

# FUTURE VISION BIE

One Stop for All Study Materials  
& Lab Programs



*Future Vision*

By K B Hemanth Raj

Scan the QR Code to Visit the Web Page



Or

Visit : <https://hemanthrajhemu.github.io>

Gain Access to All Study Materials according to VTU,  
CSE – Computer Science Engineering,  
ISE – Information Science Engineering,  
ECE - Electronics and Communication Engineering  
& MORE...

Join Telegram to get Instant Updates: [https://bit.ly/VTU\\_TELEGRAM](https://bit.ly/VTU_TELEGRAM)

Contact: MAIL: [futurevisionbie@gmail.com](mailto:futurevisionbie@gmail.com)

INSTAGRAM: [www.instagram.com/hemanthraj\\_hemu/](http://www.instagram.com/hemanthraj_hemu/)

INSTAGRAM: [www.instagram.com/futurevisionbie/](http://www.instagram.com/futurevisionbie/)

WHATSAPP SHARE: <https://bit.ly/FVBIESHARE>

# COMMUNICATION SYSTEMS ENGINEERING

**John G. Proakis**

**Masoud Salehi**

**2nd Ed.**



Upper Saddle River, New Jersey 07458

**<https://hemanthrajhemu.github.io>**

- 7.5 Optimum Receiver for Digitally Modulated Signals in Additive White Gaussian Noise 370
  - 7.5.1 *Correlation-Type Demodulator*, 370
  - 7.5.2 *Matched-Filter-Type Demodulator*, 375
  - 7.5.3 *The Optimum Detector*, 381
  - 7.5.4 *Demodulation and Detection of Carrier-Amplitude Modulated Signals*, 386
  - 7.5.5 *Demodulation and Detection of Carrier-Phase Modulated Signals*, 388
  - 7.5.6 *Demodulation and Detection of Quadrature Amplitude Modulated Signals*, 396
  - 7.5.7 *Demodulation and Detection of Frequency-Modulated Signals*, 398
- 7.6 Probability of Error for Signal Detection in Additive White Gaussian Noise 405
  - 7.6.1 *Probability of Error for Binary Modulation*, 405
  - 7.6.2 *Probability of Error for M-ary PAM*, 408
  - 7.6.3 *Probability of Error for Phase-Coherent PSK Modulation*, 413
  - 7.6.4 *Probability of Error for DPSK*, 417
  - 7.6.5 *Probability of Error for QAM*, 418
  - 7.6.6 *Probability of Error for M-ary Orthogonal Signals*, 423
  - 7.6.7 *Probability of Error for M-ary Biorthogonal Signals*, 428
  - 7.6.8 *Probability of Error for M-ary Simplex Signals*, 429
  - 7.6.9 *Probability of Error for Noncoherent Detection of FSK*, 430
  - 7.6.10 *Comparison of Modulation Methods*, 432
- 7.7 Performance Analysis for Wireline and Radio Communication Channels 436
  - 7.7.1 *Regenerative Repeaters*, 437
  - 7.7.2 *Link Budget Analysis for Radio Channels*, 438
- 7.8 Symbol Synchronization 442
  - 7.8.1 *Early-Late Gate Synchronizers*, 443
  - 7.8.2 *Minimum Mean-Square-Error Method*, 445
  - 7.8.3 *Maximum-Likelihood Methods*, 448
  - 7.8.4 *Spectral Line Methods*, 449
  - 7.8.5 *Symbol Synchronization for Carrier-Modulated Signals*, 451
- 7.9 Further Reading 452
  - Problems 453

## **8 DIGITAL TRANSMISSION THROUGH BANDLIMITED AWGN CHANNELS**

474

- 8.1 Digital Transmission through Bandlimited Channels 474
  - 8.1.1 *Digital PAM Transmission through Bandlimited Baseband Channels*, 478
  - 8.1.2 *Digital Transmission through Bandlimited Bandpass Channels*, 480

- 8.2 The Power Spectrum of Digitally Modulated Signals 482
  - 8.2.1 *The Power Spectrum of the Baseband Signal*, 483
  - 8.2.2 *The Power Spectrum of a Carrier-Modulated Signal*, 488
- 8.3 Signal Design for Bandlimited Channels 490
  - 8.3.1 *Design of Bandlimited Signals for Zero ISI—The Nyquist Criterion*, 492
  - 8.3.2 *Design of Bandlimited Signals with Controlled ISI—Partial Response Signals*, 497
- 8.4 Probability of Error in Detection of Digital PAM 499
  - 8.4.1 *Probability of Error for Detection of Digital PAM with Zero ISI*, 500
  - 8.4.2 *Symbol-by-Symbol Detection of Data with Controlled ISI*, 501
  - 8.4.3 *Probability of Error for Detection of Partial Response Signals*, 504
- 8.5 Digitally Modulated Signals with Memory 507
  - 8.5.1 *Modulation Codes and Modulation Signals with Memory*, 508
  - 8.5.2 *The Maximum-Likelihood Sequence Detector*, 521
  - 8.5.3 *Maximum-Likelihood Sequence Detection of Partial Response Signals*, 525
  - 8.5.4 *The Power Spectrum of Digital Signals with Memory*, 530
- 8.6 System Design in the Presence of Channel Distortion 534
  - 8.6.1 *Design of Transmitting and Receiving Filters for a Known Channel*, 535
  - 8.6.2 *Channel Equalization*, 538
- 8.7 Multicarrier Modulation and OFDM 556
  - 8.7.1 *An OFDM System Implemented via the FFT Algorithm*, 557
- 8.8 Further Reading 560
  - Problems 561

## **9 CHANNEL CAPACITY AND CODING**

576

- 9.1 Modeling of Communication Channels 576
- 9.2 Channel Capacity 579
  - 9.2.1 *Gaussian Channel Capacity*, 583
- 9.3 Bounds on Communication 586
  - 9.3.1 *Transmission of Analog Sources by PCM*, 590
- 9.4 Coding for Reliable Communication 591
  - 9.4.1 *A Tight Bound on Error Probability of Orthogonal Signals*, 592
  - 9.4.2 *The Promise of Coding*, 595
- 9.5 Linear Block Codes 601
  - 9.5.1 *Decoding and Performance of Linear Block Codes*, 606
  - 9.5.2 *Burst-Error-Correcting-Codes*, 614
- 9.6 Cyclic Codes 615
  - 9.6.1 *The Structure of Cyclic Codes*, 615

# *Digital Transmission through Bandlimited AWGN Channels*

In the preceding chapter, we considered digital communication over an AWGN channel and evaluated the probability of error performance of the optimum receiver for several different types of baseband and carrier-modulation methods. In this chapter, we treat digital communication over a channel that is modeled as a linear filter with a bandwidth limitation. Bandlimited channels most frequently encountered in practice are telephone channels, microwave LOS radio channels, satellite channels, and underwater acoustic channels.

In general, a linear filter channel imposes more stringent requirements on the design of modulation signals. Specifically, the transmitted signals must be designed to satisfy the bandwidth constraint imposed by the channel. The bandwidth constraint generally precludes the use of rectangular pulses at the output of the modulator. Instead, the transmitted signals must be shaped to restrict their bandwidth to that available on the channel. The design of bandlimited signals is one of the topics treated in this chapter.

We will see that a linear filter channel distorts the transmitted signal. The channel distortion results in intersymbol interference at the output of the demodulator and leads to an increase in the probability of error at the detector. Devices or methods for correcting or undoing the channel distortion, called *channel equalizers*, are then described.

## 8.1 DIGITAL TRANSMISSION THROUGH BANDLIMITED CHANNELS

A bandlimited channel such as a telephone wireline is characterized as a linear filter with impulse response  $c(t)$  and frequency response  $C(f)$ , where

$$C(f) = \int_{-\infty}^{\infty} c(t)e^{-j2\pi ft} dt \quad (8.1.1)$$

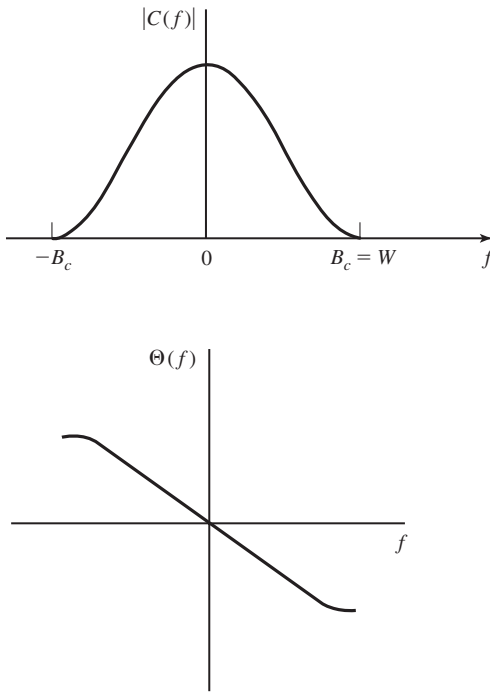


**Figure 8.1** Magnitude and phase responses of bandlimited channel.

If the channel is a baseband channel that is bandlimited to  $B_c$  Hz, then  $C(f) = 0$  for  $|f| > B_c$ . Any frequency components at the input to the channel that are higher than  $B_c$  Hz will not be passed by the channel. For this reason, we consider the design of signals for transmission through the channel that are bandlimited to  $W = B_c$  Hz, as shown in Figure 8.1. Henceforth,  $W$  will denote the bandwidth limitation of the signal and the channel.

Now, suppose that the input to a bandlimited channel is a signal waveform  $g_T(t)$ . Then, the response of the channel is the convolution of  $g_T(t)$  with  $c(t)$ ; i.e.,

$$h(t) = \int_{-\infty}^{\infty} c(\tau)g_T(t - \tau) d\tau = c(t) \star g_T(t) \quad (8.1.2)$$

or, when expressed in the frequency domain, we have

$$H(f) = C(f)G_T(f) \quad (8.1.3)$$

where  $G_T(f)$  is the spectrum (Fourier transform) of the signal  $g_T(t)$  and  $H(f)$  is the spectrum of  $h(t)$ . Thus, the channel alters or distorts the transmitted signal  $g_T(t)$ .

Let us assume that the signal at the output of the channel is corrupted by AWGN. Then, the signal at the input to the demodulator is of the form  $h(t) + n(t)$ , where  $n(t)$  denotes the AWGN. Recall from the preceding chapter that in the presence of AWGN,

a demodulator that employs a filter which is matched to the signal  $h(t)$  maximizes the SNR at its output. Therefore, let us pass the received signal  $h(t) + n(t)$  through a filter that has a frequency response

$$G_R(f) = H^*(f) e^{-j2\pi f t_0} \quad (8.1.4)$$

where  $t_0$  is some nominal time delay at which we sample the filter output.

The signal component at the output of the matched filter at the sampling instant  $t = t_0$  is

$$y_s(t_0) = \int_{-\infty}^{\infty} |H(f)|^2 df = \mathcal{E}_h, \quad (8.1.5)$$

which is the energy in the channel output  $h(t)$ . The noise component at the output of the matched filter has a zero mean and a power-spectral density

$$\mathcal{S}_n(f) = \frac{N_0}{2} |H(f)|^2 \quad (8.1.6)$$

Hence, the noise power at the output of the matched filter has a variance

$$\sigma_n^2 = \int_{-\infty}^{\infty} \mathcal{S}_n(f) df = \frac{N_0}{2} \int_{-\infty}^{\infty} |H(f)|^2 df = \frac{N_0 \mathcal{E}_h}{2} \quad (8.1.7)$$

The SNR at the output of the matched filter is

$$\left( \frac{S}{N} \right)_0 = \frac{\mathcal{E}_h^2}{N_0 \mathcal{E}_h / 2} = \frac{2\mathcal{E}_h}{N_0} \quad (8.1.8)$$

This is the result for the SNR at the output of the matched filter that was obtained in the Chapter 7 except that the received signal energy  $\mathcal{E}_h$  has replaced the transmitted signal energy  $\mathcal{E}_s$ . Compared to the previous result, the major difference in this development is that the filter impulse response is matched to the received signal  $h(t)$  instead of the transmitted signal. Note that the implementation of the matched filter at the receiver requires that  $h(t)$  or, equivalently, the channel impulse response  $c(t)$  must be known to the receiver.

### Example 8.1.1

The signal pulse  $g_T(t)$ , defined as

$$g_T(t) = \frac{1}{2} \left[ 1 + \cos \frac{2\pi}{T} \left( t - \frac{T}{2} \right) \right], \quad 0 \leq t \leq T$$

is transmitted through a baseband channel with frequency-response characteristic as shown in Figure 8.2(a). The signal pulse is illustrated in Figure 8.2(b). The channel output is corrupted by AWGN with power-spectral density  $N_0/2$ . Determine the matched filter to

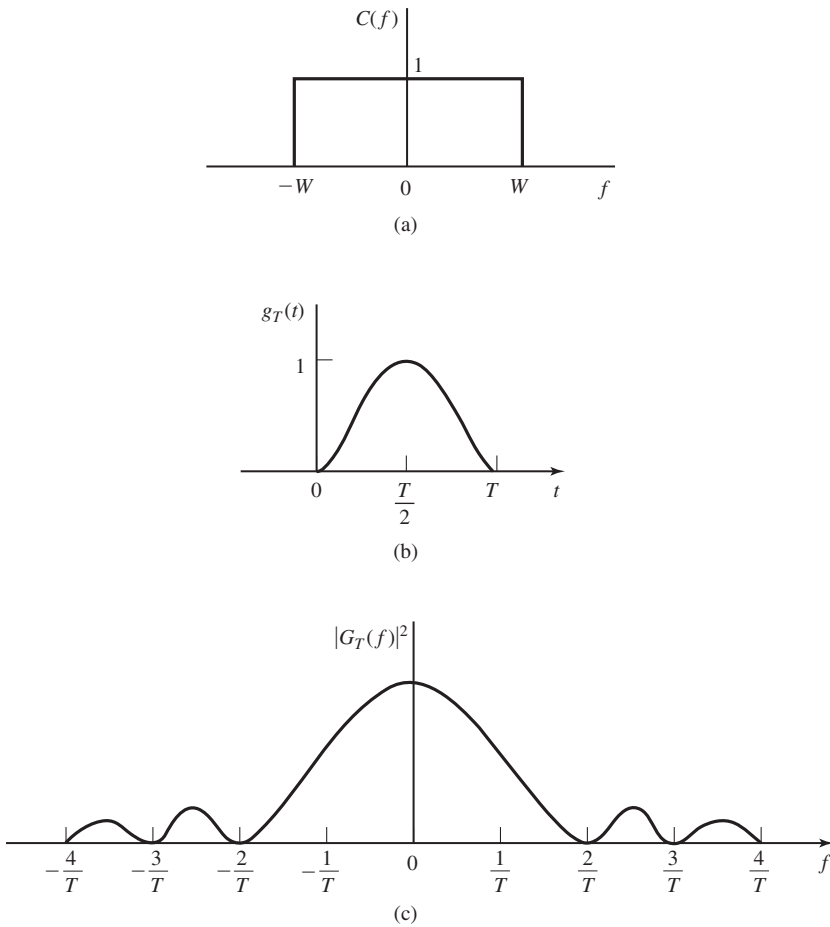


**Figure 8.2** The signal pulse in (b) is transmitted through the ideal bandlimited channel shown in (a). The spectrum of  $g_T(t)$  is shown in (c).

**Solution** This problem is most easily solved in the frequency domain. First, the spectrum of the signal pulse is

$$\begin{aligned} G_T(f) &= \frac{T}{2} \frac{\sin \pi f T}{\pi f T (1 - f^2 T^2)} e^{-j\pi f T} \\ &= \frac{T}{2} \frac{\text{sinc } \pi f T}{(1 - f^2 T^2)} e^{-j\pi f T} \end{aligned}$$

The spectrum  $|G_T(f)|^2$  is shown in Figure 8.2(c). Hence,

$$\begin{aligned} H(f) &= C(f)G_T(f) \\ &= \begin{cases} G_T(f), & |f| \leq W \\ 0, & |f| > W \end{cases} \end{aligned}$$

Then, the signal component at the output of the filter matched to  $H(f)$  is

$$\begin{aligned}\mathcal{E}_h &= \int_{-W}^W |G_T(f)|^2 df \\ &= \frac{1}{(2\pi)^2} \int_{-W}^W \frac{(\sin \pi f T)^2}{f^2(1 - f^2 T^2)^2} df \\ &= \frac{T}{(2\pi)^2} \int_{-WT}^{WT} \frac{\sin^2 \pi \alpha}{\alpha^2(1 - \alpha^2)^2} d\alpha\end{aligned}$$

The variance of the noise component is

$$\sigma_n^2 = \frac{N_0}{2} \int_{-W}^W |G_T(f)|^2 df = \frac{N_0 \mathcal{E}_h}{2}$$

Hence, the output SNR is

$$\left(\frac{S}{N}\right)_0 = \frac{2\mathcal{E}_h}{N_0}$$

In this example, we observe that the signal at the input to the channel is not bandlimited. Hence, only a part of the transmitted signal energy is received. The amount of signal energy at the output of the matched filter depends on the value of the channel bandwidth  $W$  when the signal pulse duration is fixed (see Problem 8.1). The maximum value of  $\mathcal{E}_h$ , obtained as  $W \rightarrow \infty$ , is

$$\max \mathcal{E}_h = \int_{-\infty}^{\infty} |G_T(f)|^2 df = \int_0^T g_T^2(t) dt$$

In the above development, we considered the transmission and reception of only a single signal waveform  $g_T(t)$  through a bandlimited channel with impulse response  $c(t)$ . We observed that the performance of the system is determined by  $\mathcal{E}_h$ , the energy in the received signal  $h(t)$ . To maximize the received SNR, we have to make sure that the power-spectral density of the transmitted signal matches the frequency band of the channel. To this end we must study the power-spectral density of the input signal. This will be done in Section 8.2. The impact of the channel bandwidth limitation is felt when we consider the transmission of a sequence of signal waveforms. This problem is treated in the following section.

### 8.1.1 Digital PAM Transmission through Bandlimited Baseband Channels

Let us consider the baseband PAM communication system illustrated by the functional block diagram in Figure 8.3. The system consists of a transmitting filter having an impulse response  $g_T(t)$ , the linear filter channel with AWGN, a receiving filter with impulse response  $g_R(t)$ , a sampler that periodically samples the output of the receiving filter, and a symbol detector. The sampler requires the extraction of a timing signal from the received signal as described in Section 7.8. This timing signal serves as a clock that specifies the appropriate time instants for sampling the output of the receiving filter.

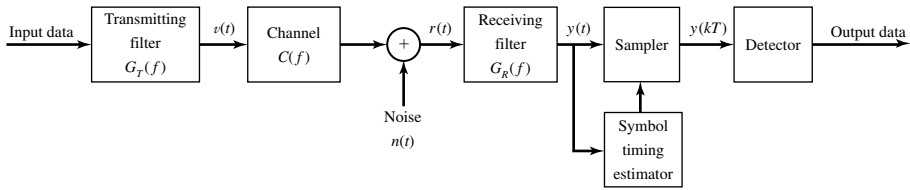


**Figure 8.3** Block diagram of digital PAM system.

First we consider digital communications by means of  $M$ -ary PAM. Hence, the input binary data sequence is subdivided into  $k$ -bit symbols and each symbol is mapped into a corresponding amplitude level that amplitude modulates the output of the transmitting filter. The baseband signal at the output of the transmitting filter (the input to the channel) may be expressed as

$$v(t) = \sum_{n=-\infty}^{\infty} a_n g_T(t - nT) \quad (8.1.9)$$

where  $T = k/R_b$  is the symbol interval ( $1/T = R_b/k$  is the symbol rate),  $R_b$  is the bit rate, and  $\{a_n\}$  is a sequence of amplitude levels corresponding to the sequence of  $k$ -bit blocks of information bits.

The channel output, which is the received signal at the demodulator, may be expressed as

$$r(t) = \sum_{n=-\infty}^{\infty} a_n h(t - nT) + n(t) \quad (8.1.10)$$

where  $h(t)$  is the impulse response of the cascade of the transmitting filter and the channel; i.e.,  $h(t) = c(t) \star g_T(t)$ ,  $c(t)$  is the impulse response of the channel, and  $n(t)$  represents the AWGN.

The received signal is passed through a linear receiving filter with impulse response  $g_R(t)$  and frequency response  $G_R(f)$ . If  $g_R(t)$  is matched to  $h(t)$ , then its output SNR is a maximum at the proper sampling instant. The output of the receiving filter may be expressed as

$$y(t) = \sum_{n=-\infty}^{\infty} a_n x(t - nT) + v(t) \quad (8.1.11)$$

where  $x(t) = h(t) \star g_R(t) = g_T(t) \star c(t) \star g_R(t)$  and  $v(t) = n(t) \star g_R(t)$  denotes the additive noise at the output of the receiving filter.

To recover the information symbols  $\{a_n\}$ , the output of the receiving filter is sampled periodically, every  $T$  seconds. Thus, the sampler produces

$$y(mT) = \sum_{n=-\infty}^{\infty} a_n x(mT - nT) + v(mT) \quad (8.1.12)$$

or, equivalently,

$$\begin{aligned} y_m &= \sum_{n=-\infty}^{\infty} a_n x_{m-n} + v_m \\ &= x_0 a_m + \sum_{n \neq m} a_n x_{m-n} + v_m \end{aligned} \quad (8.1.13)$$

where  $x_m = x(mT)$ ,  $v_m = v(mT)$ , and  $m = 0, \pm 1, \pm 2, \dots$ . A timing signal extracted from the received signal as described in Section 7.8 is used as a clock for sampling the received signal.

The first term on the right-hand side (RHS) of Equation (8.1.13) is the desired symbol  $a_m$ , scaled by the gain parameter  $x_0$ . When the receiving filter is matched to the received signal  $h(t)$ , the scale factor is

$$\begin{aligned} x_0 &= \int_{-\infty}^{\infty} h^2(t) dt = \int_{-\infty}^{\infty} |H(f)|^2 df \\ &= \int_{-W}^W |G_T(f)|^2 |C(f)|^2 df \equiv \mathcal{E}_h \end{aligned} \quad (8.1.14)$$

as indicated by the development of Equations (8.1.4) and (8.1.5). The second term on the RHS of Equation (8.1.13) represents the effect of the other symbols at the sampling instant  $t = mT$ , called the *intersymbol interference* (ISI). In general, ISI causes a degradation in the performance of the digital communication system. Finally, the third term,  $v_m$ , that represents the additive noise, is a zero-mean Gaussian random variable with variance  $\sigma_v^2 = N_0 \mathcal{E}_h / 2$ , previously given by Equation (8.1.7).

By appropriate design of the transmitting and receiving filters, it is possible to satisfy the condition  $x_n = 0$  for  $n \neq 0$ , so that the ISI term vanishes. In this case, the only term that can cause errors in the received digital sequence is the additive noise. The design of transmitting and receiving filters is considered in Section 8.3.

## 8.1.2 Digital Transmission through Bandlimited Bandpass Channels

The development given in Section 8.1.1 for baseband PAM is easily extended to carrier modulation via PAM, QAM, and PSK. In a carrier-amplitude modulated signal, the baseband PAM given by  $v(t)$  in Equation (8.1.9) modulates the carrier, so that the transmitted signal  $u(t)$  is simply

$$u(t) = v(t) \cos 2\pi f_c t \quad (8.1.15)$$

Thus, the baseband signal  $v(t)$  is shifted in frequency by  $f_c$ .

A QAM signal is a bandpass signal which, in its simplest form, may be viewed as two amplitude-modulated carrier signals in phase quadrature. That is, the QAM signal may be expressed as

$$u(t) = \sum_{n=-\infty}^{\infty} a_n \cos 2\pi f_c t - \sum_{n=-\infty}^{\infty} b_n \sin 2\pi f_c t \quad (8.1.16)$$

where

$$v_c(t) = \sum_{n=-\infty}^{\infty} a_{nc} g_T(t - nT)$$

$$v_s(t) = \sum_{n=-\infty}^{\infty} a_{ns} g_T(t - nT)$$
(8.1.17)

and  $\{a_{nc}\}$  and  $\{a_{ns}\}$  are the two sequences of amplitudes carried on the two quadrature carriers. A more compact mathematical representation of the baseband signal is the equivalent complex-valued baseband signal

$$v(t) = v_c(t) - jv_s(t)$$

$$= \sum_{n=-\infty}^{\infty} (a_{nc} - ja_{ns}) g_T(t - nT)$$

$$= \sum_{n=-\infty}^{\infty} a_n g_T(t - nT)$$
(8.1.18)

where the sequence  $\{a_n = a_{nc} - ja_{ns}\}$  is now a complex-valued sequence representing the signal points from the QAM signal constellation. The corresponding bandpass QAM signal  $u(t)$  may also be represented as

$$u(t) = \text{Re}[v(t)e^{j2\pi f_c t}]$$
(8.1.19)

In a similar manner, we can represent a digital carrier-phase modulated signal as in Equation (8.1.19), where the equivalent baseband signal is

$$v(t) = \sum_{n=-\infty}^{\infty} a_n g_T(t - nT)$$
(8.1.20)

and the sequence  $\{a_n\}$  takes the value from the set of possible (phase) values  $\{e^{-j2\pi m/M}, m = 0, 1, \dots, M-1\}$ . Thus, all three carrier-modulated signals, PAM, QAM, and PSK can be represented as in Equations (8.1.19) and (8.1.20), where the only difference is in the values taken by the transmitted sequence  $\{a_n\}$ .

The signal  $v(t)$  given by Equation (8.1.20) is called the *equivalent lowpass signal*. In the case of QAM and PSK, this equivalent lowpass signal is a baseband signal which is complex-valued because the information-bearing sequence  $\{a_n\}$  is complex-valued. In the case of PAM,  $v(t)$  is a real-valued baseband signal.

When transmitted through the bandpass channel, the received bandpass signal may be represented as

$$w(t) = \text{Re}[r(t)e^{j2\pi f_c t}]$$
(8.1.21)

where  $r(t)$  is the equivalent lowpass (baseband) signal, which may be expressed as

$$r(t) = \sum_{n=-\infty}^{\infty} a_n h(t - nT) + n(t)$$
(8.1.22)

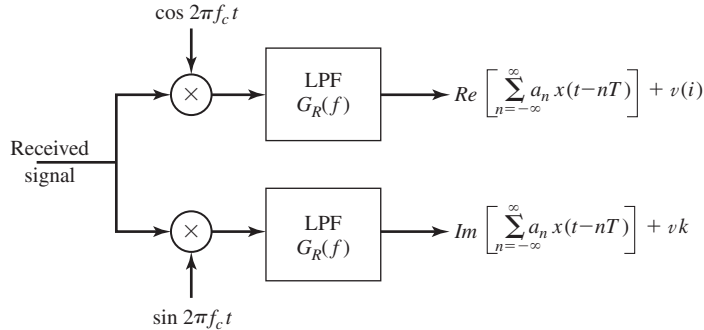


**Figure 8.4** Conversion of the bandpass received signal to baseband.

and where, as in the case of baseband transmission,  $h(t)$  is the impulse response of the cascade of the transmitting filter and the channel; i.e.,  $h(t) = c(t) \star g_T(t)$ , where  $c(t)$  is the impulse response of the equivalent lowpass channel and  $n(t)$  represents the additive Gaussian noise expressed as an equivalent lowpass (baseband) noise.

The received bandpass signal can be converted to a baseband signal by multiplying  $w(t)$  with the quadrature carrier signals  $\cos 2\pi f_c t$  and  $\sin 2\pi f_c t$  and eliminating the double frequency terms by passing the two quadrature components through separate lowpass filters, as shown in Figure 8.4. Each one of the lowpass filters is assumed to have an impulse response  $g_R(t)$ . Hence, we can represent the two quadrature components at the outputs of these lowpass filters as an equivalent complex-valued signal of the form

$$y(t) = \sum_{m=-\infty}^{\infty} a_n x(t - nT) + v(t) \quad (8.1.23)$$

which is identical to the form given by Equation (8.1.11) for the real baseband signal. Consequently, the signal design problem for bandpass signals is basically the same as that described in Section 8.1.1 for baseband signals.

In Section 8.3, we consider the design of bandlimited transmitting and receiving filters that either eliminate ISI or control ISI. However, first we will determine the power-spectral density of the transmitted digital signal. Thus, we will establish the relationship between the spectral characteristics of the transmitted signal and the channel bandwidth requirements.

## 8.2 THE POWER SPECTRUM OF DIGITALLY MODULATED SIGNALS

First, we will derive the power spectrum of a baseband signal and, then, we consider the power spectrum of the bandpass signal.

### 8.2.1 The Power Spectrum of the Baseband Signal

As shown above, the equivalent baseband transmitted signal for a digital PAM, PSK, or QAM signal is represented in the general form as

$$v(t) = \sum_{n=-\infty}^{\infty} a_n g_T(t - nT) \quad (8.2.1)$$

where  $\{a_n\}$  is the sequence of values selected from either a PAM, QAM, or PSK signal constellation corresponding to the information symbols from the source, and  $g_T(t)$  is the impulse response of the transmitting filter. Since the information sequence  $\{a_n\}$  is random,  $v(t)$  is a sample function of a random process  $V(t)$ . In this section we evaluate the power-density spectrum of  $V(t)$ . Our approach is to derive the autocorrelation function of  $V(t)$  and then to determine its Fourier transform.

First, the mean value of  $v(t)$  is

$$\begin{aligned} E[V(t)] &= \sum_{n=-\infty}^{\infty} E(a_n) g_T(t - nT) \\ &= m_a \sum_{n=-\infty}^{\infty} g_T(t - nT) \end{aligned} \quad (8.2.2)$$

where  $m_a$  is the mean value of the random sequence  $\{a_n\}$ . Note that although  $m_a$  is a constant, the term  $\sum_n g_T(t - nT)$  is a periodic function with period  $T$ . Hence, the mean value of  $V(t)$  is periodic with period  $T$ .

The autocorrelation function of  $V(t)$  is

$$R_V(t + \tau, t) = E[V^*(t) V(t + \tau)] = \sum_{n=-\infty}^{\infty} \sum_{m=-\infty}^{\infty} E(a_n^* a_m) g_T(t - nT) g_T(t + \tau - mT) \quad (8.2.3)$$

In general, we assume that the information sequence  $\{a_n\}$  is wide-sense stationary with autocorrelation sequence

$$R_a(n) = E(a_m^* a_{n+m}) \quad (8.2.4)$$

Hence, Equation (8.2.3) may be expressed as

$$\begin{aligned} R_V(t + \tau, t) &= \sum_{n=-\infty}^{\infty} \sum_{m=-\infty}^{\infty} R_a(m - n) g_T(t - nT) g_T(t + \tau - mT) \\ &= \sum_{m=-\infty}^{\infty} R_a(m) \sum_{n=-\infty}^{\infty} g_T(t - nT) g_T(t + \tau - nT - mT) \end{aligned} \quad (8.2.5)$$

We observe that the second summation in Equation (8.2.5), namely

$$\sum_{n=-\infty}^{\infty} g_T(t - nT) g_T(t + \tau - nT - mT) \quad (8.2.6)$$

is periodic with period  $T$ . Consequently, the autocorrelation function  $R_V(t + \tau, t)$  is periodic in the variable  $t$ ; i.e.,

$$R_V(t + T + \tau, t + T) = R_V(t + \tau, t) \quad (8.2.7)$$

Therefore, the random process  $V(t)$  has a periodic mean and a periodic autocorrelation. Such a random process is *cyclostationary* (see Definition 4.2.7).

The power-spectral density of a cyclostationary process can be determined by first averaging the autocorrelation function  $R_V(t + \tau, t)$  over a single period  $T$  and then computing the Fourier transform of the average autocorrelation function (see Corollary to Theorem 4.3.1). Thus, we have

$$\begin{aligned} \bar{R}_V(\tau) &= \frac{1}{T} \int_{-T/2}^{T/2} R_V(t + \tau, t) dt \\ &= \sum_{m=-\infty}^{\infty} R_a(m) \sum_{n=-\infty}^{\infty} \frac{1}{T} \int_{-T/2}^{T/2} g_T(t - nT) g_T(t + \tau - nT - mT) dt \\ &= \sum_{m=-\infty}^{\infty} R_a(m) \sum_{n=-\infty}^{\infty} \frac{1}{T} \int_{nT-T/2}^{nT+T/2} g_T(t) g_T(t + \tau - mT) dt \\ &= \frac{1}{T} \sum_{m=-\infty}^{\infty} R_a(m) \int_{-\infty}^{\infty} g_T(t) g_T(t + \tau - mT) dt \end{aligned} \quad (8.2.8)$$

We interpret the integral in Equation (8.2.8) as the time-autocorrelation function of  $g_T(t)$  and define it as [see Equation (2.3.1)]

$$R_g(\tau) = \int_{-\infty}^{\infty} g_T(t) g_T(t + \tau) dt \quad (8.2.9)$$

With this definition, the average autocorrelation function of  $V(t)$  becomes

$$\bar{R}_V(\tau) = \frac{1}{T} \sum_{m=-\infty}^{\infty} R_a(m) R_g(\tau - mT) \quad (8.2.10)$$

We observe that the expression for  $\bar{R}_V(\tau)$  in Equation (8.2.10) has the form of a convolution sum. Hence the Fourier transform of Equation (8.2.10) becomes

$$\begin{aligned} \bar{S}_V(f) &= \int_{-\infty}^{\infty} \bar{R}_V(\tau) e^{-j2\pi f\tau} d\tau \\ &= \frac{1}{T} \sum_{m=-\infty}^{\infty} R_a(m) \int_{-\infty}^{\infty} R_g(\tau - mT) e^{-j2\pi f\tau} d\tau \\ &= \frac{1}{T} S_a(f) |G_T(f)|^2 \end{aligned} \quad (8.2.11)$$

where  $\mathcal{S}_a(f)$  is the power spectrum of the information sequence  $\{a_n\}$ , defined as

$$\mathcal{S}_a(f) = \sum_{m=-\infty}^{\infty} R_a(m) e^{-j2\pi f m T} \quad (8.2.12)$$

and  $G_T(f)$  is the spectrum of the transmitting filter.  $|G_T(f)|^2$  is the Fourier transform of  $R_g(\tau)$ .

The result in Equation (8.2.11) illustrates the dependence of the power-spectral density  $\mathcal{S}_V(f)$  of the transmitted signal on (1) the spectral characteristics  $G_T(f)$  of the transmitting filter and (2) the spectral characteristics  $\mathcal{S}_a(f)$  of the information sequence  $\{a_n\}$ . Both  $G_T(f)$  and  $\mathcal{S}_a(f)$  can be designed to control the shape and form of the power spectral density of the transmitted signal.

Whereas the dependence of  $\mathcal{S}_V(f)$  on  $G_T(f)$  is easily understood, the effect of the autocorrelation properties of the information sequence  $\{a_n\}$  is more subtle. First, we observe that for an arbitrary autocorrelation  $R_a(m)$ , the corresponding power-spectral density  $\mathcal{S}_a(f)$  is periodic in frequency with period  $1/T$ . In fact, we note that  $\mathcal{S}_a(f)$ , given by Equation (8.2.12), has the form of an exponential Fourier series with  $\{R_a(m)\}$  as the Fourier coefficients. Consequently, the autocorrelation sequence  $\{R_a(m)\}$  is simply

$$R_a(m) = T \int_{-1/2T}^{1/2T} \mathcal{S}_a(f) e^{j2\pi f m T} df \quad (8.2.13)$$

Second, let us consider the case in which the information symbols in the sequence  $\{a_n\}$  are mutually uncorrelated. Then,

$$R_a(m) = \begin{cases} \sigma_a^2 + m^2, & m = 0 \\ m_a^2, & m \neq 0 \end{cases} \quad (8.2.14)$$

where  $\sigma_a^2 = E(a_n^2) - m_a^2$  is the variance of an information symbol. By substituting for  $R_a(m)$  into (8.2.12), we obtain the power-spectral density

$$\mathcal{S}_a(f) = \sigma_a^2 + m_a^2 \sum_{m=-\infty}^{\infty} e^{-j2\pi f m T} \quad (8.2.15)$$

The term involving the summation on the RHS of Equation (8.2.15) is periodic with period  $1/T$ . It may be viewed as the exponential Fourier series of a periodic train of impulses where each impulse has an area  $1/T$  (see Table 2.1). Therefore, Equation (8.2.15) can be expressed as

$$\mathcal{S}_a(f) = \sigma_a^2 + \frac{m_a^2}{T} \sum_{m=-\infty}^{\infty} \delta\left(f - \frac{m}{T}\right) \quad (8.2.16)$$

Substitution of this expression into  $\mathcal{S}_V(f)$  given by Equation (8.2.11) yields the desired result for the power spectral density of the transmitted signal  $\mathcal{V}(f)$  when the sequence

of information symbols is uncorrelated; i.e.,

$$S_V(f) = \frac{\sigma_a^2}{T} |G_T(f)|^2 + \frac{m_a^2}{T^2} \sum_{m=-\infty}^{\infty} \left| G_T \left( \frac{m}{T} \right) \right|^2 \delta \left( f - \frac{m}{T} \right) \quad (8.2.17)$$

The expression for the power-spectral density of the transmitted signal given by Equation (8.2.17) is purposely separated into two terms to emphasize the two different types of spectral components. The first term  $\sigma_a^2 |G_T(f)|^2 / T$  is the continuous spectrum and its shape depends of  $G_T(f)$ . The second term in Equation (8.2.17) consists of discrete frequency components spaced  $1/T$  apart in frequency. Each spectral line has a power that is proportional to  $|G_T(f)|^2$  evaluated at  $f = m/T$ . We note that the discrete frequency components can be eliminated by selecting the information symbol sequence  $\{a_n\}$  to have zero mean. This condition is usually imposed in digital-modulation methods because discrete spectral lines are considered to be undesirable. To be specific, the mean  $m_a$  in digital PAM, PSK, or QAM signals is easily forced to be zero by selecting the signal constellation points to be symmetrically positioned in the complex plane relative to the origin. Under the condition that  $m_a = 0$ , we have

$$S_V(f) = \frac{\sigma_a^2}{T} |G_T(f)|^2 \quad (8.2.18)$$

Thus, the system designer can control the spectral characteristics of the transmitted digital PAM signal. The following example illustrates the spectral shaping resulting from  $g_T(t)$ .

### Example 8.2.1

Determine the power-spectral density in Equation (8.2.17), when  $g_T(t)$  is the rectangular pulse shown in Figure 8.5(a).

**Solution** The Fourier transform of  $g_T(t)$  is

$$G_T(f) = AT \frac{\sin \pi f T}{\pi f T} e^{-j\pi f T}$$

Hence,

$$\begin{aligned} |G_T(f)|^2 &= (AT)^2 \left( \frac{\sin \pi f T}{\pi f T} \right)^2 \\ &= (AT)^2 \text{sinc}^2(fT) \end{aligned}$$

This spectrum is illustrated in Figure 8.5(b). We note that it contains nulls at multiples of  $1/T$  in frequency and that it decays inversely as the square of the frequency variable. As a consequence of the spectral nulls in  $G_T(f)$ , all but one of the discrete spectral components in Equation (8.2.17) vanish. Thus, upon substitution for  $|G_T(f)|^2$  into Equation (8.12.17), we obtain the result

$$\begin{aligned} S_V(f) &= \sigma_a^2 A^2 T \left( \frac{\sin \pi f T}{\pi f T} \right)^2 + A^2 m_a^2 \delta(f) \\ &= \sigma_a^2 A^2 T \text{sinc}^2(fT) + A^2 m_a^2 \delta(f) \end{aligned}$$

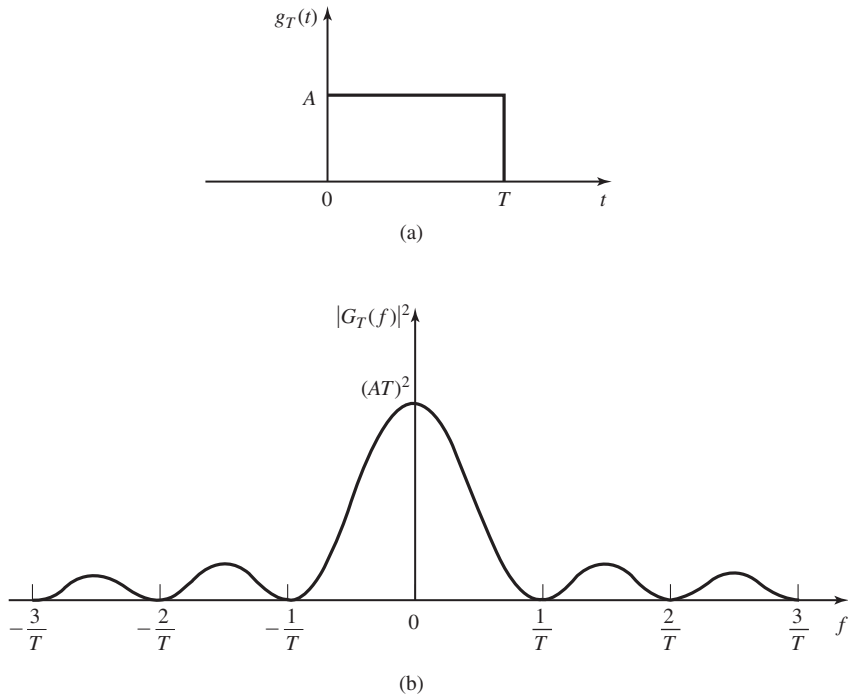


**Figure 8.5** A rectangular pulse  $g_T(t)$  and its energy density spectrum  $|G_T(f)|^2$ .

Example 8.2.2 illustrates the spectral shaping that can be achieved by operations performed on the input information sequence.

### Example 8.2.2

Consider a binary sequence  $\{b_n\}$ , from which we form the symbols

$$a_n = b_n + b_{n-1}$$

The  $\{b_n\}$  are assumed to be uncorrelated binary valued ( $\pm 1$ ) random variables, each having a zero mean and a unit variance. Determine the power-spectral density of the transmitted signal.

**Solution** The autocorrelation function of the sequence  $\{a_n\}$  is

$$\begin{aligned} R_a(m) &= E[a_n a_{n+m}] \\ &= E[(b_n + b_{n-1})(b_{n+m} + b_{n+m-1})] \\ &= \begin{cases} 2 & m = 0 \\ 1 & m = \pm 1 \\ 0, & \text{otherwise} \end{cases} \end{aligned}$$

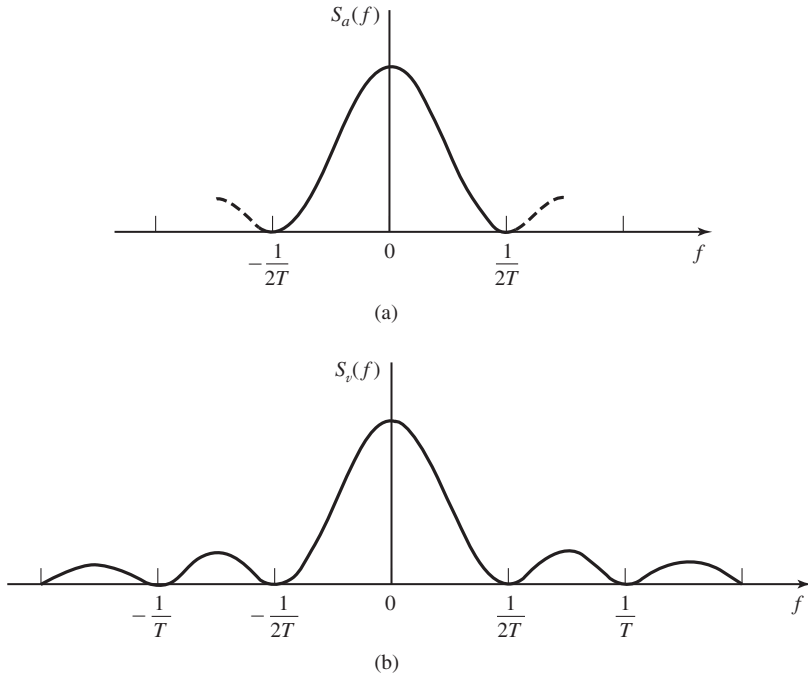


**Figure 8.6** Power-density spectra for (a) information sequence and (b) PAM modulated signal.

Hence, the power-spectral density of the input sequence is

$$\begin{aligned} S_a(f) &= 2(1 + \cos 2\pi fT) \\ &= 4 \cos^2 \pi fT \end{aligned}$$

and the corresponding power spectrum for the modulated signal is, from Equation (8.2.17),

$$S_V(f) = \frac{4}{T} |G_T(f)|^2 \cos^2 \pi fT$$

Figure 8.6 illustrates the power-density spectrum  $S_a(f)$  of the input sequence, and the corresponding  $S_V(f)$  when  $G_T(f)$  is the spectrum of the rectangular pulse.

As demonstrated in the example, the transmitted signal spectrum can be shaped by having a correlated sequence  $\{a_n\}$  as the input to the modulator.

### 8.2.2 The Power Spectrum of a Carrier-Modulated Signal

In Section 8.2.1, we showed that the power spectrum of the equivalent baseband signal  $v(t)$  given by Equation (8.2.1) for PAM, QAM, and PSK is

$$S_V(f) = \frac{1}{2} S_a(f) |G_T(f)|^2 \quad (8.2.19)$$

where  $\mathcal{S}_a(f)$  is the power spectrum of the information sequence  $\{a_n\}$ , defined as

$$\mathcal{S}_a(f) = \sum_{m=-\infty}^{\infty} R_a(m) e^{-j2\pi f m T} \quad (8.2.20)$$

and  $R_a(m)$  is the autocorrelation of the information sequence  $\{a_n\}$ ; i.e.

$$R_a(m) = E[a_n^* a_{n+m}] \quad (8.2.21)$$

The relationship between the power spectrum of the baseband signal to the power spectrum of the bandpass signal is relatively simple. Let us consider the bandpass PAM signal as an example. The autocorrelation function of the bandpass signal

$$u(t) = v(t) \cos 2\pi f_c t$$

is

$$\begin{aligned} R_U(t + \tau, t) &= E[U(t)U(t + \tau)] \\ &= E[V(t)V(t + \tau)] \cos 2\pi f_c t \cos 2\pi f_c (t + \tau) \\ &= R_V(t + \tau, t) \cos 2\pi f_c t \cos 2\pi f_c (t + \tau) \end{aligned}$$

By expressing the product of the two cosine functions in terms of the cosine of the difference plus the sum of the two angles, we obtain

$$R_U(t + \tau, t) = \frac{1}{2} R_V(t + \tau, t) [\cos 2\pi f_c \tau + \cos 2\pi f_c (2t + \tau)]$$

Then, the average of  $R_U(t + \tau, t)$  over a single period  $T$  yields

$$\bar{R}_U(\tau) = \frac{1}{2} \bar{R}_V(\tau) \cos 2\pi f_c \tau \quad (8.2.22)$$

where the second term involving the double frequency term averages to zero for each period of  $\cos 4\pi f_c t$ .

The Fourier transform of  $\bar{R}_U(t)$  yields the power spectrum of the bandpass signal as

$$\mathcal{S}_U(f) = \frac{1}{4} [\mathcal{S}_V(f - f_c) + \mathcal{S}_V(f + f_c)] \quad (8.2.23)$$

Although the derivation that resulted in Equation (8.2.23) was carried out for a bandpass PAM signal, the same expression applies to QAM and PSK. The three bandpass signals differ only in the autocorrelation  $R_a(m)$  of the sequence  $\{a_n\}$  and, hence, in the power spectrum  $\mathcal{S}_a(f)$  of  $\{a_n\}$ .

### 8.3 SIGNAL DESIGN FOR BANDLIMITED CHANNELS

Recall from Section 8.1.1 that the output of the transmitting filter in a digital PAM or PSK or QAM communication system may be expressed as

$$v(t) = \sum_{n=-\infty}^{\infty} a_n g_T(t - nT) \quad (8.3.1)$$

and the output of the channel, which is the received signal at the demodulator, may be expressed as

$$r(t) = \sum_{n=-\infty}^{\infty} a_n h(t - nT) + n(t) \quad (8.3.2)$$

where  $h(t) = c(t) \star g_T(t)$ ,  $c(t)$  is the impulse response of the channel,  $g_T(t)$  is the impulse response of the transmitting filter, and  $n(t)$  is a sample function of an additive, white Gaussian noise process.

In this section, we consider the problem of designing a bandlimited transmitting filter. The design will be done first under the condition that there is no channel distortion. Later, we consider the problem of filter design when the channel distorts the transmitted signal. Since  $H(f) = C(f)G_T(f)$ , the condition for distortion-free transmission is that the frequency response characteristic  $C(f)$  of the channel have a constant magnitude and a linear phase over the bandwidth of the transmitted signal; i.e.,

$$C(f) = \begin{cases} C_0 e^{-j2\pi f t_0}, & |f| \leq W \\ 0, & |f| > W \end{cases} \quad (8.3.3)$$

where  $W$  is the available channel bandwidth,  $t_0$  represents an arbitrary finite delay, which we set to zero for convenience, and  $C_0$  is a constant gain factor which we set to unity for convenience. Thus, under the condition that the channel is distortion-free,  $H(f) = G_T(f)$  for  $|f| \leq W$  and zero for  $|f| > W$ . Consequently, the matched filter has a frequency response  $H^*(f) = G_T^*(f)$  and its output at the periodic sampling times  $t = mT$  has the form

$$y(mT) = x(0)a_m + \sum_{n \neq m} a_n x(mT - nT) + v(mT) \quad (8.3.4)$$

or, more simply,

$$y_m = x_0 a_m + \sum_{n \neq m} a_n x_{m-n} + v_m \quad (8.3.5)$$

where  $x(t) = g_T(t) \star g_R(t)$  and  $v(t)$  is the output response of the matched filter to the input AWGN process  $n(t)$ .

The middle term on the RHS of Equation (8.3.5) represents the ISI. The amount of ISI and noise that is present in the received signal can be viewed on an oscilloscope. Specifically, we may display the received signal on the vertical input with the horizontal sweep rate set at  $1/T$ . The resulting oscilloscope display is called an *eye pattern* because

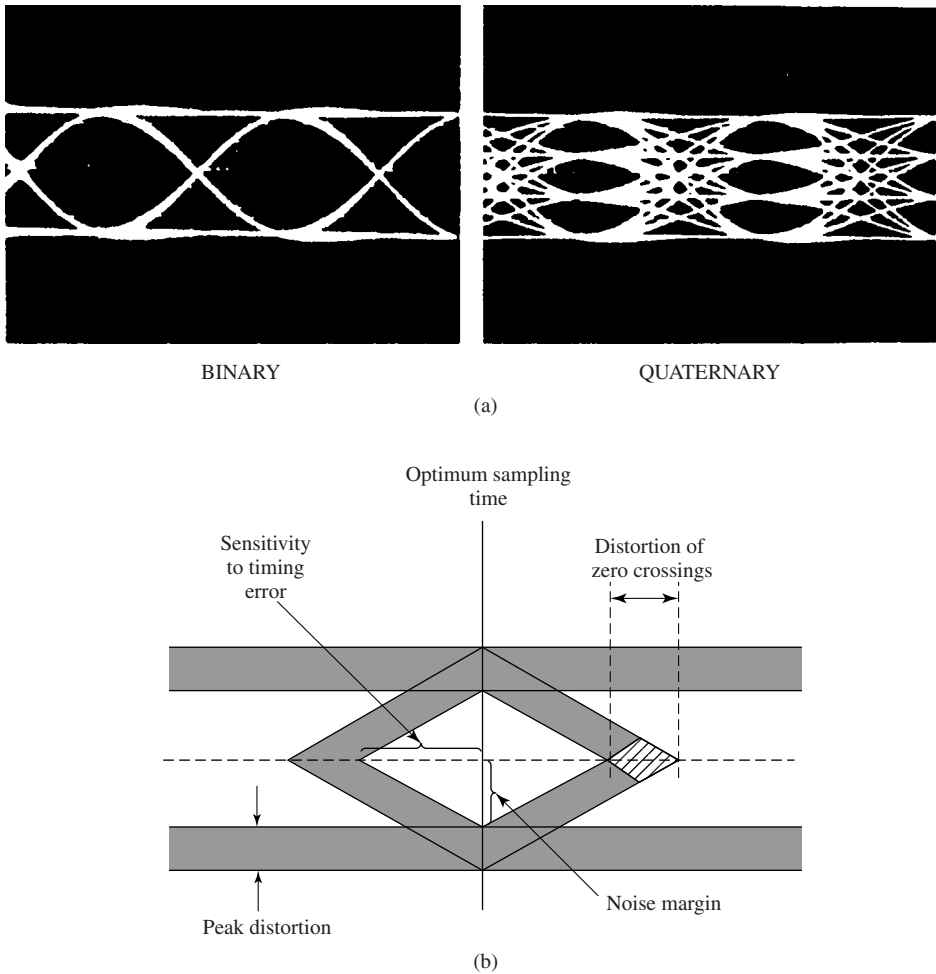


**Figure 8.7** Eye patterns. (a) Examples of eye patterns for binary and quaternary amplitude-shift keying (or PAM) and (b) Effect of ISI on eye opening.

of its resemblance to the human eye. Examples of two eye patterns, one for binary PAM and the other for quaternary ( $M = 4$ ) PAM, are illustrated in Figure 8.7(a).

The effect of ISI is to cause the eye to close, thereby reducing the margin for additive noise to cause errors. Figure 8.7(b) illustrates the effect of ISI in reducing the opening of the eye. Note that ISI distorts the position of the zero crossings and causes a reduction in the eye opening. As a consequence, the system is more sensitive to a synchronization error and exhibits a smaller margin against additive noise.

Below we consider the problem of signal design under two conditions, namely, (1) that there is no ISI at the sampling instants and (2) that a controlled amount of ISI is allowed.

<https://hemanthrajhemu.github.io>

### 8.3.1 Design of Bandlimited Signals for Zero ISI—The Nyquist Criterion

As indicated above, in a general digital communication system that transmits through a bandlimited channel, the Fourier transform of the signal at the output of the receiving filter is given by  $X(f) = G_T(f)C(f)G_R(f)$  where  $G_T(f)$  and  $G_R(f)$  denote the transmitter and receiver filters frequency responses and  $C(f)$  denotes the frequency response of the channel. We have also seen that the output of the receiving filter, sampled at  $t = mT$  is given by

$$y_m = x(0)a_m + \sum_{\substack{n=-\infty \\ n \neq m}}^{\infty} x(mT - nT)a_n + v(mT) \quad (8.3.6)$$

To remove the effect of ISI, it is necessary and sufficient that  $x(mT - nT) = 0$  for  $n \neq m$  and  $x(0) \neq 0$ , where without loss of generality we can assume  $x(0) = 1$ .<sup>†</sup> This means that the overall communication system has to be designed such that

$$x(nT) = \begin{cases} 1, & n = 0 \\ 0, & n \neq 0 \end{cases} \quad (8.3.7)$$

In this section, we derive the necessary and sufficient condition for  $X(f)$  in order for  $x(t)$  to satisfy the above relation. This condition is known as the *Nyquist pulse-shaping criterion* or *Nyquist condition for zero ISI* and is stated in the following theorem.

**Theorem 8.3.1 [Nyquist].** A necessary and sufficient condition for  $x(t)$  to satisfy

$$x(nT) = \begin{cases} 1, & n = 0 \\ 0, & n \neq 0 \end{cases} \quad (8.3.8)$$

is that its Fourier transform  $X(f)$  satisfy

$$\sum_{m=-\infty}^{\infty} X\left(f + \frac{m}{T}\right) = T \quad (8.3.9)$$

*Proof.* In general,  $x(t)$  is the inverse Fourier transform of  $X(f)$ . Hence,

$$x(t) = \int_{-\infty}^{\infty} X(f)e^{j2\pi ft} df \quad (8.3.10)$$

At the sampling instants  $t = nT$ , this relation becomes

$$x(nT) = \int_{-\infty}^{\infty} X(f)e^{j2\pi fnT} df \quad (8.3.11)$$

Let us break up the integral in Equation (8.3.11) into integrals covering the finite range

<sup>†</sup>The choice of  $x(0)$  is equivalent to the choice of a constant gain factor in the receiving filter. This constant gain factor has no effect on the overall system performance since it scales both the signal and the noise.

of  $1/T$ . Thus, we obtain

$$\begin{aligned}
 x(nT) &= \sum_{m=-\infty}^{\infty} \int_{(2m-1)/2T}^{(2m+1)/2T} X(f) e^{j2\pi f n T} df \\
 &= \sum_{m=-\infty}^{\infty} \int_{-1/2T}^{1/2T} X\left(f + \frac{m}{T}\right) e^{j2\pi f n T} dt \\
 &= \int_{-1/2T}^{1/2T} \left[ \sum_{m=-\infty}^{\infty} X\left(f + \frac{m}{T}\right) \right] e^{j2\pi f n T} dt \\
 &= \int_{-1/2T}^{1/2T} Z(f) e^{j2\pi f n T} dt \tag{8.3.12}
 \end{aligned}$$

where we have defined  $Z(f)$  by

$$Z(f) = \sum_{m=-\infty}^{\infty} X\left(f + \frac{m}{T}\right) \tag{8.3.13}$$

Obviously,  $Z(f)$  is a periodic function with period  $\frac{1}{T}$ , and therefore it can be expanded in terms of its Fourier series coefficients  $\{z_n\}$  as

$$Z(f) = \sum_{m=-\infty}^{\infty} z_n e^{j2\pi n f T} \tag{8.3.14}$$

where

$$z_n = T \int_{-\frac{1}{2T}}^{\frac{1}{2T}} Z(f) e^{-j2\pi n f T} df \tag{8.3.15}$$

Comparing Equations (8.3.15) and (8.3.12) we obtain

$$z_n = T x(-nT) \tag{8.3.16}$$

Therefore, the necessary and sufficient conditions for Equation (8.3.8) to be satisfied is that

$$z_n = \begin{cases} T & n = 0 \\ 0, & n \neq 0 \end{cases} \tag{8.3.17}$$

which, when substituted into Equation (8.3.14), yields

$$Z(f) = T \tag{8.3.18}$$

or, equivalently,

$$\sum_{m=-\infty}^{\infty} X\left(f + \frac{m}{T}\right) = T \tag{8.3.19}$$

This concludes the proof of the theorem. ■

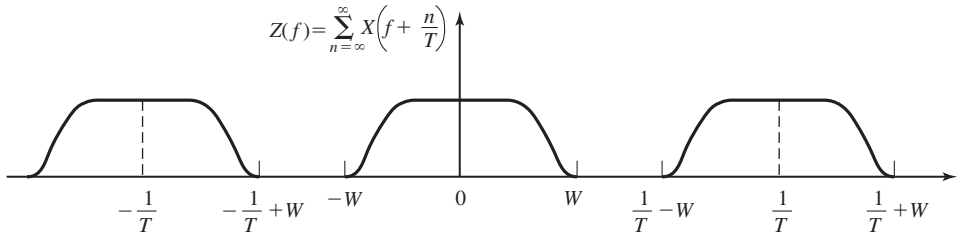


**Figure 8.8** Plot of  $Z(f)$  for the case  $T < \frac{1}{2W}$ .

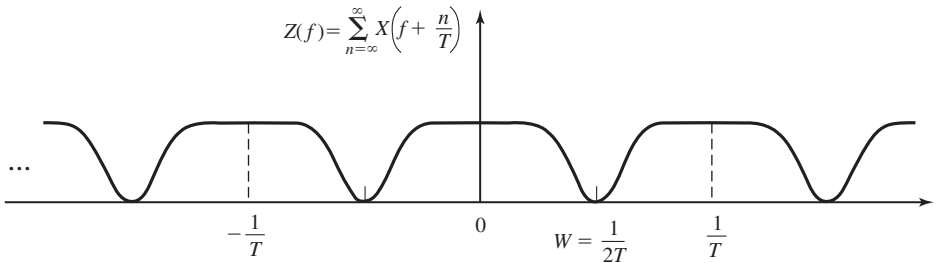


**Figure 8.9** Plot of  $Z(f)$  for the case  $T = \frac{1}{2W}$ .

Now, suppose that the channel has a bandwidth of  $W$ . Then  $C(f) \equiv 0$  for  $|f| > W$  and consequently,  $X(f) = 0$  for  $|f| > W$ . We distinguish three cases:

1.  $T < \frac{1}{2W}$ , or equivalently,  $\frac{1}{T} > 2W$ . Since  $Z(f) = \sum_{n=-\infty}^{+\infty} X(f + \frac{n}{T})$  consists of nonoverlapping replicas of  $X(f)$ , separated by  $\frac{1}{T}$  as shown in Figure 8.8, there is no choice for  $X(f)$  to ensure  $Z(f) \equiv T$  in this case, and there is no way that we can design a system with no ISI.
2.  $T = \frac{1}{2W}$ , or equivalently,  $\frac{1}{T} = 2W$  (the Nyquist rate). In this case, the replications of  $X(f)$ , separated by  $\frac{1}{T}$ , are about to overlap as shown in Figure 8.9. It is clear that in this case there exists only one  $X(f)$  that results in  $Z(f) = T$ , namely,

$$X(f) = \begin{cases} T & |f| < W \\ 0, & \text{otherwise} \end{cases} \quad (8.3.20)$$

or,  $X(f) = T \Pi(\frac{f}{2W})$ , which results in

$$x(t) = \text{sinc}\left(\frac{t}{T}\right) \quad (8.3.21)$$

This means that the smallest value of  $T$  for which transmission with zero ISI is possible is  $T = \frac{1}{2W}$  and for this value,  $x(t)$  has to be a sinc function. The difficulty with this choice of  $x(t)$  is that it is noncausal and therefore nonrealizable. To make it realizable, usually a delayed version of it; i.e.,  $\text{sinc}(\frac{t-t_0}{T})$  is used and  $t_0$  is chosen such that for  $t < 0$ , we have  $\text{sinc}(\frac{t-t_0}{T}) \approx 0$ . Of course with this choice of

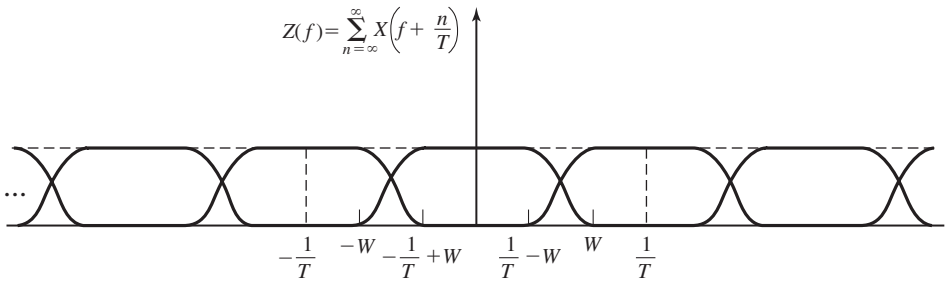


Figure 8.10 Plot of  $Z(f)$  for the case  $T > 1/2W$ .

$x(t)$ , the sampling time must also be shifted to  $mT + t_0$ . A second difficulty with this pulse shape is that its rate of convergence to zero is slow. The tails of  $x(t)$  decay as  $1/t$ , consequently, a small mistiming error in sampling the output of the matched filter at the demodulator results in an infinite series of ISI components. Such a series is not absolutely summable because of the  $1/t$  rate of decay of the pulse and, hence, the sum of the resulting ISI does not converge.

3. For  $T > \frac{1}{2W}$ ,  $Z(f)$  consists of overlapping replications of  $X(f)$  separated by  $\frac{1}{T}$ , as shown in Figure 8.10. In this case, there exist numerous choices for  $X(f)$ , such that  $Z(f) \equiv T$ .

A particular pulse spectrum, for the  $T > \frac{1}{2W}$  case, that has desirable spectral properties and has been widely used in practice is the raised cosine spectrum. The raised cosine frequency characteristic is given as (see Problem 8.11)

$$X_{rc}(f) = \begin{cases} T, & 0 \leq |f| \leq (1 - \alpha)/2T \\ \frac{T}{2} \left[ 1 + \cos \frac{\pi T}{\alpha} \left( |f| - \frac{1-\alpha}{2T} \right) \right], & \frac{1-\alpha}{2T} \leq |f| \leq \frac{1+\alpha}{2T} \\ 0, & |f| > \frac{1+\alpha}{2T} \end{cases} \quad (8.3.22)$$

where  $\alpha$  is called the *rolloff factor*, which takes values in the range  $0 \leq \alpha \leq 1$ . The bandwidth occupied by the signal beyond the Nyquist frequency  $\frac{1}{2T}$  is called the *excess bandwidth* and is usually expressed as a percentage of the Nyquist frequency. For example, when  $\alpha = \frac{1}{2}$ , the excess bandwidth is 50%, and when  $\alpha = 1$  the excess bandwidth is 100%. The pulse  $x(t)$  having the raised cosine spectrum is

$$\begin{aligned} x(t) &= \frac{\sin \pi t/T}{\pi t/T} \frac{\cos(\pi \alpha t/T)}{1 - 4\alpha^2 t^2/T^2} \\ &= \text{sinc}(t/T) \frac{\cos(\pi \alpha t/T)}{1 - 4\alpha^2 t^2/T^2} \end{aligned} \quad (8.3.23)$$

Note that  $x(t)$  is normalized so that  $x(0) = 1$ . Figure 8.11 illustrates the raised cosine spectral characteristics and the corresponding pulses for  $\alpha = 0, 1/2, 1$ . We note that

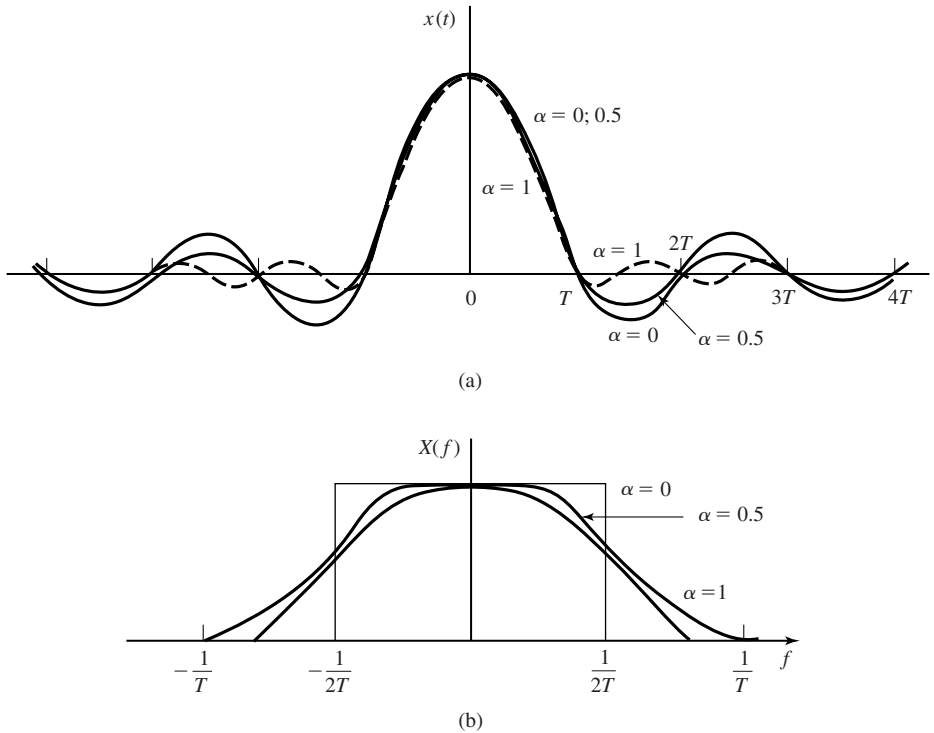


**Figure 8.11** Pulses having a raised cosine spectrum.

for  $\alpha = 0$ , the pulse reduces to  $x(t) = \text{sinc}(t/T)$ , and the symbol rate  $1/T = 2W$ . When  $\alpha = 1$ , the symbol rate is  $1/T = W$ . In general, the tails of  $x(t)$  decay as  $1/t^3$  for  $\alpha > 0$ . Consequently, a mistiming error in sampling leads to a series of intersymbol interference components that converges to a finite value.

Due to the smooth characteristics of the raised cosine spectrum, it is possible to design practical filters for the transmitter and the receiver that approximate the overall desired frequency response. In the special case where the channel is ideal with  $C(f) = \Pi(\frac{f}{2W})$ , we have

$$X_{\text{rc}}(f) = G_T(f)G_R(f) \quad (8.3.24)$$

In this case, if the receiver filter is matched to the transmitter filter we have  $X_{\text{rc}}(f) = G_T(f)G_R(f) = |G_T(f)|^2$ . Ideally,

$$G_T(f) = \sqrt{|X_{\text{rc}}(f)|} e^{-j2\pi f t_0} \quad (8.3.25)$$

and  $G_R(f) = G_T^*(f)$ , where  $t_0$  is some nominal delay that is required to assure physical realizability of the filter. Thus, the overall raised cosine spectral characteristic is split evenly between the transmitting filter and the receiving filter. We should also note that

### 8.3.2 Design of Bandlimited Signals with Controlled ISI—Partial Response Signals

As we have observed from our discussion of signal design for zero ISI, it is necessary to reduce the symbol rate  $1/T$  below the Nyquist rate of  $2W$  symbols/sec in order to realize practical transmitting and receiving filters. On the other hand, suppose we choose to relax the condition of zero ISI and, thus, achieve a symbol transmission rate of  $2W$  symbols/sec. By allowing for a controlled amount of ISI, we can achieve this symbol rate.

We have already seen in that the condition of zero ISI is  $x(nT) = 0$  for  $n \neq 0$ . However, suppose that we design the bandlimited signal to have controlled ISI at one time instant. This means that we allow one additional nonzero value in the samples  $\{x(nT)\}$ . The ISI that we introduce is deterministic or “controlled” and, hence, it can be taken into account at the receiver, as discussed next.

One special case that leads to (approximately) physically realizable transmitting and receiving filters is specified by the samples<sup>†</sup>

$$x(nT) = \begin{cases} 1, & n = 0, 1 \\ 0, & \text{otherwise} \end{cases} \quad (8.3.26)$$

Now, using Equation (8.3.16), we obtain

$$z_n = \begin{cases} T & n = 0, -1 \\ 0, & \text{otherwise} \end{cases} \quad (8.3.27)$$

which when substituted into Equation (8.3.14) yields

$$Z(f) = T + T e^{-j2\pi fT} \quad (8.3.28)$$

As in the preceding section, it is impossible to satisfy the above equation for  $T < \frac{1}{2W}$ . However, for  $T = \frac{1}{2W}$ , we obtain

$$\begin{aligned} X(f) &= \begin{cases} \frac{1}{2W} [1 + e^{-j\frac{\pi f}{W}}], & |f| < W \\ 0, & \text{otherwise} \end{cases} \\ &= \begin{cases} \frac{1}{W} e^{-j\frac{\pi f}{2W}} \cos\left(\frac{\pi f}{2W}\right), & |f| < W \\ 0, & \text{otherwise} \end{cases} \end{aligned} \quad (8.3.29)$$

Therefore,  $x(t)$  is given by

$$x(t) = \text{sinc}(2Wt) + \text{sinc}(2Wt - 1) \quad (8.3.30)$$

This pulse is called a duobinary signal pulse. It is illustrated, along with its magnitude spectrum in Figure 8.12. We note that the spectrum decays to zero smoothly, which means that physically realizable filters can be designed that approximate this spectrum very closely. Thus, a symbol rate of  $2W$  is achieved.

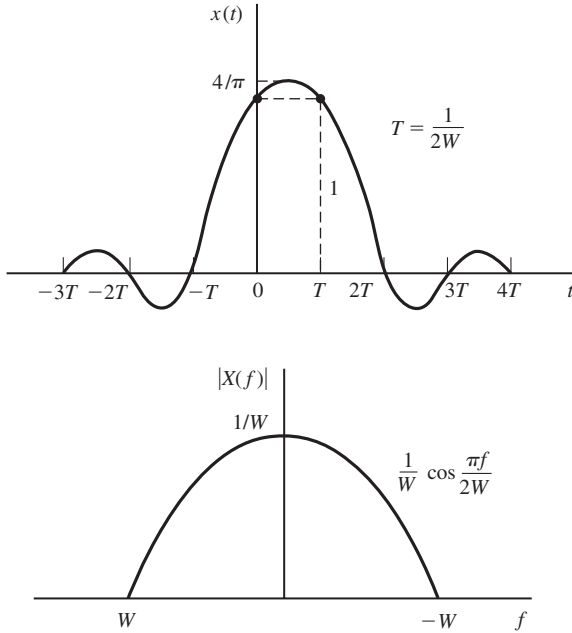


**Figure 8.12** Time domain and frequency-domain characteristics of a duobinary signal.

Another special case that leads to (approximately) physically realizable transmitting and receiving filters is specified by the samples

$$x\left(\frac{n}{2W}\right) = x(nT) = \begin{cases} 1, & n = -1 \\ -1, & n = 1 \\ 0, & \text{otherwise} \end{cases} \quad (8.3.31)$$

The corresponding pulse  $x(t)$  is given as

$$x(t) = \text{sinc}(t + T)/T - \text{sinc}(t - T)/T \quad (8.3.32)$$

and its spectrum is

$$X(f) = \begin{cases} \frac{1}{2W} e^{j\pi f/W} - e^{-j\pi f/W} = \frac{j}{W} \sin \frac{\pi f}{W}, & |f| \leq W \\ 0, & |f| > W \end{cases} \quad (8.3.33)$$

This pulse and its magnitude spectrum are illustrated in Figure 8.13. It is called a *modified duobinary signal pulse*. It is interesting to note that the spectrum of this signal has a zero at  $f = 0$ , making it suitable for transmission over a channel that does not pass dc.

One can obtain other interesting and physically realizable filter characteristics, as shown by Kretzmer (1966) and Lucky et al. (1968), by selecting different values for the samples  $\{x(n/2W)\}$  and more than two nonzero samples. However, as we select more nonzero samples, the problem of unraveling the controlled ISI becomes more

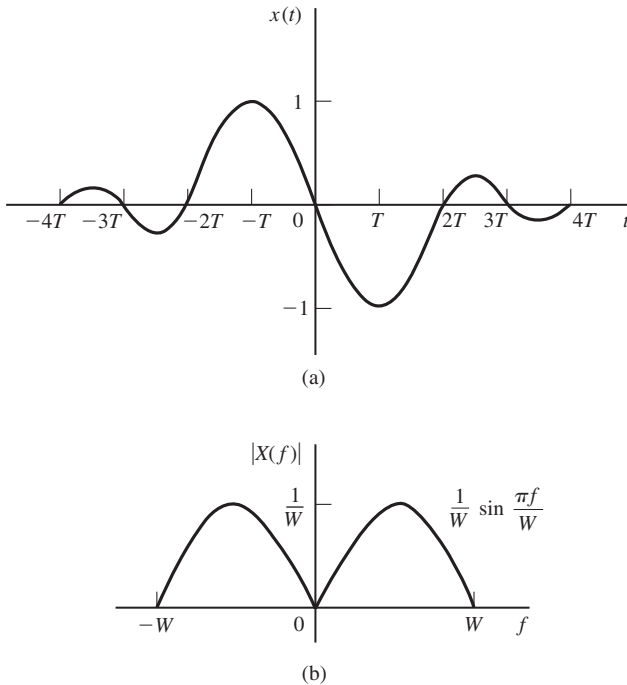


**Figure 8.13** Time domain and frequency domain characteristics of a modified duobinary signal.

In general, the class of bandlimited signals pulses that have the form

$$x(t) = \sum_{n=-\infty}^{\infty} x\left(\frac{n}{2W}\right) \frac{\sin 2\pi W(t - n/2W)}{2\pi W(t - n/2W)} \quad (8.3.34)$$

and their corresponding spectra

$$X(f) = \begin{cases} \frac{1}{2W} \sum_{n=-\infty}^{\infty} x\left(\frac{n}{2W}\right) e^{-jn\pi f/W}, & |f| \leq W \\ 0, & |f| > W \end{cases} \quad (8.3.35)$$

are called *partial response signals* when controlled ISI is purposely introduced by selecting two or more nonzero samples from the set  $\{x(n/2W)\}$ . The resulting signal pulses allow us to transmit information symbols at the Nyquist rate of  $2W$  symbols per second. The detection of the received symbols in the presence of controlled ISI is described in Sections 8.4 and 8.5.

## 8.4 PROBABILITY OF ERROR IN DETECTION OF DIGITAL PAM

In this section we evaluate the performance of the receiver for demodulating and detecting an  $M$ -ary PAM signal in the presence of additive, white Gaussian noise at its input. First, we consider the case in which the transmitter and receiver filters  $G_T(f)$  and  $G_R(f)$  are designed for zero ISI. Then, we consider the case in which  $G_T(f)$  and  $G_R(f)$  are designed such that  $x(t) = g(t) + g(t - T)$  is either a duobinary signal

or a modified duobinary signal. Although our focus in this section is the performance evaluation of PAM, our treatment can be generalized to two-dimensional modulations, such as PSK and QAM, and multidimensional signals.

#### 8.4.1 Probability of Error for Detection of Digital PAM with Zero ISI

In the absence of ISI, the received signal sample at the output of the receiving matched filter has the form

$$y_m = x_0 a_m + v_m \quad (8.4.1)$$

where

$$x_0 = \int_{-W}^W |G_T(f)|^2 df = \mathcal{E}_g \quad (8.4.2)$$

and  $v_m$  is the additive Gaussian noise which has zero mean and variance

$$\sigma_v^2 = \mathcal{E}_g N_0 / 2 \quad (8.4.3)$$

In general,  $a_m$  takes one of  $M$  possible equally spaced amplitude values with equal probability. Given a particular amplitude level, the problem is to determine the probability of error.

The problem of evaluating the probability of error for digital PAM in a bandlimited, additive white Gaussian noise channel, in the absence of ISI, is identical to the evaluation of the error probability for  $M$ -ary PAM as given in Section 7.6.2. The final result that is obtained from the derivation is

$$P_M = \frac{2(M-1)}{M} Q \left[ \sqrt{\frac{2\mathcal{E}_g}{N_0}} \right] \quad (8.4.4)$$

But  $\mathcal{E}_g = 3\mathcal{E}_{av}/(M^2 - 1)$ ,  $\mathcal{E}_{av} = k \mathcal{E}_{bav}$  is the average energy per symbol and  $\mathcal{E}_{bav}$  is the average energy/bit. Hence,

$$P_M = \frac{2(M-1)}{M} Q \left[ \sqrt{\frac{6(\log_2 M)\mathcal{E}_{bav}}{(M^2 - 1)N_0}} \right] \quad (8.4.5)$$

This is exactly the form for the probability of error of  $M$ -ary PAM derived previously in Section 7.6.2. In the treatment of PAM given in this chapter we imposed the additional constraint that the transmitted signal is bandlimited to the bandwidth allocated for the channel. Consequently, the transmitted signal pulses were designed to be bandlimited and to have zero ISI.

In contrast, no bandwidth constraint was imposed on the PAM signals considered in Section 7.6.2. Nevertheless, the receivers (demodulators and detectors) in both cases are optimum (matched filters) for the corresponding transmitted signals. Consequently, no loss in error-rate performance results from the bandwidth constraint when the signal pulse is designed for zero ISI and the channel does not distort the transmitted signal.

### 8.4.2 Symbol-by-Symbol Detection of Data with Controlled ISI

In this section we describe a symbol-by-symbol method for detecting the information symbols at the demodulator when the received signal contains controlled ISI. This symbol detection method is relatively easy to implement. A second method, based on the maximum-likelihood criterion for detecting a sequence of symbols, is described in Section 8.5.2. This second method minimizes the probability of error but is a little more complex to implement. In particular, we consider the detection of the duobinary and the modified duobinary partial response signals. In both cases, we assume that the desired spectral characteristic  $X(f)$  for the partial response signal is split evenly between the transmitting and receiving filters; i.e.,  $|G_T(f)| = |G_R(f)| = |X(f)|^{1/2}$ .

For the duobinary signal pulse,  $x(nT) = 1$ , for  $n = 0, 1$  and zero otherwise. Hence, the samples at the output of the receiving filter have the form

$$y_m = b_m + v_m = a_m + a_{m-1} + v_m \quad (8.4.6)$$

where  $\{a_m\}$  is the transmitted sequence of amplitudes and  $\{v_m\}$  is a sequence of additive Gaussian noise samples. Let us ignore the noise for the moment and consider the binary case where  $a_m = \pm 1$  with equal probability. Then,  $b_m$  takes on one of three possible values, namely,  $b_m = -2, 0, 2$  with corresponding probabilities  $1/4, 1/2, 1/4$ . If  $a_{m-1}$  is the detected symbol from the  $(m-1)$ st signaling interval, its effect on  $b_m$ , the received signal in the  $m$ th signaling interval, can be eliminated by subtraction, thus allowing  $a_m$  to be detected. This process can be repeated sequentially for every received symbol.

The major problem with this procedure is that errors arising from the additive noise tend to propagate. For example, if  $a_{m-1}$  is in error, its effect on  $b_m$  is not eliminated but, in fact, it is reinforced by the incorrect subtraction. Consequently, the detection of  $a_m$  is also likely to be in error.

Error propagation can be avoided by *precoding* the data at the transmitter instead of eliminating the controlled ISI by subtraction at the receiver. The precoding is performed on the binary data sequence prior to modulation. From the data sequence  $\{d_n\}$  of 1's and 0's that is to be transmitted, a new sequence  $\{p_n\}$ , called the *precoded sequence* is generated. For the duobinary signal, the precoded sequence is defined as

$$p_m = d_m \ominus p_{m-1}, \quad m = 1, 2, \dots \quad (8.4.7)$$

where the symbol  $\ominus$  denotes modulo-2 subtraction.<sup>†</sup> Then, we set  $a_m = -1$  if  $p_m = 0$  and  $a_m = 1$  if  $p_m = 1$ ; i.e.,  $a_m = 2p_m - 1$ .

The noise-free samples at the output of the receiving filter are given as

$$\begin{aligned} b_m &= a_m + a_{m-1} \\ &= (2p_m - 1) + (2p_{m-1} - 1) \\ &= 2(p_m + p_{m-1} - 1) \end{aligned} \quad (8.4.8)$$

<sup>†</sup> Although this is identical to modulo-2 addition, it is convenient to view the precoding operation for duobinary in terms of modulo-2 subtraction.

**TABLE 8.1** BINARY SIGNALING WITH DUOBINARY PULSES

Data sequence $d_n$	1	1	1	0	1	0	0	1	0	0	0	1	1	0	1	
Precoded sequence $p_n$	0	1	0	1	1	0	0	0	1	1	1	1	0	1	1	0
Transmitted sequence $a_n$	-1	1	-1	1	1	-1	-1	-1	1	1	1	1	-1	1	1	-1
Received sequence $b_n$	0	0	0	2	0	-2	-2	0	2	2	2	0	0	2	0	
Decoded sequence $d_n$	1	1	1	0	1	0	0	1	0	0	0	1	1	0	1	

Consequently,

$$p_m + p_{m-1} = \frac{b_m}{2} + 1 \quad (8.4.9)$$

Since  $d_m = p_m \oplus p_{m-1}$ , it follows that the data sequence  $d_m$  is obtained from  $b_m$  by using the relation

$$d_m = \frac{b_m}{2} - 1 \pmod{2} \quad (8.4.10)$$

Consequently, if  $b_m = \pm 2$ ,  $d_m = 0$  and if  $b_m = 0$ ,  $d_m = 1$ . An example that illustrates the precoding and decoding operations is given in Table 8.1. In the presence of additive noise the sampled outputs from the receiving filter are given by Equation (8.4.6). In this case  $y_m = b_m + v_m$  is compared with the two thresholds set at +1 and -1. The data sequence  $\{d_n\}$  is obtained according to the detection rule

$$d_m = \begin{cases} 1, & \text{if } -1 < y_m < 1 \\ 0, & \text{if } |y_m| \geq 1 \end{cases} \quad (8.4.11)$$

The extension from binary PAM to multilevel PAM signaling using the duobinary pulses is straightforward. In this case the  $M$ -level amplitude sequence  $\{a_m\}$  results in a (noise-free) sequence

$$b_m = a_m + a_{m-1}, \quad m = 1, 2, \dots \quad (8.4.12)$$

which has  $2M - 1$  possible equally spaced levels. The amplitude levels are determined from the relation

$$a_m = 2p_m - (M - 1) \quad (8.4.13)$$

where  $\{p_m\}$  is the precoded sequence that is obtained from an  $M$ -level data sequence  $\{d_m\}$  according to the relation

$$p_m = d_m \ominus p_{m-1} \pmod{M} \quad (8.4.14)$$

where the possible values of the sequence  $\{d_m\}$  are 0, 1, 2, ...,  $M - 1$ .

**TABLE 8.2** FOUR-LEVEL TRANSMISSION WITH DUOBINARY PULSES

Data sequence $d_n$	0	0	1	3	1	2	0	3	3	2	0	1	0	
Preceded sequence $p_n$	0	0	0	1	2	3	3	1	2	1	1	3	2	2
Transmitted sequence $a_n$	-3	-3	-3	-1	1	3	3	-1	1	-1	-1	3	1	1
Received sequence $b_n$	-6	-6	-4	0	4	6	2	0	0	-2	2	4	2	
Decoded sequence $d_n$	0	0	1	3	1	2	0	3	3	2	0	1	0	

In the absence of noise, the samples at the output of the receiving filter may be expressed as

$$\begin{aligned} b_m &= a_m + a_{m-1} \\ &= 2[p_m + p_{m-1} - (M - 1)] \end{aligned} \quad (8.4.15)$$

Hence,

$$p_m + p_{m-1} = \frac{b_m}{2} + (M - 1) \quad (8.4.16)$$

Since  $d_m = p_m + p_{m-1} \pmod{M}$ , it follows that

$$d_m = \frac{b_m}{2} + (M - 1) \pmod{M} \quad (8.4.17)$$

An example illustrating multilevel precoding and decoding is given in Table 8.2.

In the presence of noise, the received signal-plus-noise is quantized to the nearest of the possible signal levels and the rule given above is used on the quantized values to recover the data sequence.

In the case of the modified duobinary pulse, the controlled ISI is specified by the values  $x(n/2W) = -1$ , for  $n = 1$ ,  $x(n/2W) = 1$  for  $n = -1$ , and zero otherwise. Consequently, the noise-free sampled output from the receiving filter is given as

$$b_m = a_m - a_{m-2} \quad (8.4.18)$$

where the  $M$ -level sequence  $\{a_n\}$  is obtained by mapping a precoded sequence according to the relation Equation (8.2.43) and

$$p_m = d_m \oplus p_{m-2} \pmod{M} \quad (8.4.19)$$

From these relations, it is easy to show that the detection rule for recovering the data sequence  $\{d_m\}$  from  $\{b_m\}$  in the absence of noise is

$$d_m = \frac{b_m}{2} \pmod{M} \quad (8.4.20)$$

As demonstrated above, the precoding of the data at the transmitter makes it possible to detect the received data on a symbol-by-symbol basis without having to look back at previously detected symbols. Thus, error propagation is avoided.

The symbol-by-symbol detection rule described above is not the optimum detection scheme for partial response signals. Nevertheless, symbol-by-symbol detection is relatively simple to implement and is used in many practical applications involving duobinary and modified duobinary pulse signals. Its performance is evaluated in Section 8.4.3.

### 8.4.3 Probability of Error for Detection of Partial Response Signals

In this section we determine the probability of error for detection of digital  $M$ -ary PAM signaling using duobinary and modified duobinary pulses. The channel is assumed to be an ideal bandlimited channel with additive white Gaussian noise. The model for the communications system is shown in Figure 8.14.

We consider the symbol-by-symbol detector. The performance of the optimum ML sequence detector is described in Section 8.5.3.

**Symbol-by-Symbol Detector.** At the transmitter, the  $M$ -level data sequence  $\{d_n\}$  is precoded as described previously. The precoder output is mapped into one of  $M$  possible amplitude levels. Then the transmitting filter with frequency response  $G_T(f)$  has an output

$$v(t) = \sum_{n=-\infty}^{\infty} a_n g_T(t - nT) \quad (8.4.21)$$

The partial-response function  $X(f)$  is divided equally between the transmitting and receiving filters. Hence, the receiving filter is matched to the transmitted pulse, and the cascade of the two filters results in the frequency characteristic

$$|G_T(f)G_R(f)| = |X(f)| \quad (8.4.22)$$

The matched filter output is sampled at  $t = nT = n/2W$  and the samples are fed to the decoder. For the duobinary signal, the output of the matched filter at the sampling instant may be expressed as

$$\begin{aligned} y_m &= a_m + a_{m-1} + v_m \\ &= b_m + v_m \end{aligned} \quad (8.4.23)$$

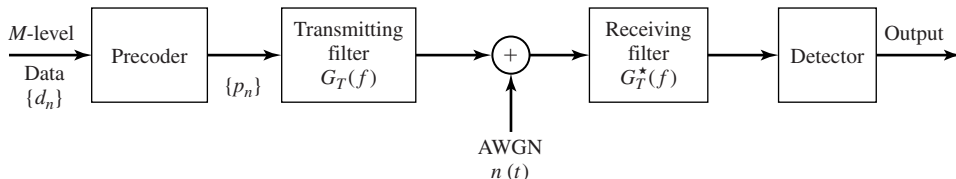


**Figure 8.14** Block diagram of modulator and demodulator for partial response signals.

where  $v_m$  is the additive noise component. Similarly, the output of the matched filter for the modified duobinary signal is

$$\begin{aligned} y_m &= a_m - a_{m-2} + v_m \\ &= b_m + v_m \end{aligned} \quad (8.4.24)$$

For binary transmission, let  $a_m = \pm d$ , where  $2d$  is the distance between signal levels. Then, the corresponding values of  $b_m$  are  $(2d, 0, -2d)$ . For  $M$ -ary PAM signal transmission, where  $a_m = \pm d, \pm 3d, \dots, \pm(M-1)d$ , the received signal levels are  $b_m = 0, \pm 2d, \pm 4d, \dots, \pm 2(M-1)d$ . Hence, the number of received levels is  $2M-1$ .

The input transmitted symbols  $\{a_m\}$  are assumed to be equally probable. Then, for duobinary and modified duobinary signals, it is easily demonstrated that, in the absence of noise, the received output levels have a (triangular) probability mass function of the form

$$P(b = 2md) = \frac{M - |m|}{M^2}, \quad m = 0, \pm 1, \pm 2, \dots, \pm(M-1) \quad (8.4.25)$$

where  $b$  denotes the noise-free received level and  $2d$  is the distance between any two adjacent received signal levels.

The channel corrupts the signal transmitted through it by the addition of white Gaussian noise with zero-mean and power-spectral density  $N_0/2$ .

We assume that a symbol error is committed whenever the magnitude of the additive noise exceeds the distance  $d$ . This assumption neglects the rare event that a large noise component with magnitude exceeding  $d$  may result in a received signal level that yields a correct symbol decision. The noise component  $v_m$  is zero-mean, Gaussian with variance

$$\begin{aligned} \sigma_v^2 &= \frac{N_0}{2} \int_{-W}^W |G_R(f)|^2 df \\ &= \frac{N_0}{2} \int_{-W}^W |X(f)| df = 2N_0/\pi \end{aligned} \quad (8.4.26)$$

for both the duobinary and the modified duobinary signals. Hence, an upper bound on the symbol probability of error is

$$\begin{aligned} P_M &< \sum_{m=-(M-2)}^{M-2} P(|y - 2md| > d \mid b = 2md) P(b = 2md) \\ &\quad + 2P(y + 2(M-1)d > d \mid b = -2(M-1)d) P(b = -2(M-1)d) \\ &= P(|y| > d \mid b = 0) \left[ 2 \sum_{m=0}^{M-1} P(b = 2md) - P(b = 0) - P(b = -2(M-1)d) \right] \\ &= \left( 1 - \frac{1}{M^2} \right) P(|y| > d \mid b = 0) \end{aligned} \quad (8.4.27)$$

But

$$\begin{aligned} P(|y| > d | b = 0) &= \frac{2}{\sqrt{2\pi}\sigma_v} \int_d^\infty e^{-x^2/2\sigma_v^2} dx \\ &= 2Q\left(\sqrt{\frac{\pi d^2}{2N_0}}\right) \end{aligned} \quad (8.4.28)$$

Therefore, the average probability of a symbol error is upper-bounded as

$$P_M < 2\left(1 - \frac{1}{M^2}\right) Q\left(\sqrt{\frac{\pi d^2}{2N_0}}\right) \quad (8.4.29)$$

The scale factor  $d$  in Equation (8.4.29) can be eliminated by expressing  $d$  in terms of the average power transmitted into the channel. For the  $M$ -ary PAM signal in which the transmitted levels are equally probable, the average power at the output of the transmitting filter is

$$\begin{aligned} P_{av} &= \frac{E(a_m^2)}{T} \int_{-W}^W |G_T(f)|^2 df \\ &= \frac{E(a_m^2)}{T} \int_{-W}^W |X(f)| df = \frac{4}{\pi T} E(a_m^2) \end{aligned} \quad (8.4.30)$$

where  $E(a_m^2)$  is the mean square value of the  $M$  signal levels, which is

$$E(a_m^2) = \frac{d^2(M^2 - 1)}{3} \quad (8.4.31)$$

Therefore,

$$d^2 = \frac{3\pi P_{av}T}{4(M^2 - 1)} \quad (8.4.32)$$

By substituting the value of  $d^2$  from Equation (8.4.32) into Equation (8.4.29), we obtain the upper-bound for the symbol error probability as

$$P_M < 2\left(1 - \frac{1}{M^2}\right) Q\left(\sqrt{\left(\frac{\pi}{4}\right)^2 \frac{6}{M^2 - 1} \frac{\mathcal{E}_{av}}{N_0}}\right) \quad (8.4.33)$$

where  $\mathcal{E}_{av}$  is the average energy/transmitted symbol, which can be also expressed in terms of the average bit energy as  $\mathcal{E}_{av} = k\mathcal{E}_{bav} = (\log_2 M)\mathcal{E}_{bav}$ .

The expression in Equation (8.4.33) for the probability of error of  $M$ -ary PAM holds for both a duobinary and a modified duobinary partial response signal. If we compare this result with the error probability of  $M$ -ary PAM with zero ISI, which can be obtained by using a signal pulse with a raised cosine spectrum, we note that the performance of partial response duobinary or modified duobinary has a loss of

$(\pi/4)^2$  or 2.1 dB. This loss in SNR is due to the fact that the detector for the partial response signals makes decisions on a symbol-by-symbol basis, thus, ignoring the inherent memory contained in the received signal at the input to the detector.

To observe the memory in the received sequence, let us look at the noise-free received sequence for binary transmission given in Table 8.1. The sequence  $\{b_m\}$  is 0, -2, 0, 2, 0, -2, 0, 2, 2, . . . . We note that it is not possible to have a transition from -2 to +2 or from +2 to -2 in one symbol interval. For example, if the signal level at the input to the detector is -2, the next signal level can be either -2 or 0. Similarly, if the signal level at a given sampling instant is 2, the signal level in the following time instant can be either 2 or 0. In other words, it is not possible to encounter a transition from -2 to 2 or vice versa between two successive received samples from the matched filter. However, a symbol-by-symbol detector does not exploit this constraint or inherent memory in the received sequence. In Section 8.5.3, we derive the performance of the ML sequence detector that exploits the inherent memory in the modulation and, consequently, regains a large part of the 2.1-dB loss suffered by the symbol-by-symbol detector.

## 8.5 DIGITALLY MODULATED SIGNALS WITH MEMORY

In our treatment of signal design for bandlimited channels in Section 8.3, we observed that we can shape the spectrum of the transmitted signal by introducing memory in the modulation. The two examples cited in that section are the duobinary and modified duobinary partial response signals. In essence, the spectrum shaping obtained with these partial response signals may be viewed as resulting from the memory introduced in the transmitted sequence of symbols; i.e., the sequence of symbols are correlated and, as a consequence, the power spectrum of the transmitted symbol sequence is colored (nonwhite).

Signal dependence among signals transmitted in different signal intervals is generally accomplished by encoding the data at the input to the modulator by means of a *modulation code*. Such a code generally places restrictions on the sequence of symbols into the modulator and, thus, introduces memory in the transmitted signal. In this section, we consider modulation signals with memory and characterize them in terms of their spectral characteristics and their performance in an additive white Gaussian noise channel. We confine our treatment to baseband signals. The generalization to bandpass signals is relatively straightforward, as we have already observed in our treatment of the spectral characteristics of digitally modulated signals.

Signal dependence among signals transmitted in different signal intervals can also result from intersymbol interference introduced by channel distortion. The memory imposed by the channel on the received signals requires that the detector at the receiver must be designed to estimate the received information symbols by observing and processing the received signal over a time duration that encompasses the channel memory. Signal detectors that function in this manner are generally called equalizers and are treated in Section 8.6.

### 8.5.1 Modulation Codes and Modulation Signals with Memory

Modulation codes are usually employed in magnetic recording, in optical recording, and in digital communications over cable systems to achieve spectral shaping of the modulated signal that matches the passband characteristics of the channel. Let us consider magnetic recording as an example.

In magnetic recording, we encounter two basic problems. One problem is concerned with the packing density that is used to write the data on the magnetic medium (disk or tape). Of course, we would like to write as many bits as possible on a single track. However, there is a limit as to how close successive bits in a sequence are stored, and this limit is imposed by the medium. Let us explore this problem further.

Figure 8.15 illustrates a block diagram of the magnetic recording system. The binary data sequence to be stored is used to generate a write current. This current may be viewed as the output of the “modulator.” The two most commonly used methods to map the data sequence into the write current waveform are the so-called NRZ (non-return-to-zero) and NRZI (non-return-to-zero-inverse) methods. These two waveforms are illustrated in Figure 8.16. We note that NRZ is identical to binary PAM in which the information bit 1 is represented by a rectangular pulse of amplitude  $A$  and the information bit 0 is represented by a rectangular pulse of amplitude  $-A$ . In contrast, the NRZI signal waveform is different from NRZ in that transitions from one amplitude level to another ( $A$  to  $-A$  or  $-A$  to  $A$ ), occur only when the information bit is a 1. No transition occurs when the information bit is a 0; i.e., the amplitude level remains the same as the previous signal level. The positive amplitude pulse results in magnetizing the medium on one (direction) polarity and the negative pulse magnetizes the medium in the opposite (direction) polarity.

Since the input data sequence is basically random with equally probable 1's and 0's, whether we use NRZ or NRZI, we will encounter level transitions for  $A$  to  $-A$  or  $-A$  to  $A$  with probability  $1/2$  for every data bit. The readback signal for a positive transition ( $-A$  to  $A$ ) is a pulse that is well modeled mathematically as

$$p(t) = \frac{1}{1 + (2t/T_{50})^2} \quad (8.5.1)$$

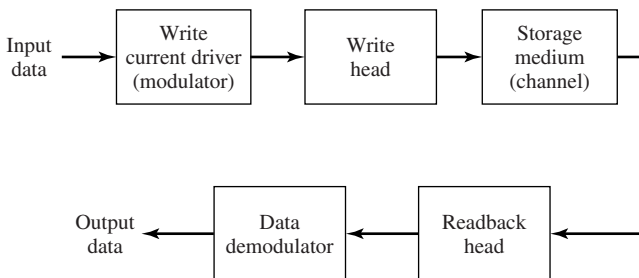


Figure 8.15 Block diagram of magnetic storage read/write system.

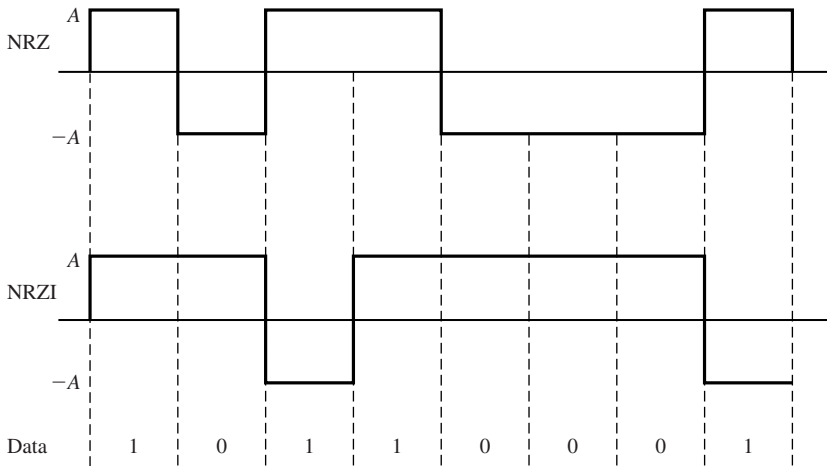


Figure 8.16 NRZ and NRZI signals.

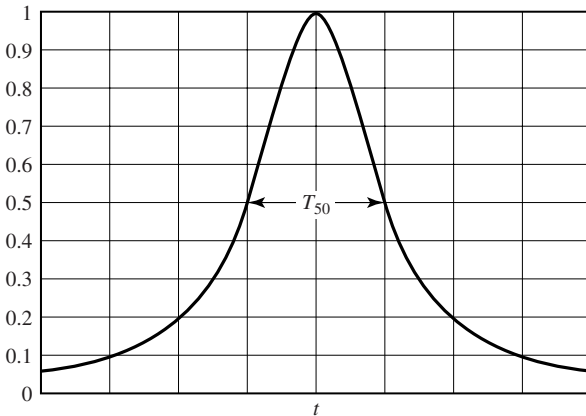
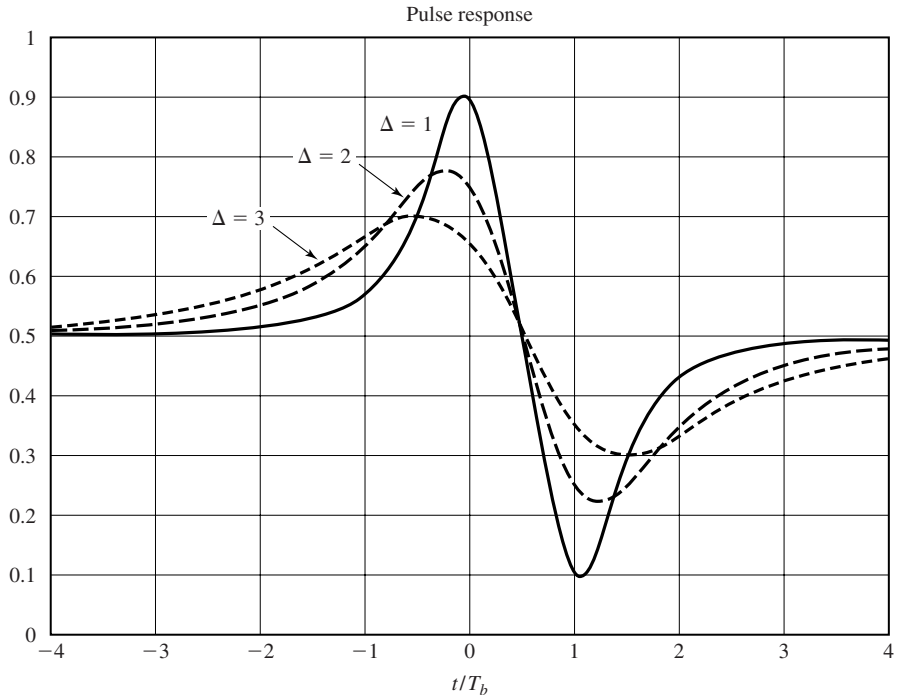


Figure 8.17 Readback pulse in magnetic recording system.

where  $T_{50}$  is defined as the width of the pulse at its 50% amplitude level, as shown in Figure 8.17. Similarly, the readback signal for a negative transition ( $A$  to  $-A$ ) is the pulse  $-p(t)$ . The value of  $T_{50}$  is determined by the characteristics of the medium and the read/write heads.

Now, suppose we write a positive transition followed by a negative transition, and let us vary the time interval between the two transitions, which we denote as  $T_b$  (the bit time interval). Figure 8.18 illustrates the readback signal pulses, which are obtained by a superposition of  $p(t)$  with  $-p(t - T_b)$ . The parameter,  $\Delta = T_{50}/T_b$ , is defined as the *normalized density*. The closer the bit transitions ( $T_b$  small), the larger will be the value of the normalized density and, hence, the larger will be the packing density. We notice that as  $\Delta$  is increased, the peak amplitudes of the readback signal



**Figure 8.18** Readback signal response to a pulse.

are reduced and are also shifted in time from the desired time instants. In other words, the pulses interfere with one another, thus, limiting the density with which we can write. This problem serves as a motivation to design modulation codes that take the original data sequence and transform (encode) it into another sequence that results in a write waveform in which amplitude transitions are spaced further apart. For example, if we use NRZI, the encoded sequence into the modulator must contain one or more 0's between 1's.

The second problem encountered in magnetic recording is the need to avoid (or minimize) having a dc content in the modulated signal (the write current), due to the frequency-response characteristics of the readback system and associated electronics. This requirement also arises in digital communication over cable channels. This problem can also be overcome by altering (encoding) the data sequence into the modulator. A class of codes that satisfy these objectives are the modulation codes described below.

**Runlength-Limited Codes.** Codes that have a restriction on the number of consecutive 1's or 0's in a sequence are generally called *runlength-limited codes*. These codes are generally described by two parameters, say  $d$  and  $\kappa$ , where  $d$  denotes the minimum number of 0's between 1's in a sequence, and  $\kappa$  denotes the maximum number of 0's between two 1's in a sequence. When used with NRZI modulation, the effect of

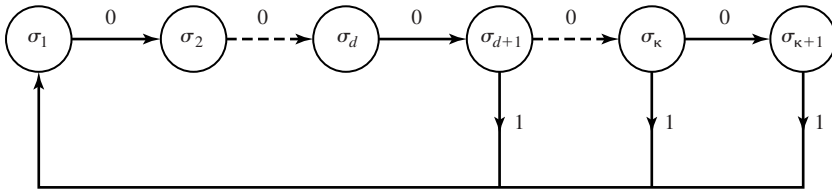


**Figure 8.19** Finite-state sequential machine for a  $(d, \kappa)$ -coded sequence.

placing  $d$  zeros between successive 1's is to spread the transitions farther apart, thus, reducing the overlap in the channel response due to successive transitions. By setting an upper limit  $\kappa$  on the runlength of 0's ensures that transitions occur frequently enough so that symbol timing information can be recovered from the received modulated signal. Runlength-limited codes are usually called  $(d, \kappa)$  codes.<sup>†</sup>

The  $(d, \kappa)$ -code sequence constraints may be represented by a finite-state sequential machine with  $\kappa + 1$  states, denoted as  $\sigma_i$ ,  $1 \leq i \leq \kappa + 1$ , as shown in Figure 8.19. We observe that an output data bit 0 takes the sequence from state  $\sigma_i$  to  $\sigma_{i+1}$ ,  $i \leq \kappa$ . The output data bit 1 takes the sequence to state  $\sigma_1$ . The output bit from the encoder may be a 1 only when the sequence is in state  $\sigma_i$ ,  $d + 1 \leq i \leq \kappa + 1$ . When the sequence is in state  $\sigma_{\kappa+1}$ , the output bit is always 1.

The finite-state sequential machine may also be represented by a *state transition matrix*, denoted as  $\mathbf{D}$ , which is a square  $(\kappa + 1) \times (\kappa + 1)$  matrix with elements  $d_{ij}$ , where

$$\begin{aligned} d_{i1} &= 1, & i &\geq d + 1 \\ d_{ij} &= 1, & j &= i + 1 \\ d_{ij} &= 0, & &\text{otherwise} \end{aligned} \quad (8.5.2)$$

### Example 8.5.1

Determine the state transition matrix for a  $(d, \kappa) = (1, 3)$  code.

**Solution** The  $(1, 3)$  code has four states. From Figure 8.19 we obtain its state transition matrix which is

$$\mathbf{D} = \begin{bmatrix} 0 & 1 & 0 & 0 \\ 1 & 0 & 1 & 0 \\ 1 & 0 & 0 & 1 \\ 1 & 0 & 0 & 0 \end{bmatrix} \quad (8.5.3)$$

An important parameter of any  $(d, \kappa)$  code is the number of sequences of a certain length, say  $n$ , which satisfy the  $(d, \kappa)$  constraints. As  $n$  is allowed to increase, the number of sequences  $N(n)$  which satisfy the  $(d, \kappa)$  constraint also increases. The number of information bits that can be uniquely represented with  $N(n)$  code sequences is

$$k = \lfloor \log_2 N(n) \rfloor$$

<sup>†</sup>Runlength-limited codes are usually called  $(d, k)$  codes, where  $k$  is the maximum runlength of zeros. We have substituted the Greek letter  $\kappa$  for  $k$ , to avoid confusion with our previous use of  $k$ .

where  $\lfloor x \rfloor$  denotes the largest integer contained in  $x$ . The maximum code rate is then  $R_c = k/n$ .

The capacity of a  $(d, \kappa)$  code is defined as

$$C(d, \kappa) = \lim_{n \rightarrow \infty} \frac{1}{n} \log_2 N(n) \quad (8.5.4)$$

Clearly,  $C(d, \kappa)$  is the maximum possible rate that can be achieved with the  $(d, \kappa)$  constraints. Shannon (1948) showed that the capacity is given as

$$C(d, \kappa) = \log_2 \lambda_{\max} \quad (8.5.5)$$

where  $\lambda_{\max}$  is the largest real eigenvalue of the state transition matrix  $\mathbf{D}$ .

### Example 8.5.2

Determine the capacity of a  $(d, \kappa) = (1, 3)$  code.

**Solution** Using the state-transition matrix given in Example 8.5.1 for the  $(1, 3)$  code, we have

$$\begin{aligned} \det(\mathbf{D} - \lambda \mathbf{I}) &= \det \begin{bmatrix} -\lambda & 1 & 0 & 0 \\ 1 & -\lambda & 1 & 0 \\ 1 & 0 & -\lambda & 1 \\ 1 & 0 & 0 & -\lambda \end{bmatrix} \\ &= \lambda^4 - \lambda^2 - \lambda - 1 = 0 \end{aligned} \quad (8.5.6)$$

The maximum real root of this polynomial is found to be  $\lambda_{\max} = 1.4656$ . Therefore, the capacity  $C(1, 3) = \log_2 \lambda_{\max} = 0.5515$ .

The capacities of  $(d, \kappa)$  codes for  $0 \leq d \leq 6$  and  $2 \leq k \leq 15$ , are given in Table 8.3. We observe that  $C(d, \kappa) < 1/2$  for  $d \geq 3$ , and any value of  $\kappa$ . The most commonly used codes for magnetic recording employ a  $d \leq 2$ , hence, their rate  $R_c$  is at least  $1/2$ .

**TABLE 8.3** CAPACITY  $C(d, \kappa)$  VERSUS RUNLENGTH PARAMETERS  $d$  AND  $\kappa$

$k$	$d = 0$	$d = 1$	$d = 2$	$d = 3$	$d = 4$	$d = 5$	$d = 6$
2	.8791	.4057					
3	.9468	.5515	.2878				
4	.9752	.6174	.4057	.2232			
5	.9881	.6509	.4650	.3218	.1823		
6	.9942	.6690	.4979	.3746	.2269	.1542	
7	.9971	.6793	.5174	.4057	.3142	.2281	.1335
8	.9986	.6853	.5293	.4251	.3432	.2709	.1993
9	.9993	.6888	.5369	.4376	.3620	.2979	.2382
10	.9996	.6909	.5418	.4460	.3746	.3158	.2633
11	.9998	.6922	.5450	.4516	.3833	.3285	.2804
12	.9999	.6930	.5471	.4555	.3894	.3369	.2924
12	.9999	.6935	.5485	.4583	.3937	.3432	.3011
14	.9999	.6938	.5495	.4602	.3968	.3478	.3074
15	.9999	.6939	.5501	.4615	.3991	.3513	.3122
$\infty$	1.000	.6942	.5515	.4650	.4057	.3620	.3282

Now, let us turn our attention to the construction of some runlength-limited codes. In general,  $(d, \kappa)$  codes can be constructed either as fixed-length codes or variable-length codes. In a fixed-length code, each bit or block of  $k$  bits, is encoded into a block of  $n > k$  bits.

In principle, the construction of a fixed-length code is straightforward. For a given block length  $n$ , we may select the subset of the  $2^n$  codewords that satisfy the specified runlength constraints. From this subset, we eliminate codewords that do not satisfy the runlength constraints when concatenated. Thus, we obtain a set of codewords that satisfies the constraints and can be used in the mapping of the input data bits to the encoder. The encoding and decoding operations can be performed by use of a look-up table.

### Example 8.5.3

Construct a  $d = 0, \kappa = 2$  code of length  $n = 3$ , and determine its efficiency.

**Solution** By listing all the codewords, we find that the following five codewords satisfy the  $(0, 2)$  constraint:  $(0\ 1\ 0)$ ,  $(0\ 1\ 1)$ ,  $(1\ 0\ 1)$ ,  $(1\ 1\ 0)$ ,  $(1\ 1\ 1)$ . We may select any four of these codewords and use them to encode the pairs of data bits  $(00, 01, 10, 11)$ . Thus, we have a rate  $k/n = 2/3$  code that satisfies the  $(0, 2)$  constraint.

The fixed-length code in this example is not very efficient. The capacity of a  $(0, 2)$  code is  $C(0, 2) = 0.8791$ , so that this code has an *efficiency* of

$$\text{efficiency} = \frac{R_c}{C(d, \kappa)} = \frac{2/3}{0.8791} = 0.76$$

Surely, better  $(0, 2)$  codes can be constructed by increasing the block length  $n$ .

In the following example, we place no restriction on the maximum runlength zeros.

### Example 8.5.4

Construct a  $d = 1, \kappa = \infty$  code of length  $n = 5$ .

**Solution** In this case, we are placing no constraint on the number of consecutive zeros. To construct the code we select from the set of 32 possible codewords, the ones that satisfy the  $d = 1$  constraint. There are eight such codewords, which implies that we can encode three information bits with each codeword. The code is given in Table 8.4. Note that the first bit of each codeword is a 0, whereas the last bit may be either 0 or 1. Consequently, the  $d = 1$  constraint is satisfied when these codewords are concatenated. This code has

**TABLE 8.4** FIXED LENGTH  $d = 1, \kappa = \infty$  CODE

Input data bits	Output coded sequence
000	00000
001	00001
010	00010
011	00100
100	00101
101	01000
110	01001
111	01010

a rate  $R_c = 3/5$ . When compared with the capacity  $C(1, \infty) = 0.6942$ , obtained from Table 8.3, the code efficiency is 0.864, which is quite acceptable.

The code construction method described in the two examples above produces fixed-length  $(d, \kappa)$  codes that are *state independent*. By “state independent,” we mean that fixed-length codewords can be concatenated without violating the  $(d, \kappa)$  constraints. In general, fixed-length, state-independent  $(d, \kappa)$  codes require large block lengths, except in cases such as those in the examples above, where  $d$  is small. Simpler (shorter-length) codes are generally possible by allowing for state-dependence and for variable-length codewords. Next, we consider codes for which both input blocks to the encoder and the output blocks may have variable length. In order for the codewords to be uniquely decodable at the receiver, the variable-length code should satisfy the prefix condition, previously described in Chapter 6.

### Example 8.5.5

Construct a simple variable-length  $d = 0, \kappa = 2$  code.

**Solution** A very simple uniquely decodable  $(0, 2)$  code is the following:

$$\begin{aligned} 0 &\rightarrow 01 \\ 10 &\rightarrow 10 \\ 11 &\rightarrow 11 \end{aligned}$$

The code in the above example has a fixed output block size but a variable input block size. In general, both the input and output blocks may be variable. The following example illustrates the latter case.

### Example 8.5.6

Construct a  $(2, 7)$  variable block size code.

**Solution** The solution to this code construction is certainly not unique nor is it trivial. We picked this example because the  $(2, 7)$  code has been widely used by IBM in many of its disk storage systems. The code is listed in Table 8.5. We observe that the input data blocks of 2, 3, and 4 bits are mapped into output data blocks of 4, 6, and 8 bits, respectively. Hence, the code rate is  $R_c = 1/2$ . Since this is the code rate for all codewords, the code is called a *fixed-rate* code. This code has an efficiency of  $0.5/0.5174 = 0.966$ . Note that this code satisfies the prefix condition.

**TABLE 8.5** CODE BOOK FOR VARIABLE-LENGTH (2,7) CODE

Input data bits	Output coded sequence
10	1000
11	0100
011	000100
010	001000
000	100100
0011	00100100
0010	00001000

**TABLE 8.6** ENCODER FOR (1, 3)  
MILLER CODE

Input data bits	Output coded sequence
0	$x0$
1	01

Another code that has been widely used in magnetic recording is the rate  $1/2$ ,  $(d, \kappa) = (1, 3)$  code given in Table 8.6. We observe that when the information bit is a 0, the first output bit is either 1, if the previous input bit was 0, or a 0, if the previous input bit was a 1. When the information bit is a 1, the encoder output is 01. Decoding of this code is simple. The first bit of the two-bit block is redundant and may be discarded. The second bit is the information bit. This code is usually called the *Miller code*. We observe that this is a state-dependent code which is described by the state diagram shown in Figure 8.20. There are two states labeled  $S_1$  and  $S_2$  with transitions as shown in the figure. When the encoder is in a state  $S_1$ , an input bit 1 results in the encoder staying in state  $S_1$  and outputs 01. This is denoted as 1/01. If the input bit is a 0 the encoder enters state  $S_2$  and outputs 00. This is denoted as 0/00. Similarly, if the encoder is in state  $S_2$ , an input bit 0 causes no transition and the encoder output is 10. On the other hand, if the input bit is a 1, the encoder enters state  $S_1$  and outputs 01.

**Trellis Representation of State-Dependent  $(d, \kappa)$  Codes.** The state diagram provides a relatively compact representation of a state-dependent code. Another way to describe such codes that have memory is by means of a graph called a *trellis*. A trellis is a graph that illustrates the state transitions as a function of time. It consists of a set of nodes representing the states that characterize the memory in the code at different instants in time and interconnections between pairs of nodes that indicate the transitions between successive instants of time. For example, Figure 8.21 shows the trellis for the  $d = 1, \kappa = 3$  Miller code whose state diagram is shown in Figure 8.20.

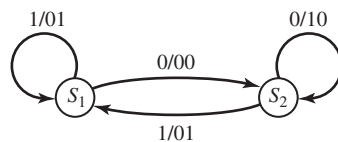


**Figure 8.20** State diagrams for  $d = 1$ ,  $\kappa = 3$  (Miller) code.

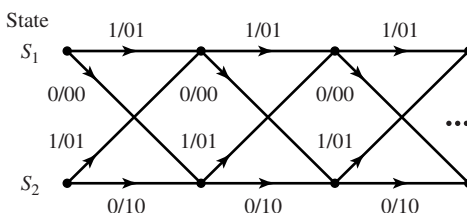


**Figure 8.21** Trellis for  $d = 1, \kappa = 3$  (Miller) code.

**The Mapping of Coded Bits Into Signal Waveforms.** The output sequence from a  $(d, \kappa)$  encoder is mapped by the modulator into signal waveforms for transmission over the channel. If the binary digit 1 is mapped into a rectangular pulse of amplitude  $A$  and the binary digit 0 is mapped into a rectangular pulse of amplitude  $-A$ , the result is a  $(d, \kappa)$ -coded NRZ modulated signal. We note that the duration of the rectangular pulses is  $T_c = R_c/R_b = R_c T_b$ , where  $R_b$  is the information (bit) rate into the encoder,  $T_b$  is the corresponding (uncoded) bit interval, and  $R_c$  is the code rate for the  $(d, \kappa)$  code.

When the  $(d, \kappa)$  code is a state-independent fixed-length code with code rate  $R_c = k/n$ , we may consider each  $n$ -bit block as generating one signal waveform of duration  $nT_c$ . Thus, we have  $M = 2^k$  signal waveforms, one for each of the  $2^k$  possible  $k$ -bit data blocks. These coded waveforms have the general form given by Equations (7.4.22) and (7.4.23). In this case, there is no dependence between the transmission of successive waveforms.

In contrast to the situation considered above, where the  $(d, \kappa)$  code is state independent and NRZ modulation is used for transmission of the coded bits, the modulation signal is no longer memoryless when NRZI is used and, or, the  $(d, \kappa)$  code is state dependent. Let us first consider the effect of mapping the coded bits into an NRZI signal waveform.

An NRZI modulated signal is itself state dependent. The signal-amplitude level is changed from its current value ( $\pm A$ ) only when the bit to be transmitted is a 1. It is interesting to note that the NRZI signal may be viewed as an NRZ signal preceded by another encoding operation, called *precoding*, of the binary sequence, as shown in Figure 8.22. The precoding operation is described mathematically by the relation

$$p_k = d_k \oplus p_{k-1}$$

where  $\{d_k\}$  is the binary sequence into the precoder,  $\{p_k\}$  is the output binary sequence from the precoder, and  $\oplus$  denotes modulo-2 addition. This type of encoding is called *differential encoding*, and is characterized by the state diagram shown in Figure 8.23(a). Then, the sequence  $\{p_k\}$  is transmitted by NRZ. Thus, when  $p_k = 1$ , the modulator output is a rectangular pulse of amplitude  $A$  and when  $p_k = 0$ , the modulator output is a rectangular pulse of amplitude  $-A$ . When the signal waveforms are superimposed on the state diagram of Figure 8.23(a), we obtain the corresponding state diagram shown in Figure 8.23(b).

It is apparent from the state diagram that differential encoding or precoding as described above introduces memory in the modulated signal. As in the case of state-dependent  $(d, \kappa)$  codes, a trellis diagram may be used to illustrate the time dependence of the modulated signal. The trellis diagram for the NRZI signal is shown in Figure 8.24. When the output of a state-dependent  $(d, \kappa)$  encoder is followed by an NRZI modulator, we may simply combine the two state diagrams into a single state diagram for the  $(d, \kappa)$

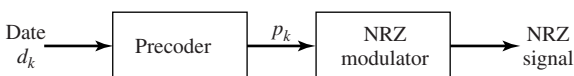


**Figure 8.22** Method for generating an NRZI signal using precoding.

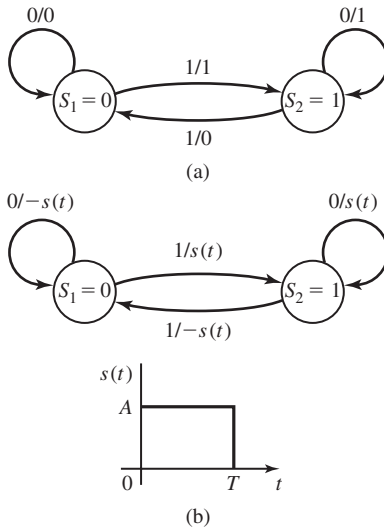


**Figure 8.23** State diagram for NRZI signal.

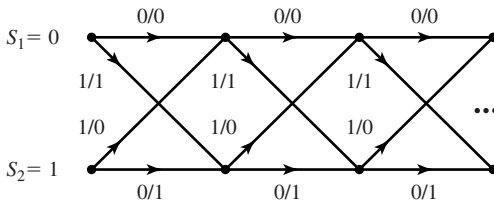


**Figure 8.24** The trellis for an NRZI signal.

code with precoding. A similar combination can be performed with the corresponding trellises. The following example illustrates the approach for the (1, 3) Miller code followed by NRZI modulation.

**Example 8.5.7**

Determine the state diagram of the combined (1, 3) Miller code followed by the precoding inherent in NRZI modulation.

**Solution** Since the (1, 3) Miller code has two states and the precoder has two states, the state diagram for the combined encoder has four states, which we denote as  $(S_M, S_N) = (\sigma_1, s_1), (\sigma_1, s_2), (\sigma_2, s_1), (\sigma_2, s_2)$ , where  $S_M = \{\sigma_1, \sigma_2\}$  represents the two states of the Miller code and  $S_N = \{s_1, s_2\}$  represents the two states of the precoder for NRZI. For each data input bit into the Miller encoder we obtain two output bits which are then precoded to yield two precoded output bits. The resulting state diagram is shown in Figure 8.25, where the first bit denotes the information bit into the Miller encoder and the next two bits represent the corresponding output of the precoder.

The trellis diagram for the Miller precoded sequence may be obtained directly from the combined state diagram or from a combination of the trellises of the two codes. The result of this combination is the four-state trellis, one stage of which is shown in Figure 8.26.

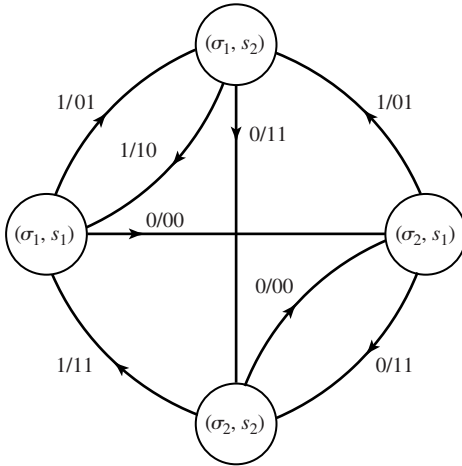


**Figure 8.25** State diagram of the Miller code followed by the precoder.

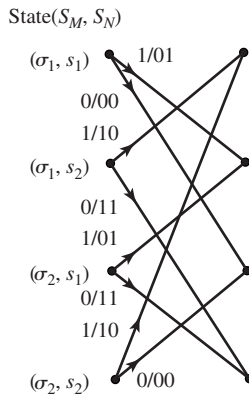


**Figure 8.26** One stage of trellis diagram for the Miller code followed by the precoder.

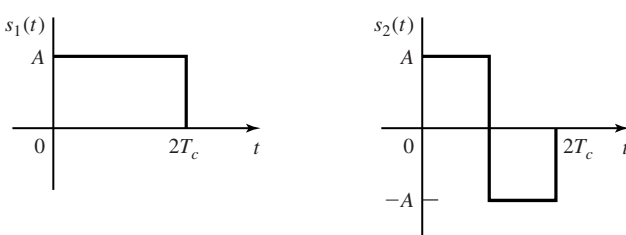


**Figure 8.27** Signal waveforms for Miller-precoded pairs of bits.

It is interesting to note that the four signal waveforms obtained by mapping each pair of bits of the Miller-precoded sequence into an NRZ signal are biorthogonal. In particular, the pair of bits 11 map into the waveform  $s_1(t)$  and the bits 01 map into the waveform  $s_2(t)$ , shown in Figure 8.27. Then, the encoded bits 00 map into  $-s_1(t)$  and the bits 10 map into  $-s_2(t)$ . Since  $s_1(t)$  and  $s_2(t)$  are orthogonal, the set of four

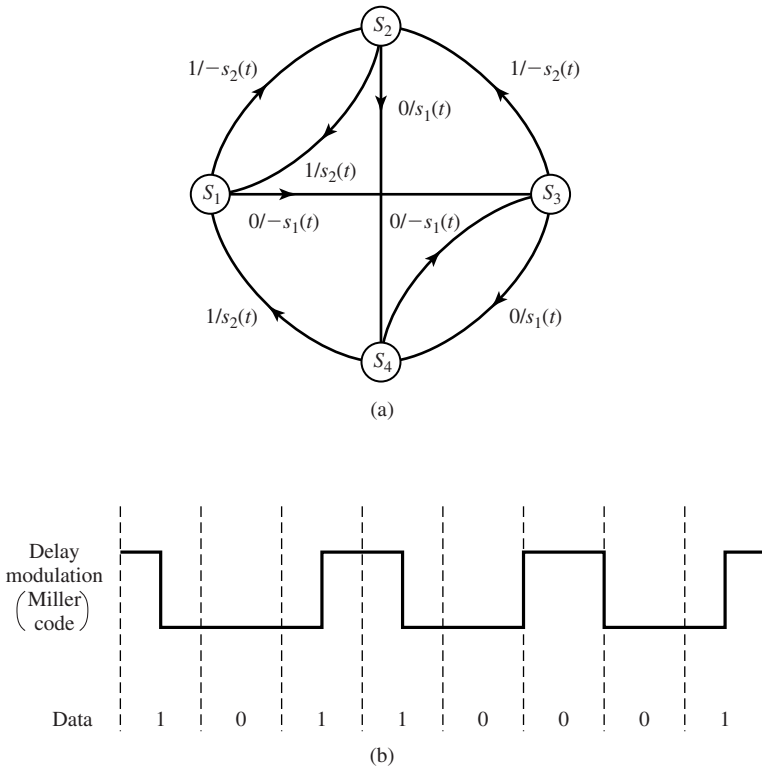


**Figure 8.28** State diagram for the Miller-precoded signal and sample waveform.

diagram for the Miller-precoded sequence we may substitute the signal waveforms from the modulator in place of the encoder output bits. This state diagram is illustrated in Figure 8.28, where the four states are simply designated as  $S_i, 1 \leq i \leq 4$ . The resulting modulated signal has also been called *delay modulation*.

Modulated signals with memory such as NRZI and Miller coded/NRZI (delay modulation) are generally characterized by a  $K$ -state Markov chain with *stationary state probabilities*  $\{p_i, i = 1, 2, \dots, K\}$ . Associated with each transition is a signal waveform  $s_j(t), j = 1, 2, \dots, K$ . Thus, the transition probability  $p_{ij}$  denotes the probability that signal waveform  $s_j(t)$  is transmitted in a given signaling interval after the transmission of the signal waveform  $s_i(t)$  in the previous signaling interval. The transition probabilities may be arranged in matrix form as

$$\mathbf{P} = \begin{bmatrix} p_{11} & p_{12} & \dots & p_{1K} \\ p_{21} & p_{22} & \dots & p_{2K} \\ \vdots & \vdots & \ddots & \vdots \\ p_{K1} & p_{K2} & \dots & p_{KK} \end{bmatrix} \quad (8.5.7)$$

where  $\mathbf{P}$  is the *transition probability matrix*. The transition probability matrix is easily obtained from the state diagram and the corresponding probabilities of occurrence of the input bits (or, equivalently, the stationary state probabilities  $\{p_i\}$ ).

For the NRZI signal with equal state probabilities  $p_1 = p_2 = 1/2$  and state diagram shown in Figure 8.23, the transition probability matrix is

$$\mathbf{P} = \begin{bmatrix} \frac{1}{2} & \frac{1}{2} \\ \frac{1}{2} & \frac{1}{2} \end{bmatrix} \quad (8.5.8)$$

Similarly, the transition probability matrix for the Miller-coded NRZI modulated signal with equally likely symbols ( $p_1 = p_2 = p_3 = p_4 = 1/4$ ) is

$$\mathbf{P} = \begin{bmatrix} 0 & \frac{1}{2} & 0 & \frac{1}{2} \\ 0 & 0 & \frac{1}{2} & \frac{1}{2} \\ \frac{1}{2} & \frac{1}{2} & 0 & 0 \\ \frac{1}{2} & 0 & \frac{1}{2} & 0 \end{bmatrix} \quad (8.5.9)$$

As we shall see later, in Section 8.5.4, the transition probability matrix is useful in determining the power-spectral density of a modulated signal with memory.

**Modulation Code for the Compact Disc System.** In the design of a modulation code for the compact disc system, several factors had to be considered. One constraint is that the maximum runlength of zeros must be sufficiently small to allow the system to synchronize from the readback signal. To satisfy this constraint,  $\kappa = 10$  was chosen. A second factor is the frequency content of the modulated signal below 20 kHz. In a CD system, the servo-control systems that keep the laser beam on a specified track and the focusing circuits are controlled by signals in the frequency range 0–20 kHz. To avoid interference with these control signals, the modulated information signal must fall above this frequency range. The runlength-limited code that was implemented for this purpose is a  $(d, \kappa) = (2, 10)$  code that results in a coded information-bearing signal that occupies the frequency range 20 kHz to 1.5 MHz.

The  $d = 2, \kappa = 10$  code selected is a fixed-length code that encodes eight information bits into 14 coded bits and is called EFM (eight-to-fourteen modulation). Since each audio signal sample is quantized to 16 bits, a 16-bit sample is divided into two 8-bit bytes and encoded. By enumerating all the 14-bit codewords, one can show that there are 267 distinct codewords that satisfy the  $(d, \kappa)$  constraints. Of these, 256 codewords are selected to form the code. However, the  $(d, \kappa)$  constraints are not satisfied when the codewords are concatenated (merged in a sequence). To remedy this problem, three additional bits are added to the 14, called “merging” bits. The three merging bits serve two purposes. First of all, if the  $d$ -constraint is not satisfied in concatenation, we choose 0’s for the merging bits. On the other hand, if the  $\kappa$ -constraint is being violated due to concatenation, we select one of the bits as 1. Since two bits are sufficient to accomplish these goals, the third merging bit may be viewed as an added

degree of freedom. This added degree of freedom allows us to use the merging bits to minimize the low-frequency content of the modulated signal. Since the merging bits carry no audio signal information, they are discarded in the readback process prior to decoding.

A measure of the low-frequency content of a digital modulated signal is the *running digital sum* (RDS), which is the difference between the total zeros and the total ones in the coded sequence accumulated from the beginning of the disc. In addition to satisfying the  $(d, \kappa)$  constraints, the three merging bits are selected so as to bring the RDS as close to zero as possible. Thus, the three merging bits are instrumental in reducing the low-frequency content below 20 kHz by an additional factor of 10 (in power).

In addition to the coded information bits and merging bits, additional bits are added for control and display (C & D), synchronization bits, and parity bits. The data bits, control bits, parity bits, and synchronization bits are arranged in a frame structure, consisting of 588 bits/frame. The frame structure is illustrated in Figure 8.29.

### 8.5.2 The Maximum-Likelihood Sequence Detector

When the signal has no memory, the symbol-by-symbol detector described in Section 7.5 is optimum in the sense of minimizing the probability of a symbol error. On the other hand, when the transmitted signal has memory; i.e., the signals transmitted in successive symbol intervals are interdependent, the optimum detector bases its decisions on observation of a sequence of received signals over successive signal intervals.

Consider as an example the NRZI signal described in Section 8.5.1. Its memory is characterized by the trellis shown in Figure 8.24. The signal transmitted in each signal interval is binary PAM. Hence, there are two possible transmitted signals corresponding to the signal points  $s_1 = -s_2 = \sqrt{\mathcal{E}_b}$ , where  $\mathcal{E}_b$  is the energy/bit. As shown in Section 7.5, the output of the matched-filter or correlation-type demodulator for binary PAM in the  $k$ th signal interval may be expressed as

$$r_k = \pm\sqrt{\mathcal{E}_b} + n_k \quad (8.5.10)$$

where  $n_k$  is a zero-mean Gaussian random variable with variance  $\sigma_n^2 = N_0/2$ . Consequently, the conditional PDFs for the two possible transmitted signals are

$$\begin{aligned} f(r_k | s_1) &= \frac{1}{\sqrt{2\pi}\sigma_n} e^{-(r_k - \sqrt{\mathcal{E}_b})^2/2\sigma_n^2} \\ f(r_k | s_2) &= \frac{1}{\sqrt{2\pi}\sigma_n} e^{-(r_k + \sqrt{\mathcal{E}_b})^2/2\sigma_n^2} \end{aligned} \quad (8.5.11)$$

Now, suppose we observe the sequence of matched-filter outputs  $r_1, r_2, \dots, r_K$ . Since the channel noise is assumed to be white and Gaussian, and  $\psi(t - iT)$ ,  $\psi(t - jT)$  for  $i \neq j$  are orthogonal, it follows that  $E(n_k n_j) = 0$ ,  $k \neq j$ . Hence, the noise sequence  $n_1, n_2, \dots, n_k$  is also white. Consequently, for any given transmitted sequence  $\mathbf{s}^{(m)}$ , the

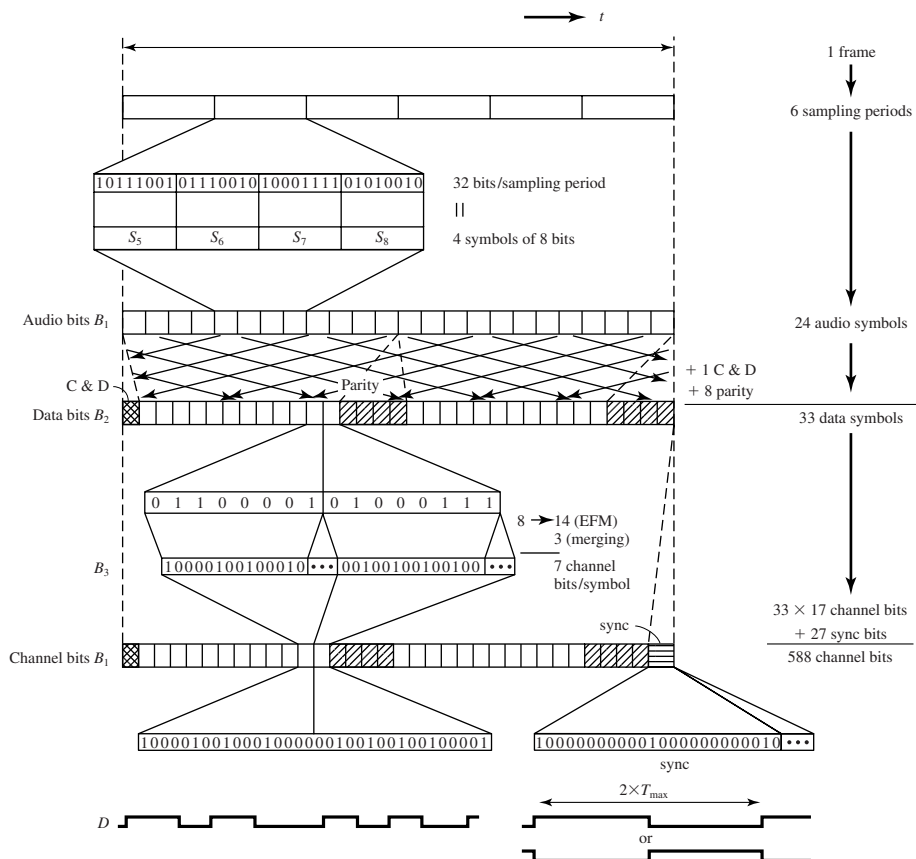


**Figure 8.29** Frame structure of data in a compact disc. The information is divided into frames; the figure gives one frame of the successive bit streams. There are six sampling periods for one frame, each sampling period giving 32 bits (16 for each of the two audio channels). These 32 bits are divided to make four symbols in the “audio bit stream”  $B_1$ . In the “data bit stream,”  $B_2$  eight parity symbols and one C & D symbol have been added to the 24 audio symbols. To scatter possible errors, the symbols of different frames in  $B_1$  are interleaved, so that the audio signals in one frame of  $B_2$  originate from different frames in  $B_1$ . The modulation translated the eight data bits of a symbol of  $B_2$  into fourteen channel bits, to which three ‘merging bits’ are added ( $B_3$ ). The frames are marked with a synchronization signal of the form illustrated (bottom right); the final result is the “channel bit stream” ( $B_1$ ) used for writing on the master disc, in such a way that each 1 indicates a pit edge ( $D$ ). (From paper by Heemskerck and Schouhamer Immink, 1982.)

joint PDF of  $r_1, r_2, \dots, r_K$  may be expressed as a product of  $k$  marginal PDFs; i.e.,

$$\begin{aligned} p(r_1, r_2, \dots, r_K | \mathbf{s}^{(m)}) &= \prod_{k=1}^K p(r_k | s_k^{(m)}) \\ &= \prod_{k=1}^K \frac{1}{\sqrt{2\pi}\sigma_n} e^{-(r_k - s_k^{(m)})^2 / 2\sigma_n^2} \\ &= \left( \frac{1}{\sqrt{2\pi}\sigma_n} \right)^K \exp \left[ - \sum_{k=1}^K (r_k - s_k^{(m)})^2 / 2\sigma_n^2 \right] \end{aligned} \quad (8.5.12)$$

where either  $s_k = \sqrt{\mathcal{E}_b}$  or  $s_k = -\sqrt{\mathcal{E}_b}$ . Then, given the received sequence  $r_1, r_2, \dots, r_K$  at the output of the matched-filter or correlation-type demodulator, the detector determines the sequence  $\mathbf{s}^{(m)} = \{s_1^{(m)}, s_2^{(m)}, \dots, s_K^{(m)}\}$  that maximizes the conditional PDF  $p(r_1, r_2, \dots, r_K | \mathbf{s}^{(m)})$ . Such a detector is called the *maximum-likelihood (ML) sequence detector*.

By taking the logarithm of Equation (8.5.12) and neglecting the terms that are independent of  $(r_1, r_2, \dots, r_K)$  we find that an equivalent ML sequence detector selects the sequence  $\mathbf{s}^{(m)}$  that minimizes the *Euclidean distance metric*

$$D(\mathbf{r}, \mathbf{s}^{(m)}) = \sum_{k=1}^K (r_k - s_k^{(m)})^2 \quad (8.5.13)$$

In searching through the trellis for the sequence that minimizes the Euclidean distance  $D(\mathbf{r}, \mathbf{s}^{(m)})$ , it may appear that we must compute the distance  $D(\mathbf{r}, \mathbf{s}^{(m)})$  for every possible path (sequence). For the NRZI example given above, which employs binary modulation, the total number of paths is  $2^K$ , where  $K$  is the number of outputs obtained from the demodulator. However, this is not the case. We may reduce the number of sequences in the trellis search by using the *Viterbi algorithm* to eliminate sequences as new data is received from the demodulator.

The Viterbi algorithm is a sequential trellis search algorithm for performing ML sequence detection. It is described in more detail in Chapter 9 as a decoding algorithm for channel-coded systems. We describe it below in the context of the NRZI signal. We assume that the search process begins initially at state  $S_1$ . The corresponding trellis is shown in Figure 8.30. At time  $t = T$ , we receive  $r_1 = s_1^{(m)} + n$ , from the demodulator

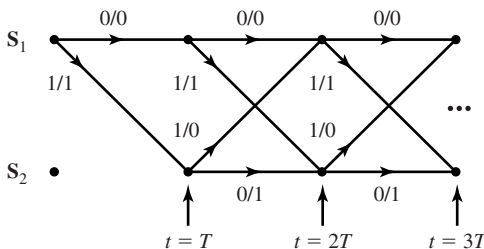


**Figure 8.30** Trellis for NRZI signal with initial state  $S_1$ .

and at  $t = 2T$  we receive  $r_2 = s_2^{(m)} + n_2$ . Since the signal memory is one bit, which we denote as  $L = 1$ , we observe that the trellis reaches its regular (steady-state) form after the first transition. Thus, upon receipt of  $r_2$  at  $t = 2T$  (and thereafter), we observe that there are two signal paths entering each of the two nodes and two signal paths leaving each node. The two paths entering node  $S_1$  at  $t = 2T$  correspond to the information bits  $(0, 0)$  and  $(1, 1)$  or, equivalently, to the signal points  $(-\sqrt{\mathcal{E}_b}, -\sqrt{\mathcal{E}_b})$  and  $(\sqrt{\mathcal{E}_b}, -\sqrt{\mathcal{E}_b})$ , respectively. The two paths entering node  $S_2$  at  $t = 2T$  correspond to the information bits  $(0, 1)$  and  $(1, 0)$  or, equivalently, to the signal points  $(-\sqrt{\mathcal{E}_b}, \sqrt{\mathcal{E}_b})$  and  $(\sqrt{\mathcal{E}_b}, \sqrt{\mathcal{E}_b})$ , respectively.

For the two paths entering node  $S_1$ , we compute the two Euclidean distance metrics

$$\begin{aligned}\mu_2(0, 0) &= (r_1 + \sqrt{\mathcal{E}_b})^2 + (r_2 + \sqrt{\mathcal{E}_b})^2 \\ \mu_2(1, 1) &= (r_1 - \sqrt{\mathcal{E}_b})^2 + (r_2 + \sqrt{\mathcal{E}_b})^2\end{aligned}\tag{8.5.14}$$

by using the outputs  $r_1$  and  $r_2$  from the demodulator. The Viterbi algorithm compares these two metrics and discards the path having the larger (greater distance) metric. The other path with the lower metric is saved and is called the *survivor* at  $t = 2T$ . The elimination of one of the two paths may be done without compromising the optimality of the trellis search, because any extension of the path with the larger distance beyond  $t = 2T$  will always have a larger metric than the survivor that is extended along the same path beyond  $t = 2T$ .

Similarly, for the two paths entering node  $S_2$  at  $t = 2T$ , we compute the two Euclidean distance metrics

$$\begin{aligned}\mu_2(0, 1) &= (r_1 + \sqrt{\mathcal{E}_b})^2 + (r_2 - \sqrt{\mathcal{E}_b})^2 \\ \mu_2(1, 0) &= (r_1 - \sqrt{\mathcal{E}_b})^2 + (r_2 - \sqrt{\mathcal{E}_b})^2\end{aligned}\tag{8.5.15}$$

by using the outputs  $r_1$  and  $r_2$  from the demodulator. The two metrics are compared and the signal path with the larger metric is eliminated. Thus, at  $t = 2T$ , we are left with two survivor paths, one at node  $S_1$  and the other at node  $S_2$ , and their corresponding metrics. The signal paths at nodes  $S_1$  and  $S_2$  are then extended along the two survivor paths.

Upon receipt of  $r_3$  at  $t = 3T$ , we compute the metrics of the two paths entering state  $S_1$ . Suppose the survivors at  $t = 2T$  are the paths  $(0, 0)$  at  $S_1$  and  $(0, 1)$  at  $S_2$ . Then, the two metrics for the paths entering  $S_1$  at  $t = 3T$  are

$$\begin{aligned}\mu_3(0, 0, 0) &= \mu_2(0, 0) + (r_3 + \sqrt{\mathcal{E}_b})^2 \\ \mu_3(0, 1, 1) &= \mu_2(0, 1) + (r_3 + \sqrt{\mathcal{E}_b})^2\end{aligned}\tag{8.5.16}$$

These two metrics are compared and the path with the larger (distance) metric is eliminated. Similarly, the metrics for the two paths entering  $S_2$  at  $t = 3T$  are

$$\begin{aligned}\mu_3(0, 0, 1) &= \mu_2(0, 0) + (r_3 - \sqrt{\mathcal{E}_b})^2 \\ \mu_3(0, 1, 0) &= \mu_2(0, 1) + (r_3 - \sqrt{\mathcal{E}_b})^2\end{aligned}\tag{8.5.17}$$

These two metrics are compared and the path with the larger (distance) metric is

This process is continued as each new signal sample is received from the demodulator. Thus, the Viterbi algorithm computes two metrics for the two signal paths entering a node at each stage of the trellis search and eliminates one of the two paths at each node. The two survivor paths are then extended forward to the next stage. Therefore, the number of paths searched in the trellis is reduced by a factor of two at each stage.

It is relatively easy to generalize the trellis search performed by the Viterbi algorithm for  $M$ -ary modulation. For example, delay modulation employs  $M = 4$  signals and is characterized by the four-state trellis shown in Figure 8.26. We observe that each state has two signal paths entering and two signal paths leaving each node. The memory of the signal is  $L = 1$ . Hence, the Viterbi algorithm will have four survivors at each stage and their corresponding metrics. Two metrics corresponding to the two entering paths are computed at each node and one of the two signal paths entering the node is eliminated at each state of the trellis. Thus, the Viterbi algorithm minimizes the number of trellis paths searched in performing ML sequence detection.

From the description of the Viterbi algorithm given above, it is unclear as to how decisions are made on the individual detected information symbols given the surviving sequences. If we have advanced to some stage, say  $K$ , where  $K \gg L$ , in the trellis and we compare the surviving sequences, we will find that, with probability approaching one, all surviving sequences will be identical in bit (or symbol) positions  $K - 5L$  and less. In a practical implementation of the Viterbi algorithm, decisions on each information bit (or symbol) are forced after a delay of  $5L$  bits (or symbols) and, hence, the surviving sequences are truncated to the  $5L$  most recent bits (or symbols). Thus, a variable delay in bit or symbol detection is avoided. The loss in performance resulting from the suboptimum detection procedure is negligible if the delay is at least  $5L$ .

### Example 8.5.8

Describe the decision rule for detecting the data sequence in an NRZI signal with a Viterbi algorithm having a delay of  $5L$  bits.

**Solution** The trellis for the NRZI signal is shown in Figure 8.30. In this case  $L = 1$ , hence the delay in bit detection is set to 5 bits. Hence, at  $t = 6T$ , we will have two surviving sequences, one for each of the two states, and the corresponding metrics  $\mu_6(b_1, b_2, b_3, b_4, b_5, b_6)$  and  $\mu_6(b'_1, b'_2, b'_3, b'_4, b'_5, b'_6)$ . At this stage, with probability nearly equal to one the bit  $b_1$  will be the same as  $b'_1$ ; i.e., both surviving sequences will have a common first branch. If  $b_1 \neq b'_1$ , we may select the bit ( $b_1$  or  $b'_1$ ) corresponding to the smaller of the two metrics. Then the first bit is dropped from the two surviving sequences. At  $t = 7T$ , the two metrics  $\mu_7(b_2, b_3, b_4, b_5, b_6, b_7)$  and  $\mu_7(b'_2, b'_3, b'_4, b'_5, b'_6, b'_7)$  will be used to determine the decision on bit  $b_2$ . This process continues at each stage of the search through the trellis for the minimum distance sequence. Thus the detection delay is fixed at 5 bits.

## 8.5.3 Maximum-Likelihood Sequence Detection of Partial Response Signals

It is clear from our previous discussion that partial response waveforms are signal waveforms with memory. This memory is conveniently represented by a trellis. For example, the trellis for the duobinary partial response signal for binary data transmission is illustrated in Figure 8.31. For binary modulation, this trellis contains two states,

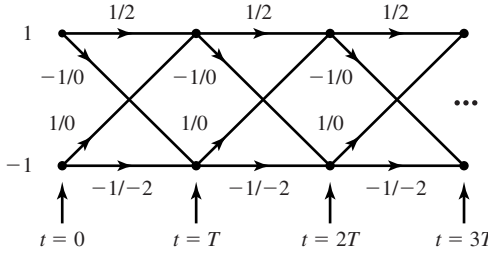


**Figure 8.31** Trellis for duobinary partial response signal.

corresponding to the two possible input values of  $a_m$ ; i.e.,  $a_m = \pm 1$ . Each branch in the trellis is labeled by two numbers. The first number on the left is the new data bit; i.e.,  $a_{m+1} = \pm 1$ . This number determines the transition to the new state. The number on the right is the received signal level.

The duobinary signal has a memory of length  $L = 1$ . Hence, for binary modulation the trellis has  $S_t = 2^L$  states. In general, for  $M$ -ary modulation, the number of trellis states is  $M^L$ .

The optimum ML sequence detector selects the most probable path through the trellis upon observing the received data sequence  $\{y_m\}$  at the sampling instants  $t = mT$ ,  $m = 1, 2, \dots$ . In general, each node in the trellis will have  $M$  incoming paths and  $M$  corresponding metrics. One out of the  $M$  incoming paths is selected as the most probable, based on the values of the metrics and the other  $M - 1$  paths and their metrics, are discarded. The surviving path at each node is then extended to  $M$  new paths, one for each of the  $M$  possible input symbols, and the search process continues. This is basically the Viterbi algorithm for performing the trellis search.

For the class of partial response signals, the received sequence  $\{y_m, 1 \leq m \leq N\}$  is generally described statistically by the joint PDF  $f(\mathbf{y}_N | \mathbf{a}_N)$ , where  $\mathbf{y}_N = (y_1, y_2, \dots, y_N)^t$  and  $\mathbf{a}_N = (a_1, a_2, \dots, a_N)^t$  and  $N > L$ . When the additive noise is zero-mean Gaussian,  $f(\mathbf{y}_N | \mathbf{a}_N)$  is a multivariate Gaussian PDF; i.e.,

$$f(\mathbf{y}_N | \mathbf{a}_N) = \frac{1}{(2\pi^{N/2})|\det(\mathbf{C})|^{1/2}} e^{-\frac{1}{2}(\mathbf{y}_N - \mathbf{b}_N)^t \mathbf{C}^{-1}(\mathbf{y}_N - \mathbf{b}_N)} \quad (8.5.18)$$

where  $\mathbf{b}_N = (b_1, b_2, \dots, b_N)^t$  is the mean of the vector  $\mathbf{y}_N$  and  $\mathbf{C}$  is the  $N \times N$  covariance matrix of  $\mathbf{y}_N$ . Then, the maximum-likelihood sequence detector selects the sequence through the trellis that maximizes the PDF  $f(\mathbf{y}_N | \mathbf{a}_N)$ .

The computations for finding the most probable sequence through the trellis is simplified by taking the natural logarithms of  $f(\mathbf{y}_N | \mathbf{a}_N)$ . Thus,

$$\ln f(\mathbf{y}_N | \mathbf{a}_N) = -\frac{N}{2} \ln(2\pi) - \frac{1}{2} \ln |\det(\mathbf{C})| - (\mathbf{y}_N - \mathbf{b}_N)^t \mathbf{C}^{-1}(\mathbf{y}_N - \mathbf{b}_N)/2 \quad (8.5.19)$$

Given the received sequence  $\{y_m\}$ , the data sequence  $\{a_m\}$  that maximizes  $\ln f(\mathbf{y}_N | \mathbf{a}_N)$  is identical to the sequence  $\{a_m\}$  that minimizes  $(\mathbf{y}_N - \mathbf{b}_N)^t \mathbf{C}^{-1}(\mathbf{y}_N - \mathbf{b}_N)$ ; i.e.,

$$\hat{\mathbf{a}}_N = \arg \min_{\mathbf{a}_N} (\mathbf{y}_N - \mathbf{b}_N)^t \mathbf{C}^{-1}(\mathbf{y}_N - \mathbf{b}_N) \quad (8.5.20)$$

The search through the trellis for the minimum distance path may be performed sequentially by use of the Viterbi algorithm. Let us consider the duobinary signal waveform with binary modulation and suppose that we begin at the initial state with  $a_0 = 1$ . Then upon receiving  $y_1 = a_1 + a_0 + v_1$  at time  $t = T$  and  $y_2 = a_2 + a_1 + v_2$  at time  $t = 2T$ , we have four candidate paths, corresponding to  $(a_1, a_2) = (1, 1), (-1, 1), (1, -1)$  and  $(-1, -1)$ . The first two candidate paths merge at state 1 at  $t = 2T$ . For the two paths merging at state 1, we compute the metrics  $\mu_2(1, 1)$  and  $\mu_2(-1, 1)$  and select the more probable path. A similar computation is performed at state  $-1$  for the two sequences  $(1, -1)$  and  $(-1, -1)$ . Thus, one of the two sequences at each node is saved and the other is discarded. The trellis search continues upon receipt of the signal sample  $y_3$  at time  $t = 3T$ , by extending the two surviving paths from time  $t = 2T$ .

The metric computations are complicated by the correlation of the noise samples at the output of the matched filter for the partial response signal. For example, in the case of the duobinary signal waveform, the correlation of the noise sequence  $\{v_m\}$  is over two successive signal samples. Hence,  $v_m$  and  $v_{m+k}$  are correlated for  $k = 1$  and uncorrelated for  $k > 1$ . In general, a partial response signal waveform with memory  $L$  will result in a correlated noise sequence at the output of the matched filter, which satisfies the condition  $E(v_m v_{m+k}) = 0$  for  $k > L$ . Ungerboeck (1974) described a sequential trellis search (Viterbi) algorithm for correlated noise (see Problem 8.26).

Some simplification in the metric computations results if we ignore the noise correlation by assuming that  $E(v_m v_{m+k}) = 0$  for  $k > 0$ . Then, by assumption the covariance matrix  $\mathbf{C} = \sigma_v^2 \mathbf{I}$  where  $\sigma_v^2 = E(v_m^2)$  and  $\mathbf{I}$  is the  $N \times N$  identity matrix. In this case, Equation (8.5.20) simplifies to

$$\begin{aligned} \hat{\mathbf{a}}_N &= \arg \min_{\mathbf{a}_N} [(\mathbf{y}_N - \mathbf{b}_N)^t (\mathbf{y}_N - \mathbf{b}_N)] \\ &= \arg \min_{\mathbf{a}_N} \left[ \sum_{m=1}^N \left( y_m - \sum_{k=0}^L x_k a_{m-k} \right)^2 \right] \end{aligned} \quad (8.5.21)$$

where

$$b_m = \sum_{k=0}^L x_k a_{m-k} \quad (8.5.22)$$

and  $x_k = x(kT)$  are the sampled values of the partial response signal waveform. In this case, the metric computations at each node of the trellis have the form

$$\mu_m(\mathbf{a}_m) = \mu_{m-1}(\mathbf{a}_{m-1}) + \left( y_m - \sum_{k=0}^L x_k a_{m-k} \right)^2 \quad (8.5.23)$$

where  $\mu_m(\mathbf{a}_m)$  are the metrics at time  $t = mT$ ,  $\mu_{m-1}(\mathbf{a}_{m-1})$  are the metrics at time  $t = (m-1)T$  and the second term on the right-hand side of Equation (8.5.23) are the new increments to the metrics based on the new received samples  $y_m$ .

As previously indicated in Section 8.5.2, ML sequence detection introduces a variable delay in detecting each transmitted information symbol. In practice, the variable

delay is avoided by truncating the surviving sequences to  $N_t$  most recent symbols, where  $N_t \gg 5L$ , thus achieving a fixed delay. In case the  $M^L$  surviving sequences at time  $t = mT$  disagree on the symbol  $a_{m-N_t}$ , the symbol in the most probable surviving sequence may be chosen. The loss in performance resulting from this truncation is negligible if  $N_t > 5L$ .

### Example 8.5.9

For the duobinary partial response signal, express the metric computations performed at  $t = 2T$  and  $t = 3T$ , based on the received signal samples  $y_m = b_m + v_m$  for  $m = 1, 2, 3$ , where the noise correlation is ignored.

**Solution** The metrics are generally given by Equation (8.5.23). Upon receipt of  $y_1$  and  $y_2$  and with  $a_0 = 1$ , the metrics for the two paths merging at state 1 are

$$\begin{aligned}\mu_2(1, 1) &= (y_1 - 2)^2 + (y_2 - 2)^2 \\ \mu_2(-1, 1) &= y_1^2 + y_2^2\end{aligned}$$

If  $\mu_2(1, 1) < \mu_2(-1, 1)$  we select the path (1, 1) as the more probable and discard (-1, 1). Otherwise, we select the path (-1, 1) and discard the path (1, 1). The path with the smaller metric is called the survivor and the sequence  $(a_1, a_2)$  and the corresponding metric are saved.

A similar computation is performed at state -1 for the sequences (1, -1) and (-1, -1). Then, we have

$$\begin{aligned}\mu_2(1, -1) &= (y_1 - 2)^2 + y_2^2 \\ \mu_2(-1, -1) &= y_1^2 + (y_2 + 2)^2\end{aligned}$$

We compare the metrics  $\mu_2(1, -1)$  and  $\mu_2(-1, -1)$  and select the sequence with the smaller metric.

Upon receipt of  $y_3$  at  $t = 3T$ , we consider the extensions of the survivor paths. Suppose that the two survivor paths are  $(a_1, a_2) = (1, 1)$  and  $(a_1, a_2) = (1, -1)$ . Then, at state 1 (at  $t = 3T$ ) we have the two merging paths  $(a_1, a_2, a_3) = (1, 1, 1)$  and  $(1, -1, 1)$ . Their corresponding metrics are

$$\begin{aligned}\mu_3(1, 1, 1) &= \mu_2(1, 1) + (y_3 - 2)^2 \\ \mu_3(1, -1, 1) &= \mu_2(1, -1) + y_3^2\end{aligned}$$

We compare the metrics for these two merging paths and select the path with the smaller metric as the survivor.

Similarly, at state -1 (at  $t = 3T$ ), we have the two merging paths (1, 1, -1) and (1, -1, -1), and their corresponding metrics

$$\begin{aligned}\mu_3(1, 1, -1) &= \mu_2(1, 1) + y_3^2 \\ \mu_3(1, -1, -1) &= \mu_2(1, -1) + (y_3 + 2)^2\end{aligned}$$

We select the path with the smaller metric as the survivor at state -1. This process continues upon receipt of additional data at  $t = kT$ ,  $k = 4, 5, \dots$

**Error Probability of the Maximum-Likelihood Sequence Detector.** In general, the computation of the exact probability of error is extremely difficult. Instead,

<https://hemanthrajhemu.github.io>

we shall determine an approximation to the probability of error, which is based on comparing the metrics of two paths which merge at a node and which are separated by the smallest Euclidean distance of all other paths. Our derivation is performed for the duobinary partial response signal waveform.

Let us consider the trellis for the duobinary partial response signal shown in Figure 8.31. We assume that we start in state 1 at  $t = 0$  and that the first two transmitted symbols are  $a_1 = 1$  and  $a_2 = 1$ . Then, at  $t = T$  we receive  $y_1 = 2d + v_1$  and at  $t = 2T$  we receive  $y_2 = 2d + v_2$ . An error is made at state 1 if the path  $(a_1, a_2) = (-1, 1)$  is more probable than the path  $(a_1, a_2) = (1, 1)$ , given the received values of  $y_1$  and  $y_2$ . This path error event is the dominant path error event and, hence, it serves as a good approximation to the probability of error for the ML sequence detector.

We recall that the metric for the path  $(a_1, a_2) = (1, 1)$  is

$$\mu_2(1, 1) = [y_1 - 2d \quad y_2 - 2d] \mathbf{C}^{-1} \begin{bmatrix} y_1 - 2d \\ y_2 - 2d \end{bmatrix} \quad (8.5.24)$$

where the covariance matrix  $\mathbf{C}$  is given by (see Problem 8.30)

$$\mathbf{C} = \frac{2N_0}{\pi} \begin{bmatrix} 1 & \frac{1}{3} \\ \frac{1}{3} & 1 \end{bmatrix} \quad (8.5.25)$$

For the path  $(a_1, a_2) = (-1, 1)$ , the corresponding metric is

$$\mu_2(-1, 1) = [y_1 \quad y_2] \mathbf{C}^{-1} \begin{bmatrix} y_1 \\ y_2 \end{bmatrix} \quad (8.5.26)$$

The probability of a path error event is simply the probability that the metric  $\mu_2(-1, 1)$  is smaller than the metric  $\mu_2(1, 1)$ ; i.e.,

$$P_2 = P[\mu_2(-1, 1) < \mu_2(1, 1)] \quad (8.5.27)$$

By substituting  $y_1 = 2d + v_1$  and  $y_2 = 2d + v_2$  into Equations (8.5.24) and (8.5.26) we find that

$$P_2 = P(v_1 + v_2 < -2d) \quad (8.5.28)$$

Since  $v_1$  and  $v_2$  are zero-mean (correlated) Gaussian variables, their sum is also zero-mean Gaussian. The variance of the sum  $z = v_1 + v_2$  is simply  $\sigma_z^2 = 16N_0/3\pi$ . Therefore,

$$P_2 = P(z < -2d) = Q\left(\frac{2d}{\sigma_z}\right) = Q\left(\sqrt{\frac{4d^2}{\sigma_z^2}}\right) \quad (8.5.29)$$

From Equation (8.4.32) we have (with  $M = 2$ ) the expression for  $d^2$  as

$$d^2 = \frac{\pi P_{av} T}{4} = \frac{\pi \mathcal{E}_b}{4} \quad (8.5.30)$$

Hence, the probability of the path error event is

$$P_2 = Q\left(\sqrt{\frac{1.5\pi^2}{16} \left(\frac{2\mathcal{E}_b}{N_0}\right)}\right) \quad (8.5.31)$$

First, we note that this path error event results in one bit-error in the sequence of two bits. Hence, the bit-error probability is  $P_2/2$ . Second, there is a reduction in SNR of  $10 \log(1.5\pi^2/16) = -0.34$  dB relative to the case of no intersymbol interference. This small SNR degradation is apparently the penalty incurred in exchange for the bandwidth efficiency of the partial response signal. Finally, we observe that the ML sequence detector has gained back 1.76 dB of the 2.1 dB degradation inherent in the symbol-by-symbol detector.

### 8.5.4 The Power Spectrum of Digital Signals with Memory

In Section 8.5.1, we demonstrated that state-dependent modulation codes resulted in modulated signals with memory. Such signals were described by Markov chains which are basically graphs that include the possible “states” of the modulator with corresponding state probabilities  $\{p_i\}$ , and state transitions with corresponding state transition probabilities  $\{p_{ij}\}$ .

The power-spectral density of digitally modulated signals that are characterized by Markov chains may be derived by following the basic procedure given in Section 8.2. Thus, we may determine the autocorrelation function and then evaluate its Fourier transform to obtain the power-spectral density. For signals that are generated by a Markov chain with transition probability matrix  $\mathbf{P}$ , as generally given by Equation (8.5.7), the power-spectral density of the modulated signal may be expressed in the general form

$$\begin{aligned} \mathcal{S}(f) = & \frac{1}{T^2} \sum_{n=-\infty}^{\infty} \left| \sum_{i=1}^K p_i S_i \left( \frac{n}{T} \right) \right|^2 \delta \left( f - \frac{n}{T} \right) + \frac{1}{T} \sum_{i=1}^K p_i |S'_i(f)|^2 \\ & + \frac{2}{T} \operatorname{Re} \left[ \sum_{i=1}^K \sum_{j=1}^K p_i S_i^*(f) S'_j(f) P_{ij}(f) \right] \end{aligned} \quad (8.5.32)$$

where  $K$  is the number of states of the modulator,  $S_i(f)$  is the Fourier transform of the signal waveform  $s_i(t)$ ,  $S'_i(f)$  is the Fourier transform of  $s'_i(t)$ , where  $s'_i(t) = s_i(t) - \sum_{k=1}^K p_k s_k(t)$ , and  $P_{ij}(f)$  is the Fourier transform of the discrete-time sequence  $p_{ij}(n)$ , defined as

$$P_{ij}(f) = \sum_{n=1}^{\infty} p_{ij}(n) e^{-j2\pi n f T} \quad (8.5.33)$$

The term  $p_{ij}(n)$  denotes the probability that a signal  $s_j(t)$  is transmitted  $n$  signaling intervals after the transmission of  $s_i(t)$ . Hence,  $\{p_{ij}(n)\}$  are the transition probabilities in the transition probability matrix  $\mathbf{P}^n$ . Note that when  $n = 1$ ,  $\mathbf{P}^n \equiv \mathbf{P}$ , which is the

**Example 8.5.10**

Determine the power-spectral density of the NRZI signal.

**Solution** The NRZI signal is characterized by the transition probability matrix

$$\mathbf{P} = \begin{bmatrix} \frac{1}{2} & \frac{1}{2} \\ \frac{1}{2} & \frac{1}{2} \end{bmatrix}$$

We note that  $\mathbf{P}^n = \mathbf{P}$  for all  $n > 1$ . Hence, with  $K = 2$  states and  $g_T(t) = s_1(t) = -s_2(t)$ , we obtain

$$\begin{aligned} \mathcal{S}(f) &= \frac{(2p-1)^2}{T^2} \sum_{n=-\infty}^{\infty} \left| G_T\left(\frac{n}{T}\right) \right|^2 \delta\left(f - \frac{n}{T}\right) \\ &\quad + \frac{4p(1-p)}{T} |G_T(f)|^2 \end{aligned} \quad (8.5.34)$$

where for a rectangular pulse of amplitude  $A$ ,

$$\begin{aligned} |G_T(f)|^2 &= (AT)^2 \left( \frac{\sin \pi f T}{\pi f T} \right)^2 \\ &= (AT)^2 \text{sinc}^2(fT) \end{aligned}$$

We observe that when  $p = 1/2$  (equally probable signals) the impulse spectrum vanishes and  $\mathcal{S}(f)$  reduces to

$$\mathcal{S}(f) = \frac{1}{T} |G_T(f)|^2$$

We observe that the power spectrum of the NRZI signal for equally probable signals is identical to the expression in (8.2.18), which applies to an uncorrelated sequence  $\{a_n\}$  into the modulator. Hence, we conclude that the simple precoding operation in NRZI does not result in a correlated sequence.

**Example 8.5.11**

Determine the power spectral density of the delay modulated (Miller encoded) signal described in Section 8.5.1.

**Solution** The transition probability matrix of a delay modulated signal is [see Equation (8.5.9)]

$$\mathbf{P} = \begin{bmatrix} 0 & \frac{1}{2} & 0 & \frac{1}{2} \\ 0 & 0 & \frac{1}{2} & \frac{1}{2} \\ \frac{1}{2} & \frac{1}{2} & 0 & 0 \\ \frac{1}{2} & 0 & \frac{1}{2} & 0 \end{bmatrix}$$

The state probabilities are  $p_i = 1/4$ , for  $i = 1, 2, 3, 4$ . Powers of  $\mathbf{P}$  are easily obtained by use of the relation (see Problem 8.8)

$$\mathbf{P}^4 \gamma = \frac{1}{-1-\gamma} \gamma \quad (8.5.35)$$

where  $\gamma$  is the signal correlation matrix with elements

$$\gamma_{ij} = \frac{1}{T} \int_0^T s_i(t)s_j(t) dt$$

and the four signals  $\{s_i(t), i = 1, 2, 3, 4\}$  are shown in Figure 8.27, where  $s_3(t) = -s_2(t)$  and  $s_4(t) = -s_1(t)$ . It is easily seen that

$$\gamma = \begin{bmatrix} 1 & 0 & 0 & -1 \\ 0 & 1 & -1 & 0 \\ 0 & -1 & 1 & 0 \\ -1 & 0 & 0 & 1 \end{bmatrix} \quad (8.5.36)$$

Consequently, powers of  $\mathbf{P}$  can be generated from the relation

$$\mathbf{P}^{k+4}\gamma = -\frac{1}{4}\mathbf{P}^k\gamma, \quad k \geq 1 \quad (8.5.37)$$

With the aid of these relations, the power spectral density of the delay modulated signal is obtained from Equation (8.5.32). It may be expressed in the form

$$\begin{aligned} S(f) = \frac{1}{2(\pi fT)^2(17 + 8 \cos 8\pi fT)} [23 - 2 \cos \pi fT - 22 \cos 2\pi fT \\ - 12 \cos 3\pi fT + 5 \cos 4\pi fT + 12 \cos 5\pi fT + 2 \cos 6\pi fT \\ - 8 \cos 7\pi fT + 2 \cos 8\pi fT] \end{aligned} \quad (8.5.38)$$

The power-spectral densities of the NRZI and the delay modulated signal are shown in Figure 8.32. We observe that the NRZI signal has a lowpass power spectrum with a peak of  $f = 0$ . On the other hand, the delay modulated signal has very little power in the vicinity of  $f = 0$ . It also has a relatively narrow power-spectral density. These two characteristics make it particularly suitable for use in magnetic recording storage

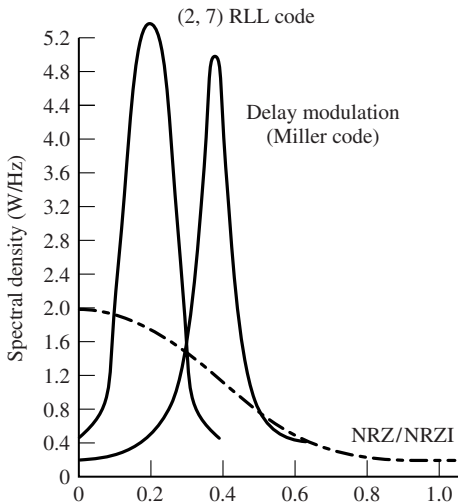


**Figure 8.32** Power-spectral density (one-sided) of Miller code (delay modulation), and NRZ/NRZI baseband

channels which use flux-sensing heads for writing on and reading off a disk. Also shown for comparison in Figure 8.32 is the power-spectral density of the modulated signal generated by a  $(d, \kappa) = (2, 7)$  code followed by NRZI. The  $(2, 7)$  runlength-limited code, previously given in Table 8.5, is also widely used in magnetic recording channels.

When there is no memory in the modulation method, the signal waveform transmitted in each signaling interval is independent of the waveforms transmitted in previous signaling intervals. The power-spectral density of the resulting signal may still be expressed in the form of Equation (8.5.32) if the transition probability matrix is replaced by

$$\mathbf{P} = \begin{bmatrix} p_1 & p_2 & \dots & p_K \\ p_1 & p_2 & \dots & p_K \\ \vdots & \vdots & & \vdots \\ p_1 & p_2 & \dots & p_K \end{bmatrix} \quad (8.5.39)$$

and we impose the condition that  $\mathbf{P}^n = \mathbf{P}$  for all  $n > 1$ , as a consequence of the memoryless modulation. Under these conditions, the expression for  $\mathcal{S}(f)$  given Equation (8.5.32) reduces to the simpler form

$$\begin{aligned} \mathcal{S}(f) = & \frac{1}{T^2} \sum_{n=-\infty}^{\infty} \left| \sum_{i=1}^K p_i S_i \left( \frac{n}{T} \right) \right|^2 \delta \left( f - \frac{n}{T} \right) + \frac{1}{T} \sum_{i=1}^K p_i (1 - p_i) |S_i(f)|^2 \\ & - \frac{2}{T} \sum_{i=1}^K \sum_{\substack{j=1 \\ i < j}}^K p_i p_j \operatorname{Re} [S_i(f) S_j^*(f)] \end{aligned} \quad (8.5.40)$$

We observe that our previous result for the power-spectral density of memoryless PAM modulation given by Equation (8.2.17) is a special case of the expression in Equation (8.5.40). Specifically, if we have  $K = M$  signals which are amplitude-scaled versions of a basic pulse  $g_T(t)$ ; i.e.,  $s_m(t) = a_m g_T(t)$ , where  $a_m$  is the signal amplitude, then  $S_m(f) = a_m G_T(f)$  and Equation (8.5.40) becomes

$$\begin{aligned} \mathcal{S}(f) = & \frac{1}{T^2} \left( \sum_{i=1}^M a_i p_i \right)^2 \sum_{n=-\infty}^{\infty} \left| G_T \left( \frac{n}{T} \right) \right|^2 \delta \left( f - \frac{n}{T} \right) \\ & + \frac{1}{T} \left[ \sum_{i=1}^M p_i (1 - p_i) a_i^2 - 2 \sum_{i=1}^M \sum_{j=1}^M p_i p_j a_i a_j \right] |G_T(f)|^2 \end{aligned} \quad (8.5.41)$$

If we compare Equation (8.2.17) with Equation (8.5.41), we find that these expressions are identical, where the mean and variance of the information sequence is

$$\begin{aligned} m_a &= \sum_{i=1}^M a_i p_i \\ \sigma_a^2 &= \sum_{i=1}^M p_i (1 - p_i) a_i^2 - 2 \sum_{i=1}^M \sum_{j=1}^M p_i p_j a_i a_j \end{aligned} \quad (8.5.42)$$

Therefore Equation (8.5.40) is the more general form for the power-spectral density of memoryless modulated signals, since it applies to signals that may have different pulse shapes.

## 8.6 SYSTEM DESIGN IN THE PRESENCE OF CHANNEL DISTORTION

In Section 8.3.1 we described a signal design criterion that results in zero ISI at the output of the receiving filter. Recall that a signal pulse  $x(t)$  will satisfy the condition of zero ISI at the sampling instants  $t = nT$ ,  $n = \pm 1, \pm 2, \dots$ , if its spectrum  $X(f)$  satisfies the condition given by Equation (8.3.9). From this condition we concluded that for ISI free transmission over a channel, the transmitter-receiver filters and the channel transfer function must satisfy

$$G_T(f)C(f)G_R(f) = X_{rc}(f) \quad (8.6.1)$$

where  $X_{rc}(f)$  denotes the Fourier transform of an appropriate raised cosine pulse whose parameters depend on the channel bandwidth  $W$  and the transmission interval  $T$ . Obviously, there are an infinite number of transmitter-receiver filter pairs that satisfy the above condition. In this section, we are concerned with the design of a digital communication system that suppresses ISI in a channel with distortion. We first present a brief coverage of various types of channel distortion and then we consider the design of transmitter and receiver filters.

We distinguish two types of distortion. *Amplitude distortion* results when the amplitude characteristic  $|C(f)|$  is not constant for  $|f| \leq W$ . The second type of distortion, called *phase distortion*, results when the phase characteristic  $\Theta_c(f)$  is nonlinear in frequency.

Another view of phase distortion is obtained by considering the derivative of  $\Theta_c(f)$ . Thus, we define the *envelope delay* characteristic as (see Problems 2.57 and 8.40)

$$\tau(f) = -\frac{1}{2\pi} \frac{d\Theta_c(f)}{df} \quad (8.6.2)$$

When  $\Theta_c(f)$  is linear in  $f$ , the envelope delay is constant for all frequencies. In this case, all frequencies in the transmitted signal pass through the channel with the same fixed-time delay. In such a case, there is no phase distortion. However, when  $\Theta_c(f)$  is nonlinear, the envelope delay  $\tau(f)$  varies with frequency and the various frequency components in the input signal undergo different delays in passing through the channel. In such a case we say that the transmitted signal has suffered from *delay distortion*.

Both amplitude and delay distortion cause intersymbol interference in the received signal. For example, let us assume that we have designed a pulse with a raised cosine spectrum that has zero ISI at the sampling instants. An example of such a pulse is illustrated in Figure 8.33(a). When the pulse is passed through a channel filter with constant amplitude  $|C(f)| = 1$  for  $|f| < W$  and a quadratic phase characteristic (linear envelope delay), the received pulse at the output of the channel is shown in Figure 8.33(b). Note that the periodic zero crossings have been shifted by the delay distortion, so that the

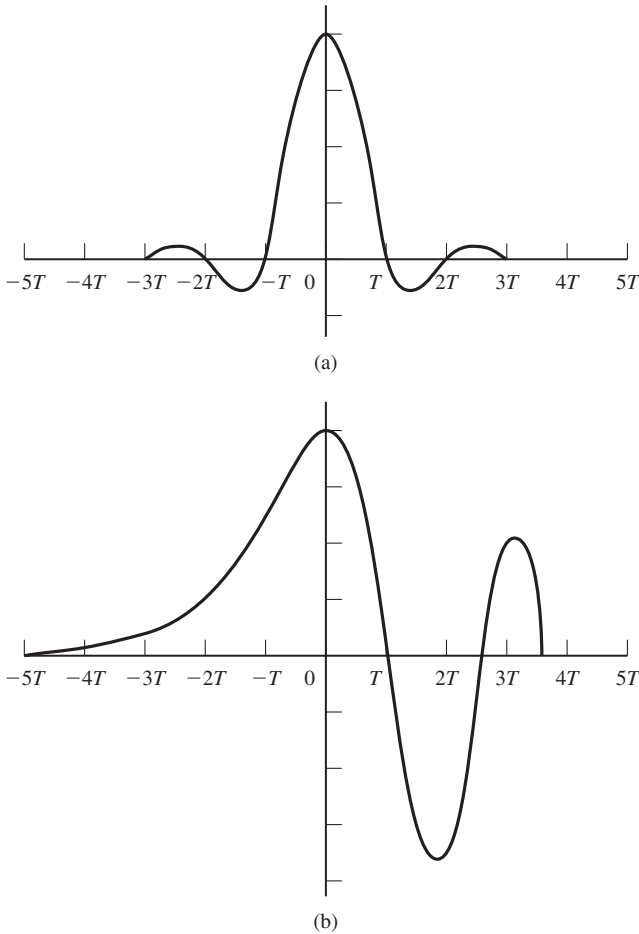


**Figure 8.33** Effect of channel distortion in (a) channel input and (b) channel output.

resulting pulse suffers from ISI. Consequently, a sequence of successive pulses would be smeared into one another and the peaks of the pulses would no longer be distinguishable due to the ISI.

Next, we consider two problems. First, we consider the design of transmitting and receiving filters in the presence of channel distortion when the channel characteristics are known. Second, we consider the design of special filters, called channel equalizers, that automatically and adaptively correct for the channel distortion when the channel characteristics; i.e.,  $|C(f)|$  and  $\angle\Theta_c(f)$ , are unknown.

### 8.6.1 Design of Transmitting and Receiving Filters for a Known Channel

In this section, we assume that the channel frequency response characteristic  $C(f)$  is known and consider the problem of designing a transmitting filter and a receiving

<https://hemanthrajhemu.github.io>

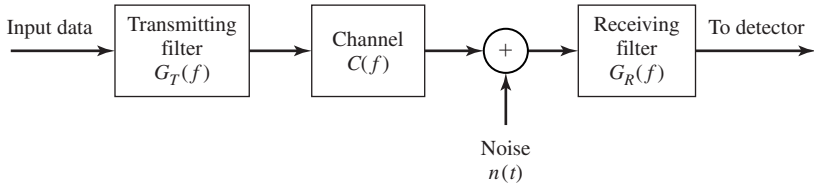


**Figure 8.34** System configuration for design of  $G_T(f)$  and  $G_R(f)$ .

filter that maximize the SNR at the output of the receiving filter and results in zero ISI. Figure 8.34 illustrates the overall system under consideration.

For the signal component, we must satisfy the condition

$$G_T(f)C(f)G_R(f) = X_{rc}(f)e^{-j\pi f t_0}, \quad |f| \leq W \quad (8.6.3)$$

where  $X_{rc}(f)$  is the desired raised cosine spectrum that yields zero ISI at the sampling instants, and  $t_0$  is a time delay which is necessary to ensure the physical realizability of the transmitter and receiver filters.

The noise at the output of the receiving filter may be expressed as

$$v(t) = \int_{-\infty}^{\infty} n(t - \tau)g_R(\tau) d\tau \quad (8.6.4)$$

where  $n(t)$  is the input to the filter. The noise  $n(t)$  is assumed to be zero-mean Gaussian. Hence,  $v(t)$  is zero-mean Gaussian, with a power-spectral density

$$S_v(f) = S_n(f)|G_R(f)|^2 \quad (8.6.5)$$

where  $S_n(f)$  is the spectral density of the noise process  $n(t)$ .

For simplicity, we consider binary PAM transmission. Then, the sampled output of the matched filter is

$$y_m = x_0 a_m + v_m = a_m + v_m \quad (8.6.6)$$

where  $x_0$  is normalized to unity,  $a_m = \pm d$ , and  $v_m$  represents the noise term which is zero-mean Gaussian with variance

$$\sigma_v^2 = \int_{-\infty}^{\infty} S_n(f)|G_R(f)|^2 df \quad (8.6.7)$$

Consequently, the probability of error is

$$P_2 = \frac{1}{\sqrt{2\pi}} \int_{d/\sigma_v}^{\infty} e^{-y^2/2} dy = Q\left(\sqrt{\frac{d^2}{\sigma_v^2}}\right) \quad (8.6.8)$$

Now, suppose that we select the filter at the transmitter to have the frequency response

$$G_T(f) = \frac{\sqrt{X_{rc}(f)}}{C(f)} e^{-j2\pi f t_0} \quad (8.6.9)$$

where  $t_0$  is a suitable delay to ensure causality. Then, the cascade of the transmit filter and the channel results in the frequency response

$$G_T(f)C(f) = \sqrt{X_{rc}(f)} e^{-j2\pi f t_0} \quad (8.6.10)$$

In the presence of additive white Gaussian noise, the filter at the receiver is designed to be matched to the received signal pulse. Hence, its frequency response

$$G_R(f) = \sqrt{X_{rc}(f)} e^{-j2\pi f t_r} \quad (8.6.11)$$

where  $t_r$  is an appropriate delay.

Let us compute the SNR  $d^2/\sigma_v^2$  for these filter characteristics. The noise variance is

$$\sigma_v^2 = \frac{N_0}{2} \int_{-\infty}^{\infty} |G_R(f)|^2 df = \frac{N_0}{2} \int_{-W}^W X_{rc}(f) df = \frac{N_0}{2} \quad (8.6.12)$$

The average transmitted power is

$$P_{av} = \frac{E(a_m^2)}{T} \int_{-\infty}^{\infty} g_T^2(t) dt = \frac{d^2}{T} \int_{-W}^W \frac{X_{rc}(f)}{|C(f)|^2} df \quad (8.6.13)$$

and, hence,

$$d^2 = P_{av} T \left[ \int_{-W}^W \frac{X_{rc}(f)}{|C(f)|^2} df \right]^{-1} \quad (8.6.14)$$

Therefore, the SNR  $d^2/\sigma_v^2$  is given as

$$\frac{d^2}{\sigma_v^2} = \frac{2P_{av} T}{N_0} \left[ \int_{-W}^W \frac{X_{rc}(f)}{|C(f)|^2} df \right]^{-1} \quad (8.6.15)$$

We note that the term,

$$10 \log_{10} \int_{-W}^W \frac{X_{rc}(f)}{|C(f)|^2} df \quad (8.6.16)$$

with  $|C(f)| \leq 1$  for  $|f| \leq W$ , represents the loss in performance in dB of the communication system due to channel distortion. When the channel is ideal,  $|C(f)| = 1$  for  $|f| \leq W$  and, hence, there is no performance loss. We also note that this loss is entirely due to amplitude distortion in the channel, because the phase distortion has been totally compensated by the transmit filter.

### Example 8.6.1

Determine the magnitude of the transmitting and receiving filter characteristics for a binary communication system that transmits data at a rate of 4800 bits/sec over a channel with frequency (magnitude) response

$$|C(f)| = \frac{1}{\sqrt{1 + \left(\frac{f}{W}\right)^2}}, \quad |f| \leq W$$

where  $W = 4800$  Hz. The additive noise is zero-mean, white, Gaussian with spectral density  $N_0/2 = 10^{-15}$  W/Hz.

**Solution** Since  $W = 1/T = 4800$  we use a signal pulse with a raised cosine spectrum and  $\alpha = 1$ . Thus,

$$\begin{aligned} X_{\text{rc}}(f) &= \frac{T}{2}[1 + \cos(\pi T|f|)] \\ &= T \cos^2\left(\frac{\pi|f|}{9600}\right) \end{aligned}$$

Then,

$$|G_T(f)| = \sqrt{T \left[ 1 + \left( \frac{f}{W} \right)^2 \right]} \cos \frac{\pi|f|}{9600}, \quad |f| \leq 4800 \text{ Hz}$$

$$|G_R(f)| = \sqrt{T} \cos \frac{\pi|f|}{9600}, \quad |f| \leq 4800 \text{ Hz}$$

and  $|G_T(f)| = |G_R(f)| = 0$  for  $|f| > 4800$  Hz

### 8.6.2 Channel Equalization

In the preceding section, we described the design of transmitting and receiving filters for digital PAM transmission when the frequency response characteristics of the channel are known. Our objective was to design these filters for zero ISI at the sampling instants. This design methodology is appropriate when the channel is precisely known and its characteristics do not change with time.

In practice we often encounter channels whose frequency response characteristics are either unknown or change with time. For example, in data transmission over the dial-up telephone network, the communication channel will be different every time we dial a number, because the channel route will be different. Once a connection is made, however, the channel will be time-invariant for a relatively long period of time. This is an example of a channel whose characteristics are unknown a priori. Examples of time-varying channels are radio channels, such as ionospheric propagation channels. These channels are characterized by time-varying frequency response characteristics. These types of channels are examples where the optimization of the transmitting and receiving filters, as described in Section 8.6.1, is not possible.

Under these circumstances, we may design the transmitting filter to have a square-root raised cosine frequency response; i.e.,

$$G_T(f) = \begin{cases} \sqrt{X_{\text{rc}}(f)} e^{-j2\pi f t_0}, & |f| \leq W \\ 0, & |f| > W \end{cases}$$

and the receiving filter, with frequency response  $G_R(f)$ , to be matched to  $G_T(f)$ . Therefore,

$$|G_T(f)||G_R(f)| = X_{\text{rc}}(f) \quad (8.6.17)$$

Then, due to channel distortion, the output of the receiving filter is

$$y(t) = \sum_{n=-\infty}^{\infty} a_n x(t - nT) + v(t) \quad (8.6.18)$$

where  $x(t) = g_T(t) \star c(t) \star g_R(t)$ . The filter output may be sampled periodically to produce the sequence

$$\begin{aligned} y_m &= \sum_{n=-\infty}^{\infty} a_n x_{m-n} + v_m \\ &= x_0 a_m + \sum_{\substack{n=-\infty \\ n \neq m}}^{+\infty} a_n x_{m-n} + v_m \end{aligned} \quad (8.6.19)$$

where  $x_n = x(nT)$ ,  $n = 0, \pm 1, \pm 2, \dots$ . The middle term on the right-hand side of Equation (8.6.19) represents the ISI.

In any practical system, it is reasonable to assume that the ISI affects a finite number of symbols. Hence, we may assume that  $x_n = 0$  for  $n < -L_1$  and  $n > L_2$ , where  $L_1$  and  $L_2$  are finite, positive integers. Consequently, the ISI observed at the output of the receiving filter may be viewed as being generated by passing the data sequence  $\{a_m\}$  through an FIR filter with coefficients  $\{x_n, -L_1 \leq n \leq L_2\}$ , as shown in Figure 8.35. This filter is called the *equivalent discrete-time channel filter*. Since its input is the discrete information sequence (binary or  $M$ -ary), the output of the discrete-time channel filter may be characterized as the output of a finite-state machine corrupted by additive Gaussian noise. Hence, the noise-free output of the filter is described by a trellis having  $M^L$  states where  $L = L_1 + L_2$ .

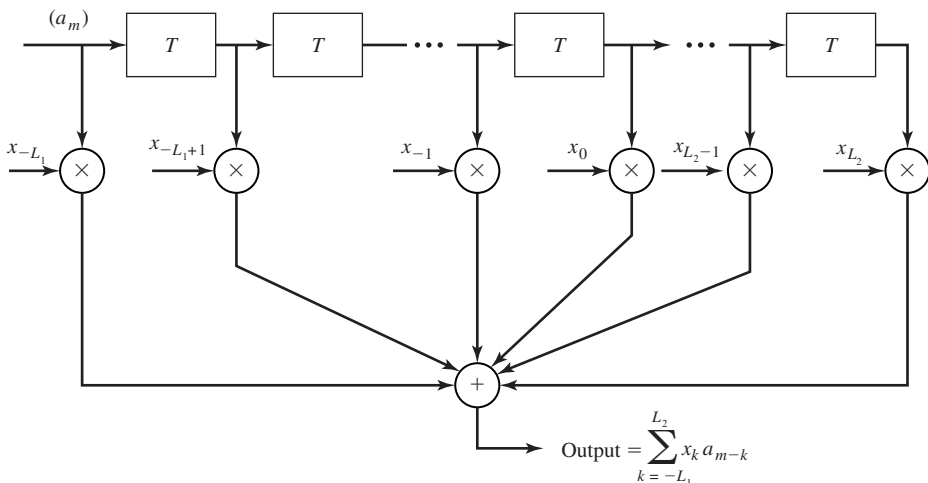


Figure 8.35 Equivalent discrete-time channel filter.

**Maximum-Likelihood Sequence Detection.** The optimum detector for the information sequence  $\{a_m\}$  based on the observation of the received sequence  $\{y_m\}$ , given by Equation (8.6.19), is a ML sequence detector. The detector is akin to the ML sequence detector described in the context of detecting partial response signals which have controlled ISI. The Viterbi algorithm provides a method for searching through the trellis for the ML signal path. To accomplish this search, the equivalent channel filter coefficients  $\{x_n\}$  must be known or measured by some method. At each stage of the trellis search, there are  $M^L$  surviving sequences with  $M^L$  corresponding Euclidean distance path metrics.

Due to the exponential increase in the computational complexity of the Viterbi algorithm with the span (length  $L$ ) of the ISI, this type of detection is practical only when  $M$  and  $L$  are small. For example in mobile cellular telephone systems which employ digital transmission of speech signals,  $M$  is usually selected to be small; e.g.,  $M = 2$  or 4, and  $2 \leq L \leq 5$ . In this case, the ML sequence detector may be implemented with reasonable complexity. However, when  $M$  and  $L$  are large, the ML sequence detector becomes impractical. In such a case other more practical but suboptimum methods are used to detect the information sequence  $\{a_m\}$  in the presence of ISI. Nevertheless, the performance of the ML sequence detector for a channel with ISI serves as a benchmark for comparing its performance with that of suboptimum methods. Two suboptimum methods are described below.

**Linear Equalizers.** To compensate for the channel distortion, we may employ a linear filter with adjustable parameters. The filter parameters are adjusted on the basis of measurements of the channel characteristics. These adjustable filters are called *channel equalizers* or, simply, *equalizers*.

On channels whose frequency-response characteristics are unknown, but time-invariant, we may measure the channel characteristics, adjust the parameters of the equalizer, and once adjusted, the parameters remain fixed during the transmission of data. Such equalizers are called *preset equalizers*. On the other hand, *adaptive equalizers* update their parameters on a periodic basis during the transmission of data.

First, we consider the design characteristics for a linear equalizer from a frequency domain viewpoint. Figure 8.36 shows a block diagram of a system that employs a linear filter as a channel equalizer.

The demodulator consists of a receiving filter with frequency response  $G_R(f)$  in cascade with a channel equalizing filter that has a frequency response  $G_E(f)$ . Since

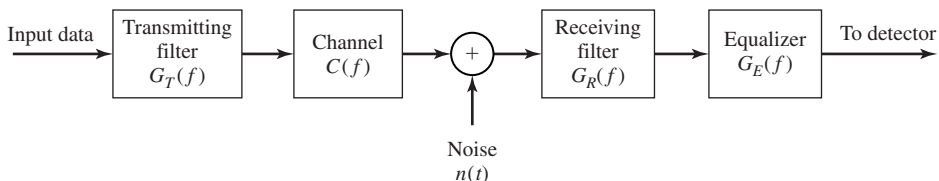


**Figure 8.36** Block diagram of a system with an equalizer.

$G_R(f)$  is matched to  $G_T(f)$  and they are designed so that their product satisfies Equation (8.6.17),  $|G_E(f)|$  must compensate for the channel distortion. Hence, the equalizer frequency response must equal the inverse of the channel response; i.e.,

$$G_E(f) = \frac{1}{C(f)} = \frac{1}{|C(f)|} e^{-j\Theta_c(f)} |f| \leq W \quad (8.6.20)$$

where  $|G_E(f)| = 1/|C(f)|$  and the equalizer phase characteristic  $\Theta_E(f) = -\Theta_c(f)$ . In this case, the equalizer is said to be the *inverse channel filter* to the channel response.

We note that the inverse channel filter completely eliminates ISI caused by the channel. Since it forces the ISI to be zero at the sampling times  $t = nT$ , the equalizer is called a *zero-forcing equalizer*. Hence, the input to the detector is of the form

$$y_m = a_m + v_m$$

where  $v_m$  is the noise component, which is zero-mean Gaussian with a variance

$$\begin{aligned} \sigma_v^2 &= \int_{-\infty}^{\infty} \mathcal{S}_n(f) |G_R(f)|^2 |G_E(f)|^2 df \\ &= \int_{-W}^W \frac{\mathcal{S}_n(f) |X_{rc}(f)|}{|C(f)|^2} df \end{aligned} \quad (8.6.21)$$

where  $\mathcal{S}_n(f)$  is the power-spectral density of the noise. When the noise is white,  $\mathcal{S}_n(f) = N_0/2$  and the variance becomes

$$\sigma_v^2 = \frac{N_0}{2} \int_{-W}^W \frac{|X_{rc}(f)|}{|C(f)|^2} df \quad (8.6.22)$$

In general, the noise variance at the output of the zero-forcing equalizer is higher than the noise variance at the output of the optimum receiving filter  $|G_R(f)|$  given by Equation (8.6.12) for the case in which the channel is known.

### Example 8.6.2

The channel given in Example 8.6.1 is equalized by a zero-forcing equalizer. Assuming that the transmitting and receiving filters satisfy Equation (8.6.17), determine the value of the noise variance at the sampling instants and the probability of error.

**Solution** When the noise is white, the variance of the noise at the output of the zero-forcing equalizer (input to the detector) is given by Equation (8.6.22). Hence,

$$\begin{aligned} \sigma_v^2 &= \frac{N_0}{2} \int_{-W}^W \frac{|X_{rc}(f)|}{|C(f)|^2} df \\ &= \frac{TN_0}{2} \int_{-W}^W \left[ 1 + \left( \frac{f}{W} \right)^2 \right] \cos^2 \frac{\pi|f|}{2W} df \\ &= N_0 \int_0^1 (1 + x^2) \cos^2 \frac{\pi x}{2} dx \\ &= \left( \frac{2}{3} - \frac{1}{\pi^2} \right) N_0 \end{aligned}$$

The average transmitted power is

$$\begin{aligned} P_{av} &= \frac{(M^2 - 1)d^2}{3T} \int_{-W}^W |G_T(f)|^2 df \\ &= \frac{(M^2 - 1)d^2}{3T} \int_{-W}^W |X_{rc}(f)| df \\ &= \frac{(M^2 - 1)d^2}{3T} \end{aligned}$$

The general expression for the probability of error is given as

$$P_M = \frac{2(M - 1)}{M} Q \left( \sqrt{\frac{3P_{av}T}{(M^2 - 1)(2/3 - 1/\pi^2)N_0}} \right)$$

If the channel were ideal, the argument of the Q-function would be  $6P_{av}T/(M^2 - 1)N_0$ . Hence, the loss in performance due to the nonideal channel is given by the factor  $2(2/3 - 1/\pi^2) = 1.133$  or 0.54 dB.

Let us now consider the design of a linear equalizer from a time-domain viewpoint. We noted previously that in real channels, the ISI is limited to a finite number of samples, say  $L$  samples. As a consequence, in practice the channel equalizer is approximated by a finite duration impulse response (FIR) filter, or transversal filter, with adjustable tap coefficients  $\{c_n\}$ , as illustrated in Figure 8.37. The time delay  $\tau$  between adjacent taps may be selected as large as  $T$ , the symbol interval, in which case the FIR equalizer is called a *symbol-spaced equalizer*. In this case the input to the equalizer is the sampled sequence given by Equation (8.6.19). However, we note that when  $1/T < 2W$ , frequencies in the received signal above the folding frequency  $1/T$

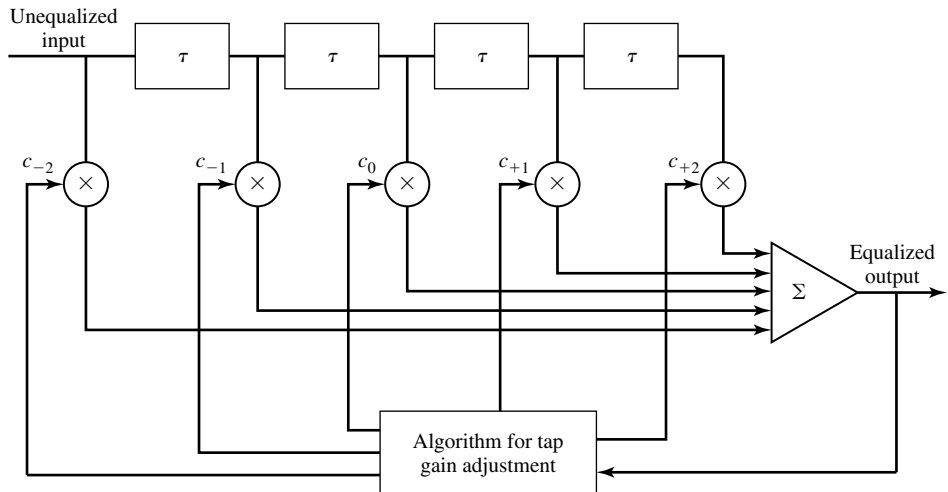


Figure 8.37 Linear transversal filter.

are aliased into frequencies below  $1/T$ . In this case, the equalizer compensates for the aliased channel-distorted signal.

On the other hand, when the time delay  $\tau$  between adjacent taps is selected such that  $1/\tau \geq 2W > 1/T$ , no aliasing occurs and, hence, the inverse channel equalizer compensates for the true channel distortion. Since  $\tau < T$ , the channel equalizer is said to have *fractionally spaced taps* and it is called a *fractionally spaced equalizer*. In practice,  $\tau$  is often selected as  $\tau = T/2$ . Notice that, in this case, the sampling rate at the output of the filter  $G_R(f)$  is  $\frac{2}{T}$ .

The impulse response of the FIR equalizer is

$$g_E(t) = \sum_{n=-N}^N c_n \delta(t - n\tau) \quad (8.6.23)$$

and the corresponding frequency response is

$$G_E(f) = \sum_{n=-N}^N c_n e^{-j2\pi f n\tau} \quad (8.6.24)$$

where  $\{c_n\}$  are the  $(2N + 1)$  equalizer coefficients, and  $N$  is chosen sufficiently large so that the equalizer spans the length of the ISI; i.e.,  $2N + 1 \geq L$ . Since  $X(f) = G_T(f)C(f)G_R(f)$  and  $x(t)$  is the signal pulse corresponding to  $X(f)$ , then the equalized output signal pulse is

$$q(t) = \sum_{n=-N}^N c_n x(t - n\tau) \quad (8.6.25)$$

The zero-forcing condition can now be applied to the samples of  $q(t)$  taken at times  $t = mT$ . These samples are

$$q(mT) = \sum_{n=-N}^N c_n x(mT - n\tau), \quad m = 0, \pm 1, \dots, \pm N \quad (8.6.26)$$

Since there are  $2N + 1$  equalizer coefficients, we can control only  $2N + 1$  sampled values of  $q(t)$ . Specifically, we may force the conditions

$$q(mT) = \sum_{n=-N}^N c_n x(mT - n\tau) = \begin{cases} 1, & m = 0 \\ 0, & m = \pm 1, \pm 2, \dots, \pm N \end{cases} \quad (8.6.27)$$

which may be expressed in matrix form as  $\mathbf{X}\mathbf{c} = \mathbf{q}$ , where  $\mathbf{X}$  is a  $(2N + 1) \times (2N + 1)$  matrix with elements  $\{x(mT - n\tau)\}$ ,  $\mathbf{c}$  is the  $(2N + 1)$  coefficient vector and  $\mathbf{q}$  is the  $(2N + 1)$  column vector with one nonzero element. Thus, we obtain a set of  $2N + 1$  linear equations for the coefficients of the zero-forcing equalizer.

We should emphasize that the FIR zero-forcing equalizer does not completely eliminate ISI because it has a finite length. However, as  $N$  is increased the residual ISI can be reduced and in the limit as  $N \rightarrow \infty$ , the ISI is completely eliminated.

**Example 8.6.3**

Consider a channel distorted pulse  $x(t)$ , at the input to the equalizer, given by the expression

$$x(t) = \frac{1}{1 + \left(\frac{2t}{T}\right)^2}$$

where  $1/T$  is the symbol rate. The pulse is sampled at the rate  $2/T$  and equalized by a zero-forcing equalizer. Determine the coefficients of a five-tap zero-forcing equalizer.

**Solution** According to Equation (8.6.27), the zero-forcing equalizer must satisfy the equations

$$q(mT) = \sum_{n=-2}^2 c_n x(mT - nT/2) = \begin{cases} 1, & m = 0 \\ 0, & m = \pm 1, \pm 2 \end{cases}$$

The matrix  $\mathbf{X}$  with elements  $x(mT - nT/2)$  is given as

$$\mathbf{X} = \begin{bmatrix} \frac{1}{5} & \frac{1}{10} & \frac{1}{17} & \frac{1}{26} & \frac{1}{37} \\ 1 & \frac{1}{2} & \frac{1}{5} & \frac{1}{10} & \frac{1}{17} \\ \frac{1}{5} & \frac{1}{2} & 1 & \frac{1}{2} & \frac{1}{5} \\ \frac{1}{17} & \frac{1}{10} & \frac{1}{5} & \frac{1}{2} & 1 \\ \frac{1}{37} & \frac{1}{26} & \frac{1}{17} & \frac{1}{10} & \frac{1}{5} \end{bmatrix} \quad (8.6.28)$$

The coefficient vector  $\mathbf{C}$  and the vector  $\mathbf{q}$  are given as

$$\mathbf{c} = \begin{bmatrix} c_{-2} \\ c_{-1} \\ c_0 \\ c_1 \\ c_2 \end{bmatrix} \quad \mathbf{q} = \begin{bmatrix} 0 \\ 0 \\ 1 \\ 0 \\ 0 \end{bmatrix} \quad (8.6.29)$$

Then, the linear equations  $\mathbf{X}\mathbf{c} = \mathbf{q}$  can be solved by inverting the matrix  $\mathbf{X}$ . Thus, we obtain

$$\mathbf{c}_{\text{opt}} = \mathbf{X}^{-1}\mathbf{q} = \begin{bmatrix} -2.2 \\ 4.9 \\ -3 \\ 4.9 \\ -2.2 \end{bmatrix} \quad (8.6.30)$$

One drawback to the zero-forcing equalizer is that it ignores the presence of additive noise. As a consequence, its use may result in significant noise enhancement. This is easily seen by noting that in a frequency range where  $C(f)$  is small, the channel equalizer  $G_E(f) = 1/C(f)$  compensates by placing a large gain in that frequency range. Consequently, the noise in that frequency range is greatly enhanced. An alternative is to relax the zero ISI condition and select the channel equalizer characteristic such that the combined power in the residual ISI and the additive noise at the output of the equalizer is minimized. A channel equalizer that is optimized based on the minimum mean-square-error (MMSE) criterion accomplishes the desired goal.

To elaborate, let us consider the noise-corrupted output of the FIR equalizer which is

$$z(t) = \sum_{n=-N}^N c_n y(t - n\tau) \quad (8.6.31)$$

where  $y(t)$  is the input to the equalizer, given by Equation (8.6.18). The output is sampled at times  $t = mT$ . Thus, we obtain

$$z(mT) = \sum_{n=-N}^N c_n y(mT - n\tau) \quad (8.6.32)$$

The desired response sample at the output of the equalizer at  $t = mT$  is the transmitted symbol  $a_m$ . The error is defined as the difference between  $a_m$  and  $z(mT)$ . Then, the mean-square-error (MSE) between the actual output sample  $z(mT)$  and the desired values  $a_m$  is

$$\begin{aligned} \text{MSE} &= E[z(mT) - a_m]^2 \\ &= E \left[ \sum_{n=-N}^N c_n y(mT - n\tau) - a_m \right]^2 \\ &= \sum_{n=-N}^N \sum_{k=-N}^N c_n c_k R_Y(n - k) - 2 \sum_{k=-N}^N c_k R_{AY}(k) + E(a_m^2) \end{aligned} \quad (8.6.33)$$

where the correlations are defined as

$$\begin{aligned} R_Y(n - k) &= E[y(mT - n\tau)y(mT - k\tau)] \\ R_{AY}(k) &= E[y(mT - k\tau)a_m] \end{aligned} \quad (8.6.34)$$

and the expectation is taken with respect to the random information sequence  $\{a_m\}$  and the additive noise.

The MMSE solution is obtained by differentiating Equation (8.6.33) with respect to the equalizer coefficients  $\{c_n\}$ . Thus, we obtain the necessary conditions for the MMSE as

$$\sum_{n=-N}^N c_n R_Y(n - k) = R_{YA}(k), \quad k = 0, \pm 1, 2, \dots, \pm N \quad (8.6.35)$$

These are  $(2N + 1)$  linear equations for the equalizer coefficients. In contrast to the zero-forcing solution described previously, these equations depend on the statistical properties (the autocorrelation) of the noise as well as the ISI through the autocorrelation  $R_Y(n)$ .

In practice, we would not normally know the autocorrelation  $R_Y(n)$  and the crosscorrelation  $R_{AY}(n)$ . However, these correlation sequences can be estimated by

**<https://hemanthrajhemu.github.io>**

transmitting a test signal over the channel and using the time average estimates

$$\begin{aligned}\hat{R}_Y(n) &= \frac{1}{K} \sum_{k=1}^K y(kT - n\tau)y(kT) \\ \hat{R}_{AY}(n) &= \frac{1}{K} \sum_{k=1}^K y(kT - n\tau) a_k\end{aligned}\tag{8.6.36}$$

in place of the ensemble averages to solve for the equalizer coefficients given by Equation (8.6.35).

**Adaptive Equalizers.** We have shown that the tap coefficients of a linear equalizer can be determined by solving a set of linear equations. In the zero-forcing optimization criterion, the linear equations are given by Equation (8.6.27). On the other hand, if the optimization criterion is based on minimizing the MSE, the optimum equalizer coefficients are determined by solving the set of linear equations given by Equation (8.6.35).

In both cases, we may express the set of linear equations in the general matrix form

$$\mathbf{B}\mathbf{c} = \mathbf{d}\tag{8.6.37}$$

where  $\mathbf{B}$  is a  $(2N + 1) \times (2N + 1)$  matrix,  $\mathbf{c}$  is a column vector representing the  $2N + 1$  equalizer coefficients, and  $\mathbf{d}$  is a  $(2N + 1)$ -dimensional column vector. The solution of Equation (8.6.37) yields

$$\mathbf{c}_{\text{opt}} = \mathbf{B}^{-1}\mathbf{d}\tag{8.6.38}$$

In practical implementations of equalizers, the solution of Equation (8.6.37) for the optimum coefficient vector is usually obtained by an iterative procedure that avoids the explicit computation of the inverse of the matrix  $\mathbf{B}$ . The simplest iterative procedure is the method of steepest descent, in which one begins by choosing arbitrarily the coefficient vector  $\mathbf{c}$ , say  $\mathbf{c}_0$ . This initial choice of coefficients corresponds to a point on the criterion function that is begin optimized. For example, in the case of the MSE criterion, the initial guess  $\mathbf{c}_0$  corresponds to a point on the quadratic MSE surface in the  $(2N + 1)$ -dimensional space of coefficients. The gradient vector, defined as  $\mathbf{g}_0$ , which is the derivative of the MSE with respect to the  $2N + 1$  filter coefficients, is then computed at this point on the criterion surface and each tap coefficient is changed in the direction opposite to its corresponding gradient component. The change in the  $j$ th tap coefficient is proportional to the size of the  $j$ th gradient component.

For example, the gradient vector, denoted as  $\mathbf{g}_k$ , for the MSE criterion, found by taking the derivatives of the MSE with respect to each of the  $2N + 1$  coefficients, is

$$\mathbf{g}_k = \mathbf{B}\mathbf{c}_k - \mathbf{d}, \quad k = 0, 1, 2, \dots\tag{8.6.39}$$

Then the coefficient vector  $\mathbf{c}_k$  is updated according to the relation

$$\mathbf{c}_{k+1} = \mathbf{c}_k - \Delta\mathbf{g}_k\tag{8.6.40}$$

where  $\Delta$  is the *step-size parameter* for the iterative procedure. To ensure convergence of the iterative method,  $\Delta$  must be chosen such that, in each case, the

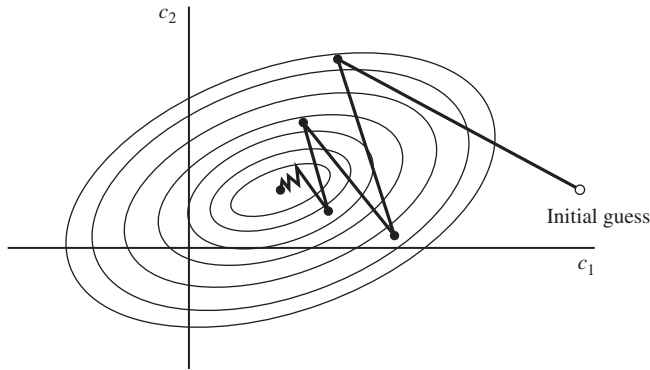


**Figure 8.38** Example of convergence characteristics of a gradient algorithm. (From *Introduction to Adaptive Arrays*, by R.A. Monzigo and T.W. Miller; ©1980 by John Wiley & Sons. Reprinted with permission of the publisher.)

gradient vector  $\mathbf{g}_k$  converges toward zero; i.e.,  $\mathbf{g}_k \rightarrow \mathbf{0}$  as  $k \rightarrow \infty$ , and the coefficient vector  $\mathbf{c}_k \rightarrow \mathbf{c}_{\text{opt}}$  as illustrated in Figure 8.38 based on two-dimensional optimization. In general, convergence of the equalizer tap coefficients to  $\mathbf{c}_{\text{opt}}$  cannot be attained in a finite number of iterations with the steepest-descent method. However, the optimum solution  $\mathbf{c}_{\text{opt}}$  can be approached as closely as desired in a few hundred iterations. In digital communication systems that employ channel equalizers, each iteration corresponds to a time interval for sending one symbol and, hence, a few hundred iterations to achieve convergence to  $\mathbf{c}_{\text{opt}}$  corresponds to a fraction of a second.

Adaptive channel equalization is required for channels whose characteristics change with time. In such a case, the ISI varies with time. The channel equalizer must track such time variations in the channel response and adapt its coefficients to reduce the ISI. In the context of the above discussion, the optimum coefficient vector  $\mathbf{c}_{\text{opt}}$  varies with time due to time variations in the matrix  $\mathbf{B}$  and, for the case of the MSE criterion, time variations in the vector  $\mathbf{d}$ . Under these conditions, the iterative method described above can be modified to use estimates of the gradient components. Thus, the algorithm for adjusting the equalizer tap coefficients may be expressed as

$$\hat{\mathbf{c}}_{k+1} = \hat{\mathbf{c}}_k - \Delta \hat{\mathbf{g}}_k \quad (8.6.41)$$

where  $\hat{\mathbf{g}}_k$  denotes an estimate of the gradient vector  $\mathbf{g}_k$  and  $\hat{\mathbf{c}}_k$  denotes the estimate of the tap coefficient vector.

In the case of the MSE criterion, the gradient vector  $\mathbf{g}_k$  given by Equation (8.6.39) may also be expressed as (see Problem 8.46).

$$\mathbf{g}_k = -E(e_k \mathbf{y}_k)$$

An estimate  $\hat{\mathbf{g}}_k$  of the gradient vector at the  $k$ th iteration is computed as

$$\hat{\mathbf{g}}_k = -e_k \mathbf{y}_k \quad (8.6.42)$$

where  $e_k$  denotes the difference between the desired output from the equalizer at the  $k$ th time interval and the actual output ( $T$ ), and  $\mathbf{y}_k$  denotes the column vector of  $M+1$

received signal values contained in the equalizer at time instant  $k$ . The *error signal*  $e_k$  is expressed as

$$e_k = a_k - z_k \quad (8.6.43)$$

where  $z_k = z(kT)$  is the equalizer output given by Equation (8.6.32) and  $a_k$  is the desired symbol. Hence, by substituting Equation (8.6.42) into Equation (8.6.41), we obtain the adaptive algorithm for optimizing the tap coefficients (based on the MSE criterion) as

$$\hat{\mathbf{c}}_{k+1} = \hat{\mathbf{c}}_k + \Delta e_k \mathbf{y}_k \quad (8.6.44)$$

Since an estimate of the gradient vector is used in Equation (8.6.44) the algorithm is called a *stochastic gradient algorithm*. It is also known as the *LMS algorithm*.

A block diagram of an adaptive equalizer that adapts its tap coefficients according to Equation (8.6.44) is illustrated in Figure 8.39. Note that the difference between the desired output  $a_k$  and the actual output  $z_k$  from the equalizer is used to form the error signal  $e_k$ . This error is scaled by the step-size parameter  $\Delta$ , and the scaled error signal  $\Delta e_k$  multiplies the received signal values  $\{y(kT - n\tau)\}$  at the  $2N + 1$  taps. The products  $\Delta e_k y(kT - n\tau)$  at the  $(2N + 1)$  taps are then added to the previous values of the tap coefficients to obtain the updated tap coefficients, according to Equation (8.6.44). This computation is repeated for each received symbol. Thus, the equalizer coefficients are updated at the symbol rate.

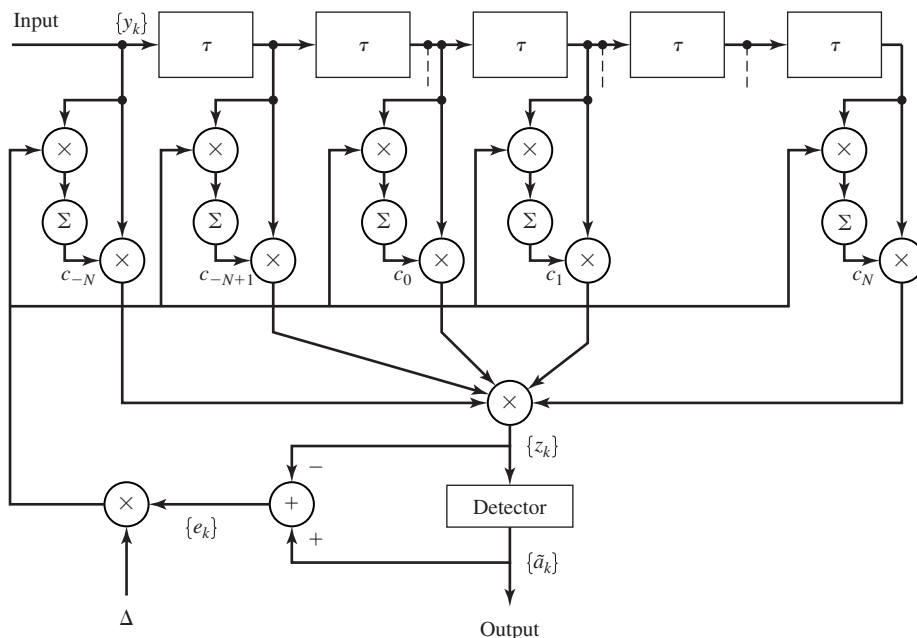


Figure 8.39 Linear adaptive equalizer based on the MSE criterion.

Initially, the adaptive equalizer is trained by the transmission of a known pseudo-random sequence  $\{a_m\}$  over the channel. At the demodulator, the equalizer employs the known sequence to adjust its coefficients. Upon initial adjustment, the adaptive equalizer switches from a *training mode* to a *decision-directed mode*, in which case the decisions at the output of the detector are sufficiently reliable so that the error signal is formed by computing the difference between the detector output and the equalizer output; i.e.,

$$e_k = \tilde{a}_k - z_k \quad (8.6.45)$$

where  $\tilde{a}_k$  is the output of the detector. In general, decision errors at the output of the detector occur infrequently and, consequently, such errors have little effect on the performance of the tracking algorithm given by Equation (8.6.44).

A rule of thumb for selecting the step-size parameter so as to ensure convergence and good tracking capabilities in slowly varying channels is

$$\Delta = \frac{1}{5(2N + 1)P_R} \quad (8.6.46)$$

where  $P_R$  denotes the received signal-plus-noise power, which can be estimated from the received signal.

The convergence characteristics of the stochastic gradient algorithm in Equation (8.6.44) is illustrated in Figure 8.40. These graphs were obtained from a computer simulation of an 11-tap adaptive equalizer operating a channel with a rather modest amount of ISI. The input signal-plus-noise power  $P_R$  was normalized to unity. The rule of thumb given in Equation (8.6.46) for selecting the step size gives  $\Delta = 0.018$ . The effect of making  $\Delta$  too large is illustrated by the large jumps in MSE as shown for  $\Delta = 0.115$ . As  $\Delta$  is decreased, the convergence is slowed somewhat, but a lower MSE is achieved, indicating that the estimated coefficients are closer to  $\mathbf{c}_{\text{opt}}$ .

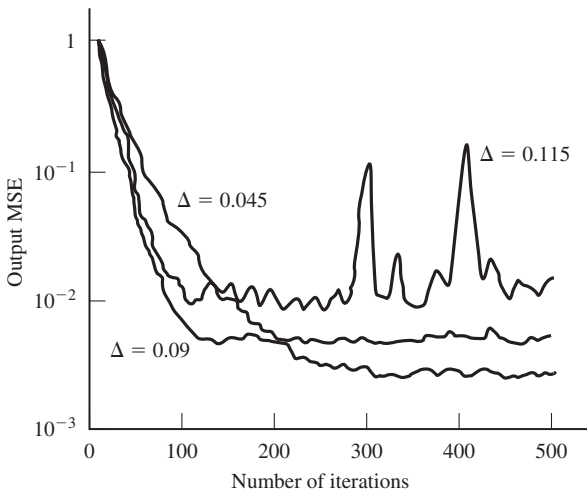


**Figure 8.40** Initial convergence characteristics of the LMS algorithm with different step sizes. (From *Digital Signal Processing* by J. G. Proakis and D. G. Manolakis; ©1988, Macmillan. Reprinted with permission of the publisher.)

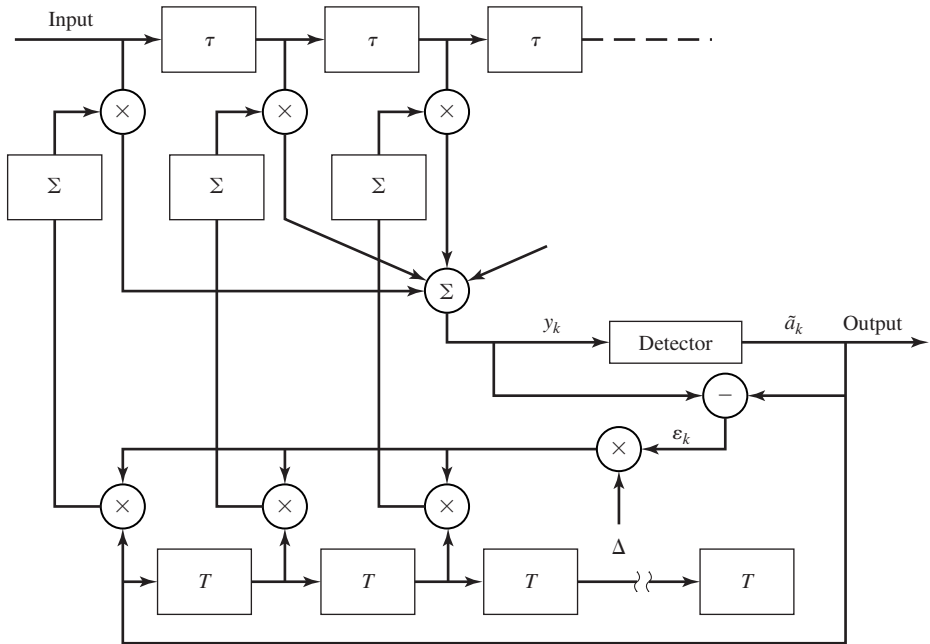
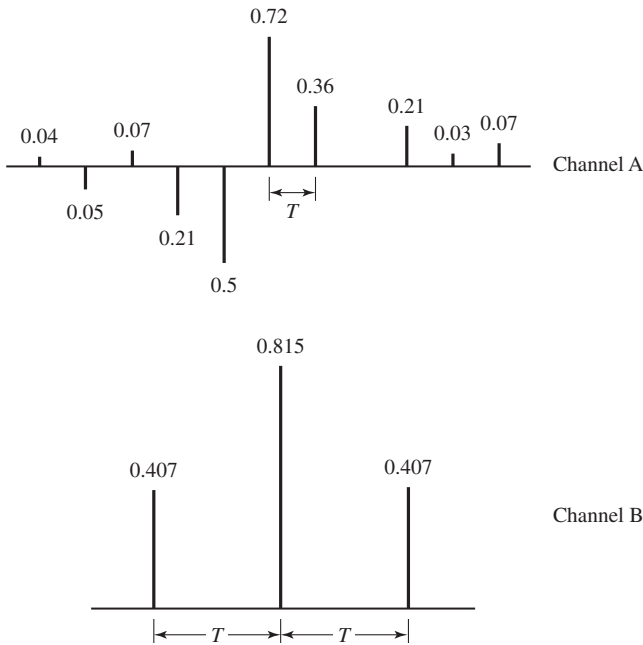


Figure 8.41 An adaptive zero-forcing equalizer.

Although we have described in some detail the operation of an adaptive equalizer which is optimized on the basis of the MSE criterion, the operation of an adaptive equalizer based on the zero-forcing method is very similar. The major difference lies in the method for estimating the gradient vectors  $\mathbf{g}_k$  at each iteration. A block diagram of an adaptive zero-forcing equalizer is shown in Figure 8.41. For more details on the tap coefficient update method for a zero-forcing equalizer, the reader is referred to the papers by Lucky (1965, 1966); and the texts by Lucky, Salz, and Weldon (1968); and Proakis (2001).

**Decision-Feedback Equalizer.** The linear filter equalizers described above are very effective on channels, such as wireline telephone channels, where the ISI is not severe. The severity of the ISI is directly related to the spectral characteristics and not necessarily to the time span of the ISI. For example, consider the ISI resulting from two channels which are illustrated in Figure 8.42. The time span for the ISI in Channel A is 5 symbol intervals on each side of the desired signal component, which has a value of 0.72. On the other hand, the time span for the ISI in Channel B is one symbol interval on each side of the desired signal component, which has a value of 0.815. The energy of the total response is normalized to unity for both channels.

In spite of the shorter ISI span, Channel B results in more severe ISI. This is evidenced in the frequency response characteristics of these channels, which are shown in Figure 8.43. We observe that Channel B has a spectral null (the frequency response

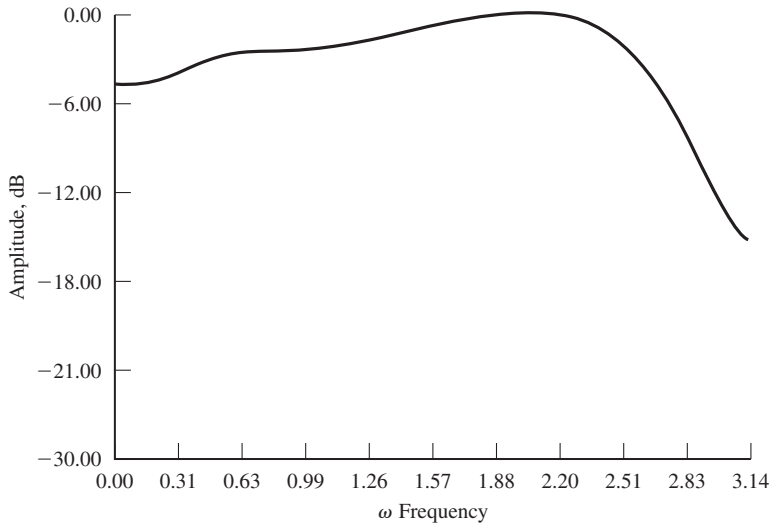


**Figure 8.42** Two channels with ISI.

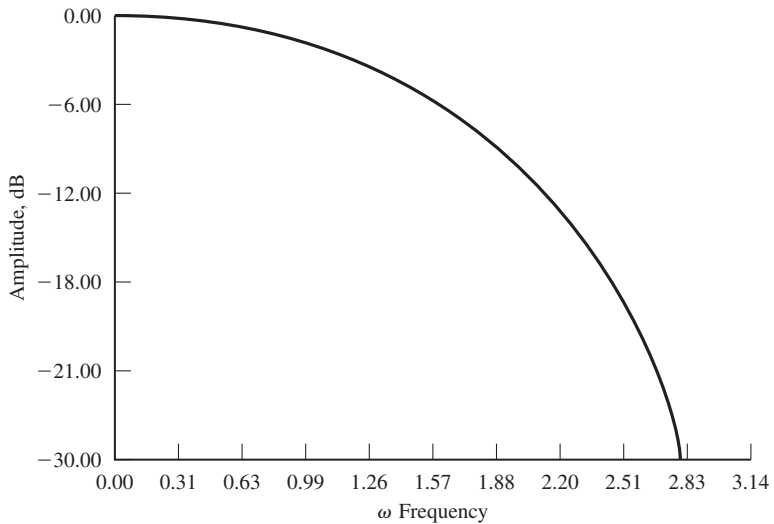
not occur in the case of Channel A. Consequently, a linear equalizer will introduce a large gain in its frequency response to compensate for the channel null. Thus, the noise in Channel B will be enhanced much more than in Channel A. This implies that the performance of the linear equalizer for Channel B will be significantly poorer than that for Channel A. This fact is borne out by the computer simulation results for the performance of the linear equalizer for the two channels, as shown in Figure 8.44. Hence, the basic limitation of a linear equalizer is that it performs poorly on channels having spectral nulls. Such channels are often encountered in radio communications, such as ionospheric transmission at frequencies below 30 MHz and mobile radio channels, such as those used for cellular radio communications.

A *decision-feedback equalizer* (DFE) is a nonlinear equalizer that employs previous decisions to eliminate the ISI caused by previously detected symbols on the current symbol to be detected. A simple block diagram for a DFE is shown in Figure 8.45. The DFE consists of two filters. The first filter is called a *feedforward filter* and it is generally a fractionally spaced FIR filter with adjustable tap coefficients. This filter is identical in form to the linear equalizer described above. Its input is the received filtered signal  $y(t)$ . The second filter is a *feedback filter*. It is implemented as an FIR filter with symbol-spaced taps having adjustable coefficients. Its input is the set of previously detected symbols. The output of the feedback filter is subtracted from the output of the feedforward filter to form the input to the detector. Thus, we have

$$z_m = \sum_{n=0}^{N_1} c_n y(mT - n\tau) - \sum_{n=0}^{N_2} b_n \tilde{a}_{m-n} \quad (8.6.47)$$



(a)



(b)

**Figure 8.43** Amplitude spectra for (a) channel A shown in Figure 8.42(a) and (b) channel B shown in Figure 8.42(b).

where  $\{c_n\}$  and  $\{b_n\}$  are the adjustable coefficients of the feedforward and feedback filters, respectively,  $\tilde{a}_{m-n}$ ,  $n = 1, 2, \dots, N_2$  are the previously detected symbols,  $N_1$  is the length of the feedforward filter and  $N_2$  is the length of the feedback filter. Based on the input  $z_m$ , the detector determines which of the possible transmitted symbols is closest in distance to the input signal  $z_m$ . Thus, it makes its decision and outputs  $\tilde{a}_m$ .

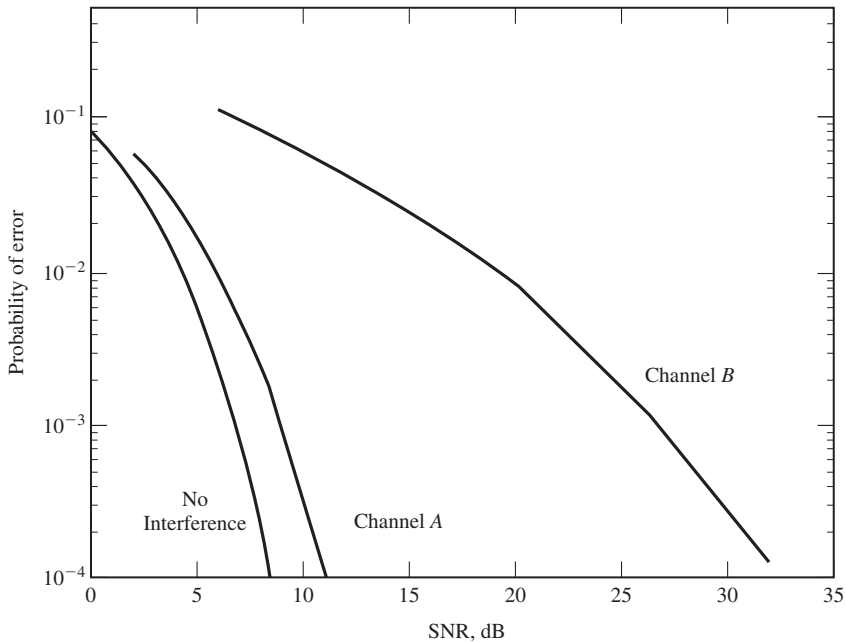


**Figure 8.44** Error-rate performance of linear MSE equalizer.

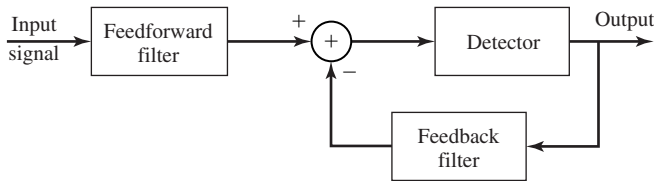


**Figure 8.45** Block diagram of DFE.

What makes the DFE nonlinear is the nonlinear characteristic of the detector which provides the input to the feedback filter.

The tap coefficients of the feedforward and feedback filters are selected to optimize some desired performance measure. For mathematical simplicity, the MSE criterion is usually applied and a stochastic gradient algorithm is commonly used to implement an adaptive DFE. Figure 8.46 illustrates the block diagram of an adaptive DFE whose tap coefficients are adjusted by means of the LMS stochastic gradient algorithm. Figure 8.47 illustrates the probability of error performance of the DFE, obtained by computer simulation, for binary PAM transmission over Channel B. The gain in performance relative to that of a linear equalizer is clearly evident.

We should mention that decision errors from the detector that are fed to the feedback filter have a small effect on the performance of the DFE. In general, a small

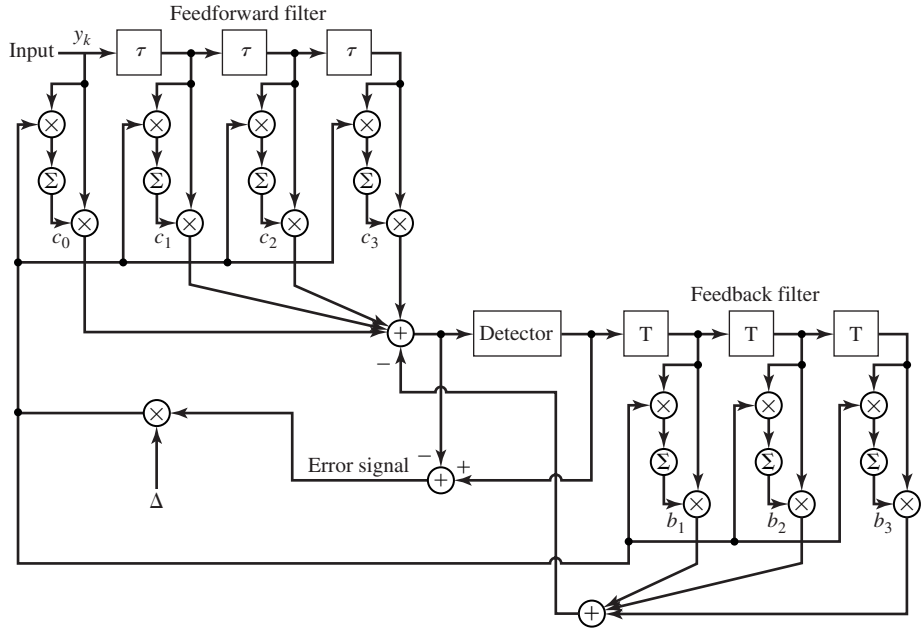


Figure 8.46 Adaptive DFE.

loss in performance of one to two dB is possible at error rates below  $10^{-2}$ , but the decision errors in the feedback filters are not catastrophic.

Although the DFE outperforms a linear equalizer, it is not the optimum equalizer from the viewpoint of minimizing the probability of error. As indicated previously, the optimum detector in a digital communication system in the presence of ISI is a ML symbol sequence detector. It is particularly appropriate for channels with severe ISI, when the ISI spans only a few signals. For example Figure 8.48 illustrates the error probability performance of the Viterbi algorithm for a binary PAM signal transmitted through channel B (see Figure 8.42). For purposes of comparison, we also illustrate the probability of error for a decision feedback equalizer. Both results were obtained by computer simulation. We observe that the performance of the ML sequence detector is about 4.5-dB better than that of the DFE at an error probability of  $10^{-4}$ . Hence, this is one example where the ML sequence detector provides a significant performance gain on a channel which has a relatively short ISI span.

In conclusion, we mention that adaptive equalizers are widely used in high-speed digital communication systems for telephone channels. High-speed telephone line modems (bit rate above 2400 bps) generally include an adaptive equalizer that is implemented as an FIR filter with coefficients that are adjusted based on the MMSE criterion. Depending on the data speed, the equalizer typically spans between 20 and 70 symbols. The LMS algorithm given by Equation (8.6.44) is usually employed for

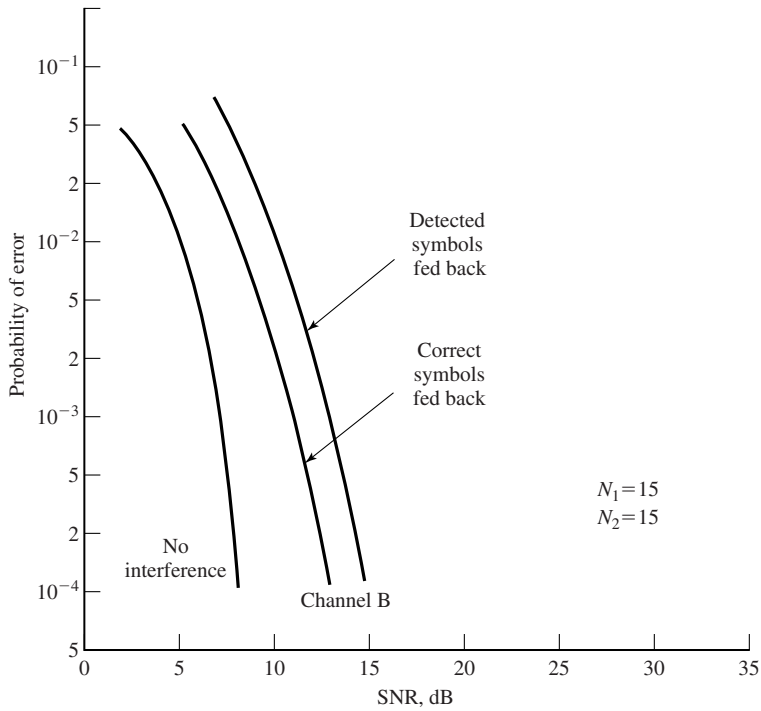


Figure 8.47 Performance of DFE with and without error propagation.

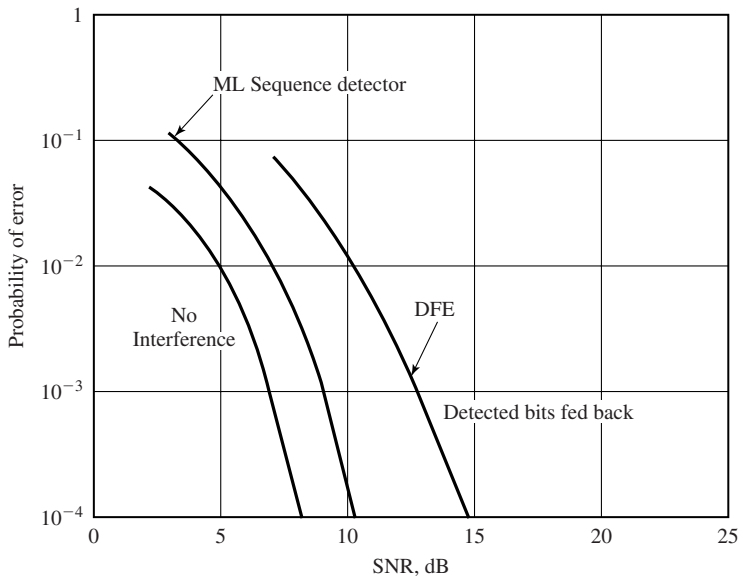


Figure 8.48 Performance of Viterbi detector and DFE for channel B

## 8.7 MULTICARRIER MODULATION AND OFDM

In the preceding sections, we considered digital transmission through nonideal channels and observed that such channels cause intersymbol interference when the reciprocal of the system rate is significantly smaller than the time dispersion (duration of the impulse response) of the nonideal channel. In such a case, a channel equalizer is employed at the receiver to compensate for the channel distortion. If the channel is a bandpass channel with a specified bandwidth, the information-bearing signal may be generated at the baseband and then translated in frequency to the passband of the channel. Thus, the information-bearing signal is transmitted on a single carrier. We also observed that intersymbol interference usually results in some performance degradation, even in the case where the optimum detector is used to recover the information symbols at the receiver.

An alternative approach to the design of a bandwidth-efficient communication system in the presence of channel distortion is to subdivide the available channel bandwidth into a number of equal-bandwidth subchannels, where the bandwidth of each subchannel is sufficiently narrow so that the frequency response characteristics of the subchannels are nearly ideal. Such a subdivision of the overall bandwidth into smaller subchannels is illustrated in Figure 8.49. Thus, we create  $K = W/\Delta f$  subchannels, where different information symbols can be transmitted simultaneously in the  $K$  subchannels. Consequently, the data is transmitted by frequency-division multiplexing (FDM).

With each subchannel, we associate a carrier

$$x_k(t) = \sin 2\pi f_k t, \quad k = 0, 1, \dots, K - 1 \quad (8.7.1)$$

where  $f_k$  is the mid-frequency in the  $k$ th subchannel. By selecting the symbol rate  $1/T$  on each of the subchannels to be equal to the separation  $\Delta f$  of adjacent subcarriers, the subcarriers are orthogonal over the symbol interval  $T$ , independent of the relative phase relationship between subcarriers; i.e.,

$$\int_0^T \sin(2\pi f_k t + \phi_k) \sin(2\pi f_j t + \phi_j) dt = 0 \quad (8.7.2)$$

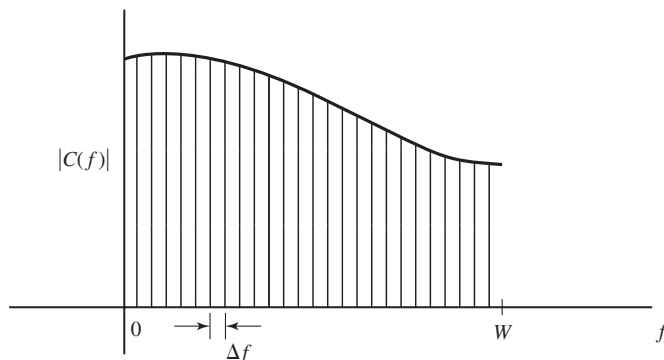


**Figure 8.49** Subdivision of the channel bandwidth  $W$  into narrowband

where  $f_k - f_j = n/T$ ,  $n = 1, 2, \dots$ , independent of the values of the phases  $\phi_k$  and  $\phi_j$ . In this case, we have orthogonal frequency-division multiplexing (OFDM).

With an OFDM system having  $K$  subchannels, the symbol rate on each subcarrier is reduced by a factor of  $N$  relative to the symbol rate on a single carrier system that employs the entire bandwidth  $W$  and transmits data at the same rate as OFDM. Hence, the symbol interval in the OFDM system is  $T = KT_s$ , where  $T_s$  is the symbol interval in the single-carrier system. By selecting  $K$  to be sufficiently large, the symbol interval  $T$  can be made significantly larger than the time duration of the channel-time dispersion. Thus, intersymbol interference can be made arbitrarily small by selection of  $K$ . In other words, each subchannel appears to have a fixed frequency response  $C(f_k)$ ,  $k = 0, 1, \dots, K - 1$ .

As long as we maintain time synchronization among the subcarriers, OFDM allows us to transmit a different number of bits/symbol on each subcarrier. Hence, subcarriers that yield a higher SNR due to a lower attenuation can be modulated to carry more bits/symbol than subchannels that yield a lower SNR (high attenuation). For example, QAM with different constellation sizes may be used in an OFDM system.

The modulator and demodulator in an OFDM system can be implemented by use of a parallel bank of filters based on the discrete Fourier transform (DFT). When the number of subchannels is large, say  $K > 25$ , the modulator and demodulator in an OFDM system are efficiently implemented by use of the fast Fourier transform algorithm (FFT) to compute the DFT. Next, we describe an OFDM system in which the modulator and demodulator are implemented based on the DFT.

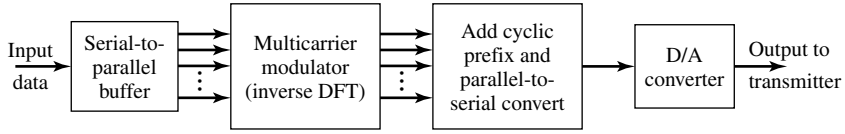
A major problem with the multicarrier modulation in general and OFDM system in particular is the high peak-to-average power ratio (PAR) that is inherent in the transmitted signal. Large signal peaks occur in the transmitted signal when the signals in the  $K$  subchannels add constructively in phase. Such large signal peaks may saturate the power amplifier at the transmitter and, thus, cause intermodulation distortion in the transmitted signal. Intermodulation distortion can be reduced and, generally, avoided by reducing the power in the transmitted signal and, thus, operating the power amplifier at the transmitter in the linear range. Such a power reduction results in inefficient operation of the OFDM system.

A variety of methods have been devised to reduce PAR in multicarrier systems. A relatively simple method is to insert different phase shifts in each of the subcarriers, where the phase shifts are selected pseudorandomly, or by means of some algorithm, to reduce the PAR. Additional methods are cited in the references cited in Section 8.8.

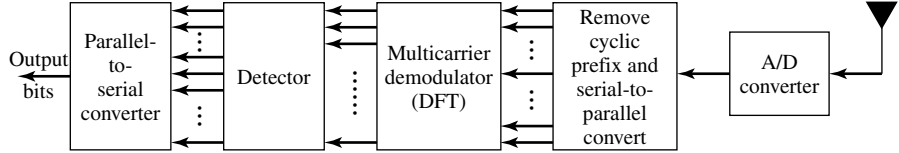
### 8.7.1 An OFDM System Implemented via the FFT Algorithm

In this section, we describe an OFDM system in which QAM is used for data transmission on each of the subcarriers and the FFT algorithm is used in the implementation of the modulator and demodulator.

The basic block diagram of the OFDM is illustrated in Figure 8.50. A serial-to-parallel buffer subdivides the information sequence into frames of  $B_f$  bits. The  $B_f$  bits in each frame are processed into  $M$  groups, where  $M$  is the number of subcarriers assigned to bits.



(a) Transmitter

**Figure 8.50** Block diagram of a multicarrier OFDM digital communication system.

Hence,

$$\sum_{i=1}^K b_i = B_f \quad (8.7.3)$$

We may view the multicarrier modulator as generating  $K$  independent QAM subchannels, where the symbol rate for each subchannel is  $1/T$  and the signal in each subchannel has a distinct QAM constellation. Hence, the number of signal points for the  $i$ th subchannel is  $M_i = 2^{b_i}$ . Let us denote the complex-valued signal points corresponding to the information signals on the  $K$  subchannels by  $X_k$ ,  $k = 0, 1, \dots, K - 1$ . These information symbols  $\{X_k\}$  represent the values of the discrete Fourier transform (DFT) of a multicarrier OFDM signal  $x(t)$ , where the modulation on each subcarrier is QAM. Since  $x(t)$  must be a real-valued signal, its  $N$ -point DFT  $\{X_k\}$  must satisfy the symmetry property  $X_{N-k} = X_k^*$ . Therefore, we create  $N = 2K$  symbols from  $K$  information symbols by defining

$$X_{N-k} = X_k^*, \quad k = 1, 2, \dots, K - 1 \quad (8.7.4)$$

$$X'_0 = \text{Re}(X_0) \quad (8.7.5)$$

$$X_N = \text{Im}(X_0) \quad (8.7.6)$$

Note that the information symbol  $X_0$  is split into two parts, both of which are real. If we denote the new sequence of symbols as  $\{X'_k, k = 0, 1, \dots, N - 1\}$ , the  $N$ -point inverse DFT (IDFT) yields the real-valued sequence

$$x_n = \frac{1}{\sqrt{N}} \sum_{k=0}^{N-1} X'_k e^{j2\pi nk/N} \quad n = 0, 1, \dots, N - 1 \quad (8.7.7)$$

where  $1/\sqrt{N}$  is simply a scale factor. This sequence  $\{x_n, 0 \leq n \leq N - 1\}$  corresponds to samples of the multicarrier OFDM signal  $x(t)$ , consisting of  $K$  subcarriers, which

may be expressed as

$$x(t) = \frac{1}{\sqrt{N}} \sum_{k=0}^{N-1} X'_k e^{j2\pi kt/T}, \quad 0 \leq t \leq T \quad (8.7.8)$$

where  $T$  is the signal duration and  $x_n = x(nT/N)$ ,  $n = 0, 1, \dots, N-1$ . The subcarrier frequencies are  $f_k = k/T$ ,  $k = 0, 1, \dots, K-1$ . The signal samples  $\{x_n\}$  generated by computing the IDFT are passed through a digital-to-analog (D/A) converter, where output, ideally, is the OFDM signal waveform  $x(t)$ .

With  $x(t)$  as the input to the channel, the channel output at the receiver may be expressed as

$$r(t) = x(t) \star c(t) + n(t) \quad (8.7.9)$$

where  $c(t)$  is the impulse response of the channel and  $\star$  denotes convolution. Since the bandwidth  $\Delta f$  of each subchannel is selected to be very small relative to the overall channel bandwidth  $W = K\Delta f$ , the symbol duration  $T = 1/\Delta f$  is large compared to the duration of the channel impulse response. To be specific, suppose that the channel impulse response spans  $m+1$  signal samples, where  $m \ll N$ . A simple way to completely avoid intersymbol interference (ISI) is to insert a time guard of duration  $mT/N$  between transmission of successive data blocks. This allows the response of the channel to die out before the next block of  $K$  symbols are transmitted.

An alternative method to avoid ISI is to append a so-called cyclic prefix to each block of  $N$  signal samples  $\{x_n, 0 \leq n \leq N-1\}$ . The cyclic prefix for the block of samples consists of the samples  $x_{N-m}, x_{N-m+1}, \dots, x_{N-1}$ . These samples are appended to the beginning of the block, thus, creating a signal sequence of length  $N+m$  samples, which may be indexed from  $n = -m$  to  $n = N-1$ , where the first  $m$  samples constitute the cyclic prefix. Then, if the sample values of the channel response are  $\{c_n, 0 \leq n \leq m\}$ , the convolution of  $\{c_n\}$  with  $\{x_n, -m \leq n \leq N-1\}$  produce the received signal  $\{r_n\}$ . Since the ISI in any pair of successive signal transmission blocks affects the first  $m$  signal samples, we discard the first  $m$  samples of  $\{r_n\}$  and demodulate the signal based on the received signal samples  $\{r_n, 0 \leq n \leq N-1\}$ .

If we view the channel characteristics in the frequency domain, the channel frequency response at the subcarrier frequencies  $f_k = k/T$  is

$$C_k = C \left( \frac{2\pi k}{N} \right) = \sum_{n=0}^m c_n e^{-j2\pi nk/N}, \quad k = 0, 1, \dots, N-1 \quad (8.7.10)$$

Since the ISI is eliminated by the use of either the cyclic prefix or the time guard band, the demodulated sequence of symbols may be expressed as

$$\hat{X}_k = C_k X'_k + \eta_k, \quad k = 0, 1, \dots, N-1 \quad (8.7.11)$$

where  $\{\hat{X}_k\}$  is the output of the  $N$ -point DFT computed by the demodulator and  $\{\eta_k\}$  is the additive noise corrupting the signal.

As illustrated in Figure 8.50, the received signal is demodulated by computing the DFT of the received signal after it has been passed through an analog-to-digital

(A/D) converter. As in the case of the OFDM modulator, the DFT computation at the demodulator is performed efficiently by use of the FFT algorithm.

In order to recover the information symbols from the values of the computed DFT, it is necessary to estimate and compensate for the channel factors  $\{C_k\}$ . The channel measurement can be accomplished by initially transmitting either a known modulated sequence on each of the subcarriers or, simply, transmitting the unmodulated subcarriers. If the channel characteristics vary slowly with time, the time variations can be tracked by using the decisions at the output of the detector in a decision-directed manner. Thus, the multicarrier OFDM system can be made to operate adaptively. The transmission rate on each of the subcarriers can be optimized by properly allocating the average transmitted power and the number of bits that are transmitted by each subcarrier. The SNR per subchannel may be defined as

$$\text{SNR}_k = \frac{T P_k |C_k|^2}{\sigma_{nk}^2} \quad (8.7.12)$$

where  $T$  is the symbol duration,  $P_k$  is the average transmitted power allocated to the  $k$ th subchannel,  $|C_k|^2$  is the squared magnitude of the frequency response of the  $k$ th subchannel, and  $\sigma_{nk}^2$  is the corresponding noise variance. In subchannels with high SNR, we transmit more bits/symbol by using a larger QAM constellation compared to subchannels with low SNR. Thus, the bit rate on each subchannel can be optimized in such a way that the error-rate performance among the subchannels is equalized to satisfy the desired specifications.

Multicarrier OFDM using QAM modulation on each of the subcarriers as described above has been implemented for a variety of applications, including high-speed transmission over telephone lines, such as digital subcarrier lines. This type of multicarrier OFDM modulation has also been called *discrete-multitone (DMT) modulation*. Multicarrier OFDM is also used in digital audio broadcasting in Europe and other parts of the world and in digital cellular communication systems.

## 8.8 FURTHER READING

The pioneering work on signal design for bandwidth-constrained channels was done by Nyquist (1928). The use of binary partial response signals was originally proposed in the paper by Lender (1963) and was later generalized by Kretzmer (1966). The problem of optimum transmitter and receiver filter design was investigated by Gerst and Diamond (1961), Tufts (1965), Smith (1965), and Berger and Tufts (1967).

Adaptive equalization for digital communication was introduced by Lucky (1965, 1966). Widrow (1966) devised the LMS algorithm for adaptively adjusting the equalizer coefficients.

The Viterbi algorithm was devised by Viterbi (1967) for the purpose of decoding convolutional codes, which are described in Chapter 9. Its use as the ML sequence detector for partial response signals and, more generally, for symbols corrupted by

intersymbol interference, was proposed and analyzed by Forney (1972) and Omura (1971). A comprehensive treatment of adaptive equalization algorithms is given in the book by Proakis (2001).

There is a large amount of literature on multicarrier digital communication systems. One of the earliest systems, described by Doeltz et al. (1957) and called Kineplex, was used for digital transmission in the high-frequency radio band. Other early work on the multicarrier system design is described in the papers by Chang (1966) and Saltzberg (1967). The use of DFT for modulation and demodulation of multicarrier OFDM systems was proposed by Weinstein and Ebert (1971). More recent references on applications of OFDM in practical systems are the papers by Chow et al. (1995) and Bingham (1990). The recent book by Bahai and Saltzberg (1999) provides a comprehensive treatment of OFDM.

The problem of PAR reduction in multicarrier systems has been investigated by many people. The interested reader may refer to the papers by Boyd (1986), Popovic (1991), Jones et al. (1994), Wilkinson and Jones (1995), Wulich (1996), Tellado and Cioffi (1998), and Tarokh and Jafarkhani (2000).

## PROBLEMS

- 8.1** In Example 8.1.1, the ideal channel of bandwidth  $W$  limits the transmitted signal energy that passes through the channel. The received signal energy as a function of the channel bandwidth is

$$\mathcal{E}_h(W) = \frac{T}{(2\pi)^2} \int_{-WT}^{WT} \frac{\sin^2 \pi \alpha}{\alpha^2(1 - \alpha^2)^2} d\alpha$$

where  $\alpha = fT$ .

1. Evaluate (numerically)  $\mathcal{E}_h(W)$  for  $W = \frac{1}{2T}, \frac{1}{T}, \frac{1.5}{T}, \frac{2}{T}, \frac{2.5}{T}, \frac{3}{T}$ , and plot  $\frac{\mathcal{E}_h(W)}{T}$  as a function of  $W$ .
2. Determine the value of  $\mathcal{E}_h(W)$  in the limit as  $W \rightarrow \infty$ . For the computation you may use the time-domain relation

$$\lim_{W \rightarrow \infty} \mathcal{E}_h(W) = \int_{-\infty}^{+\infty} g_T^2(t) dt$$

- 8.2** In a binary PAM system, the input to the detector is

$$y_m = a_m + n_m + i_m$$

where  $a_m = \pm 1$  is the desired signal,  $n_m$  is a zero-mean Gaussian random variable with variance  $\sigma_n^2$ , and  $i_m$  represents the ISI due to channel distortion. The ISI term is a random variable which takes the values,  $-\frac{1}{2}, 0, \frac{1}{2}$  with probabilities  $\frac{1}{4}, \frac{1}{2}, \frac{1}{4}$ , respectively. Determine the average probability of error as a function of  $\sigma_n^2$ .

- 8.3** In a binary PAM system, the clock that specifies the sampling of the correlator output is offset from the optimum sampling time by 10%.

1. If the signal pulse used is rectangular, determine the loss in SNR due to the mistiming.
  2. Determine the amount of intersymbol interference introduced by the mistiming and determine its effect on performance.
- 8.4 The elements of the sequence  $\{a_n\}_{n=-\infty}^{+\infty}$  are independent binary random variables taking values of  $\pm 1$  with equal probability. This data sequence is used to modulate the basic pulse  $g(t)$  shown in Figure P-8.4(a). The modulated signal is

$$X(t) = \sum_{n=-\infty}^{+\infty} a_n g(t - nT)$$

1. Find the power-spectral density of  $X(t)$ .
2. If  $g_1(t)$  [shown in Figure P-8.4(b)] is used instead of  $g(t)$ , how would the power spectrum in part 1 change?
3. In part 2, assume we want to have a null in the spectrum at  $f = \frac{1}{4T}$ . This is done by a precoding of the form  $b_n = a_n + \alpha a_{n-1}$ . Find  $\alpha$  that provides the desired null.
4. Is it possible to employ a precoding of the form  $b_n = a_n + \sum_{i=1}^N \alpha_i a_{n-i}$  for some finite  $N$  such that the final power spectrum will be identical to zero for  $\frac{1}{3T} \leq |f| \leq \frac{1}{2T}$ ? If yes, how? If no, why? (Hint: use properties of analytic functions.)

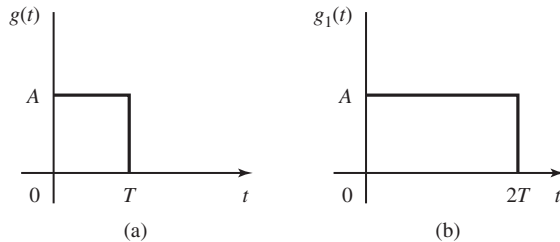


Figure P-8.4

- 8.5 The information sequence  $\{a_n\}_{n=-\infty}^{\infty}$  is a sequence of i.i.d. random variables each taking values  $+1$  and  $-1$  with equal probability. This sequence is to be transmitted at baseband by a biphase coding scheme described by

$$s(t) = \sum_{n=-\infty}^{\infty} a_n g(t - nT)$$

where  $g(t)$  is shown in Figure P-8.5.

1. Find the power-spectral density of  $s(t)$ .
2. Assume that it is desirable to have a null in the power spectrum at  $f = \frac{1}{T}$ . To this end we use a precoding scheme by introducing  $b_n = a_n + ka_{n-1}$ , where  $k$  is some constant, and then transmit the  $\{b_n\}$  sequence using the same  $g(t)$ . Is it possible to choose  $k$  to produce a frequency null at  $f = \frac{1}{T}$ ? If yes what is the appropriate value and what is the resulting power spectrum?
3. Now assume we want to have nulls at all multiples of  $f_0 = \frac{1}{2T}$ . Is it possible to have these nulls with an appropriate choice of  $k$  in the previous part? If not what kind of precoding do you suggest to result in the desired nulls?

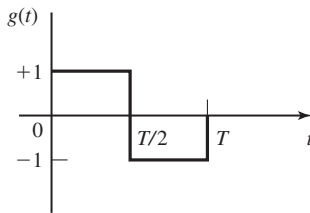


Figure P-8.5

- 8.6** The two signal waveforms for binary PSK signal transmission with discontinuous phase are

$$s_0(t) = \sqrt{\frac{2\mathcal{E}_b}{T_b}} \cos \left[ 2\pi \left( f - \frac{\Delta f}{2} \right) t + \theta_0 \right], \quad 0 \leq t \leq T$$

$$s_1(t) = \sqrt{\frac{2\mathcal{E}_b}{T_b}} \cos \left[ 2\pi \left( f + \frac{\Delta f}{2} \right) t + \theta_1 \right], \quad 0 \leq t \leq T$$

where  $\Delta f = 1/T \ll f_c$ , and  $\theta_0$  and  $\theta_1$  are uniformly distributed random variables on the interval  $(0, 2\pi)$ . The signals  $s_0(t)$  and  $s_1(t)$  are equally probable.

1. Determine the power-spectral density of the FSK signal.
  2. Show that the power-spectral density decays as  $1/f^2$  for  $f \gg f_c$ .
- 8.7** Consider a four-phase PSK signal that is represented by the equivalent lowpass signal.

$$v(t) = \sum_n a_n g(t - nT)$$

where  $a_n$  takes on one of the four possible values  $\frac{\pm 1 \pm j}{\sqrt{2}}$  with equal probability.

The sequence of information symbols  $\{a_n\}$  is statistically independent.

1. Determine and sketch the power-spectral density of  $v(t)$  when

$$g(t) = \begin{cases} A, & 0 \leq t \leq T \\ 0, & \text{otherwise} \end{cases}$$

2. Repeat part 1 when

$$g(t) = \begin{cases} A \sin \frac{\pi t}{2}, & 0 \leq t \leq T \\ 0, & \text{otherwise} \end{cases}$$

3. Compare the spectra obtained in parts 1 and 2 in terms of the 3-dB bandwidth and the bandwidth to the first spectral null.

- 8.8** Starting with the definition of the transition probability matrix for delay modulation given in Example 8.5.11, demonstrate that the relation

$$\mathbf{P}^4 \gamma = -\frac{1}{4} \gamma$$

holds and, hence,

$$\mathbf{P}^{k+4} \gamma = -\frac{1}{4} \mathbf{P}^k \gamma, \quad k \geq 1$$

- 8.9** The frequency-response characteristic of a lowpass channel can be approximated by

$$H(f) = \begin{cases} 1 + \alpha \cos 2\pi f t_0, & |\alpha| < 1, \quad |f| \leq W \\ 0, & \text{otherwise} \end{cases}$$

where  $W$  is channel bandwidth. An input signal  $s(t)$  whose spectrum is bandlimited to  $W$  Hz is passed through the channel.

1. Show that

$$y(t) = s(t) + \frac{\alpha}{2} [s(t - t_0) + s(t + t_0)]$$

Thus, the channel produces a pair of echoes.

2. Suppose the received signal  $y(t)$  is passed through a filter matched to  $s(t)$ . Determine the output of the matched filter at  $t = kT$ ,  $k = 0, \pm 1, \pm 2, \dots$ , where  $T$  is the symbol duration.
3. What is the ISI pattern resulting from the channel if  $t_0 = T$ ?

- 8.10** A wireline channel of length 1000 km is used to transmit data by means of binary PAM. Regenerative repeaters are spaced at 50-km apart along the system. Each segment of the channel has an ideal (constant) frequency response over the frequency band  $0 \leq f \leq 1200$ , and an attenuation of 1 dB/km. The channel noise is AWGN.

1. What is the highest bit rate that can be transmitted without ISI?
2. Determine the required  $\mathcal{E}_b/N_0$  to achieve a bit error of  $P_2 = 10^{-7}$  for each

3. Determine the transmitted power at each repeater to achieve the desired  $\mathcal{E}_b/N_0$ , where  $N_0 = 4.1 \times 10^{-21}$  W/Hz.
- 8.11 Show that a pulse having the raised cosine spectrum given by Equation (8.3.22) satisfies the Nyquist criterion given by Equation (8.3.9) for any value of the roll-off factor  $\alpha$ .
- 8.12 Show that for any value of  $\alpha$  the raised cosine spectrum given by Equation (8.3.22) satisfies

$$\int_{-\infty}^{+\infty} X_{rc}(f) df = 1$$

(Hint: Use the fact that  $X_{rc}(f)$  satisfies the Nyquist criterion given by Equation (8.3.9).

- 8.13 Theorem 8.3.1 gives the necessary and sufficient condition for the spectrum  $X(f)$  of the pulse  $x(t)$  that yields zero ISI. Prove that for any pulse that is bandlimited to  $|f| < 1/T$ , the zero ISI condition is satisfied if  $\text{Re}[X(f)]$ , for  $f > 0$ , consists of a rectangular function plus an arbitrary odd function about  $f = 1/2T$  and  $\text{Im}[X(f)]$  is any arbitrary even function about  $f = 1/2T$ .
- 8.14 A voice-band telephone channel has a passband characteristic in the frequency range  $300 < f < 3000$  Hz.
1. Select a symbol rate and a power efficient constellation size to achieve 9600 bits/sec signal transmission.
  2. If a square-root raised cosine pulse is used for the transmitter pulse  $g_T(t)$ , select the roll-off factor. Assume that the channel has an ideal frequency response characteristic.
- 8.15 Design an  $M$ -ary PAM system that transmits digital information over an ideal channel with bandwidth  $W = 2400$  Hz. The bit rate is 14,400 bits/sec. Specify the number of transmitted points, the number of received signal points using a duobinary signal pulse, and the required  $\mathcal{E}_b$  to achieve an error probability of  $10^{-6}$ . The additive noise is zero-mean Gaussian with a power-spectral density  $10^{-4}$  W/Hz.
- 8.16 A binary PAM signal is generated by exciting a raised cosine roll-off filter with a 50% roll-off factor and is then DSB-SC amplitude modulated on a sinusoidal carrier as illustrated in Figure P-8.16. The bit rate is 2400 bits/sec.

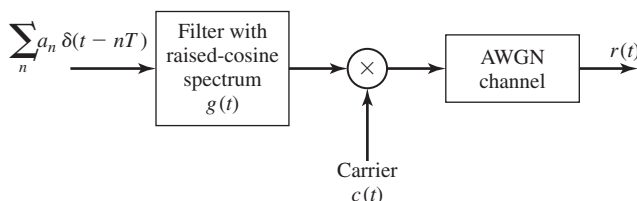
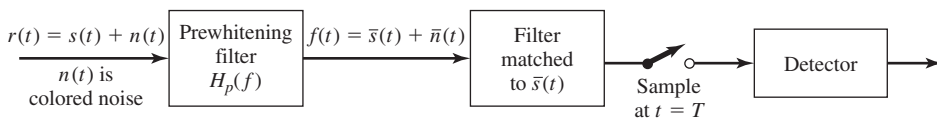


Figure P-8.16

1. Determine the spectrum of the modulated binary PAM signal and sketch it.
  2. Draw the block diagram illustrating the optimum demodulator/detector for the received signal which is equal to the transmitted signal plus additive, white Gaussian noise.
- 8.17** When the additive noise at the input to the modulator is colored, the filter matched to the signal no longer maximizes the output SNR. In such a case we may consider the use of a prefilter that “whitens” the colored noise. The prefilter is followed by a filter matched to the prefiltered signal. Towards this end, consider the configuration shown in Figure P-8.17.
1. Determine the frequency-response characteristic of the prefilter that whitens the noise.
  2. Determine the frequency-response characteristic of the filter matched to  $\bar{s}(t)$ .
  3. Consider the prefilter and the matched filter as a single “generalized matched filter.” What is the frequency-response characteristic of this filter?
  4. Determine the SNR at the input to the detector.



**Figure P-8.17**

- 8.18** A voice-band telephone channel passes the frequencies in the band from 300 to 3300 Hz. It is desired to design a modem that transmits at a symbol rate of 2400 symbols/sec, with the objective of achieving 9600 bits/sec. Select an appropriate QAM signal constellation, carrier frequency, and the roll-off factor of a pulse with a raised cosine spectrum that utilizes the entire frequency band. Sketch the spectrum of the transmitted signal pulse and indicate the important frequencies.
- 8.19** Determine the bit rate that can be transmitted through a 4 KHz voice-band telephone (bandpass) channel if the following modulation methods are used: (1) binary PSK, (2) four-phase PSK, (3) 8-point QAM, (4) binary orthogonal FSK, with noncoherent detection, (5) orthogonal four-FSK with noncoherent detection, and (6) orthogonal 8-FSK with noncoherent detection. For parts 1–3, assume that the transmitter pulse shape has a raised cosine spectrum with a 50% roll-off.
- 8.20** An ideal voice-band telephone line channel has a bandpass frequency-response characteristic spanning the frequency range 600–3000 Hz.

1. Design an  $M = 4$  PSK (quadrature PSK or QPSK) system for transmitting data at a rate of 2400 bits/sec and a carrier frequency  $f_c = 1800$ . For spectral

shaping, use a raised cosine frequency-response characteristic. Sketch a block diagram of the system and describe their functional operation.

2. Repeat part 1 if the bit rate  $R = 4800$  bits/sec.
- 8.21** A 4 KHz bandpass channel is to be used for transmission of data at a rate of 9600 bits/sec. If  $N_0/2 = 10^{-10}$  W/Hz is the spectral density of the additive, zero-mean Gaussian noise in the channel, design a QAM modulation and determine the average power that achieves a bit-error probability of  $10^{-6}$ . Use a signal pulse with a raised cosine spectrum having a roll-off factor of at least 50%.
- 8.22** Consider the transmission of data via PAM over a voice-band telephone channel that has a bandwidth of 3000 Hz. Show how the symbol rate varies as a function of the excess bandwidth. In particular, determine the symbol rate for excess bandwidths of 25%, 33%, 50%, 67%, 75%, and 100%.
- 8.23** The binary sequence 10010110010 is the input to the precoder whose output is used to modulate a duobinary transmitting filter. Construct a table as in Table 8.2 showing the precoded sequence, the transmitted amplitude levels, the received signal levels and the decoded sequence.
- 8.24** Repeat the Problem 8.23 for a modified duobinary signal pulse.
- 8.25** A precoder for a partial response signal fails to work if the desired partial response at  $n = 0$  is zero modulo  $M$ . For example, consider the desired response for  $M = 2$ :

$$x(nT) = \begin{cases} 2, & n = 0 \\ 1, & n = 1 \\ -1, & n = 2 \\ 0, & \text{otherwise} \end{cases}$$

Show why this response cannot be precoded.

- 8.26** In the case of correlated noise, the relation in the Viterbi algorithm may be expressed in general as [Ungerboeck, (1974)]

$$\mu(\mathbf{a}) = 2 \sum_n a_n r_n - \sum_n \sum_m a_n a_m x_{n-m}$$

where  $x_n = x(nT)$  is the sampled signal output of the matched filter,  $\{a_n\}$  is the data sequence, and  $\{r_n\}$  is the received signal sequence at the output of the matched filter. Determine the metric for the duobinary signal.

- 8.27** Sketch and label the trellis for a duobinary signal waveform used in conjunction with the precoding given by Equation (8.4.7). Repeat this for the modified duobinary signal waveform with the precoder given by Equation (8.4.19). Comment on any similarities and differences.
- 8.28** Consider the use of a (square-root) raised cosine signal pulse with a roll-off factor of unity for transmission of binary PAM over an ideal bandlimited channel that

passes the pulse without distortion. Thus, the transmitted signal is

$$v(t) = \sum_{k=-\infty}^{\infty} a_k g_T(t - kT_b)$$

where the signal interval  $T_b = T/2$ . Thus, the symbol rate is double of that for no ISI.

1. Determine the ISI values at the output of a matched-filter demodulator.
  2. Sketch the trellis for the ML sequence detector and label the states.
- 8.29** A binary antipodal signal is transmitted over a nonideal bandlimited channel, which introduces ISI over two adjacent symbols. For an isolated transmitted signal pulse  $s(t)$ , the (noise-free) output of the demodulator is  $\sqrt{\mathcal{E}_b}$  at  $t = T$ ,  $\sqrt{\mathcal{E}_b}/4$  at  $t = 2T$ , at zero for  $t = kT$ ,  $k > 2$ , where  $\mathcal{E}_b$  is the signal energy and  $T$  is the signaling interval.
1. Determine the average probability of error assuming that the two signals are equally probable and the additive noise is white and Gaussian.
  2. By plotting the error probability obtained in part 1 and that for the case of no ISI, determine the relative difference in SNR of the error probability of  $10^{-6}$ .
- 8.30** Show that the covariance matrix  $\mathbf{C}$  for the noise at the output of the matched filter for the duobinary pulse is given by Equation (8.5.25).
- 8.31** As indicated in Section 8.5.1, the running digital sum (RDS) is defined as the difference between the total number of accumulated zeros and the total number of accumulated ones in a sequence. If the RDS is limited to the range

$$-2 \leq \text{RDS} \leq 2$$

determine the state transition matrix and the capacity of the corresponding code.

- 8.32** Determine the capacity of a (0, 1) runlength-limited code. Compare its capacity with that of a (1,  $\infty$ ) code and explain the relationship.
- 8.33** A ternary signal format is designed for a channel that does not pass dc. The binary input information sequence is transmitted by mapping a 1 into either a positive pulse or a negative pulse, and a zero is transmitted by the absence of a pulse. Hence, for the transmission of 1's, the polarity of the pulses alternate. This is called an AMI (alternate mark inversion) code. Determine the capacity of the code.
- 8.34** Give an alternative description of the AMI code described in Problem 8.33 using the RDS with the constraint that the RDS can take only the values 0 and +1.
- 8.35** ( $kBnT$  codes) From Problem 8.33 we note that the AMI code is a “pseudoternary” code in that it transmits one bit/symbol using a ternary alphabet, which has the capacity of  $\log_2 3 = 1.58$  bits. Such a code does not provide sufficient spectral shaping. Better spectral shaping is achieved by the class of block codes designated as  $kBnT$ , where  $k$  denotes the number of information bits and  $n$  denotes the

we obtain the table shown below.

$k$	$n$	Code
1	1	1B1T
3	2	3B2T
4	3	4B3T
6	4	6B4T

Determine the efficiency of these codes by computing the ratio of the rate of the code in bits/symbol divided by  $\log_2 3$ . Note that 1B1T is the AMI code.

**8.36** This problem deals with the capacity of two  $(d, \kappa)$  codes.

1. Determine the capacity of a  $(d, \kappa)$  code that has the following state transition matrix:

$$D = \begin{bmatrix} 1 & 1 \\ 1 & 0 \end{bmatrix}$$

2. Repeat (step 1) when  $D$  is given as

$$D = \begin{bmatrix} 1 & 1 \\ 0 & 1 \end{bmatrix}$$

3. Comment on the differences between parts 1 and 2.

**8.37** A simplified model of the telegraph code consists of two symbols (Blahut, 1990). A dot consists of one time unit of line closure followed by one time unit of line open. A dash consists of three units of line closure followed by one time unit of line open.

1. If we view this code as a constrained code with symbols of equal duration, give the constraints.
2. Determine the state transition matrix.
3. Determine the capacity.

**8.38** Determine the state transition matrix for the runlength-constrained code described by the state diagram shown in Figure P-8.38. Sketch the corresponding trellis.

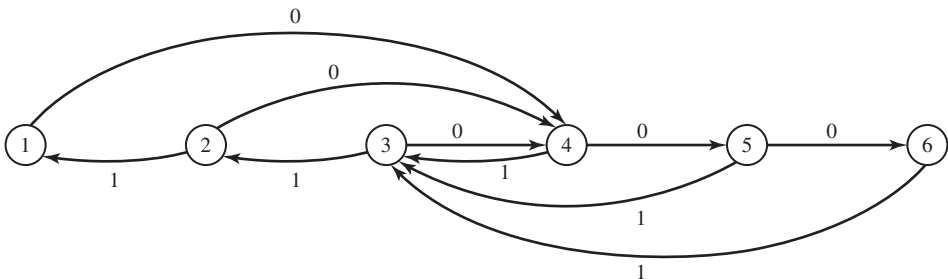


Figure P-8.38

**8.39** Determine the transition matrix for the  $(2, 7)$  runlength-limited code specified by the state diagram shown in Figure P-8.39.

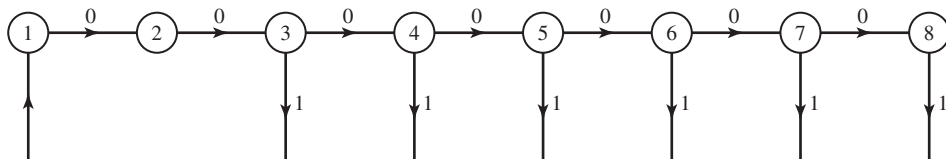


Figure P-8.39

**8.40** Determine the frequency response characteristics for the RC circuit shown in Figure P-8.40. Also determine the expression for the envelope delay.

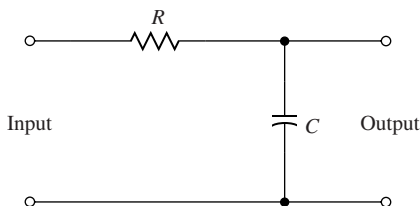


Figure P-8.40

**8.41** Consider the RC lowpass filter shown in Figure P-8.40 where  $\tau = RC = 10^{-6}$ .

1. Determine and sketch the envelope (group) delay of the filter as a function of frequency (see Problem 2.57).
2. Suppose that the input to the filter is a lowpass signal of bandwidth  $\Delta f = 1$  kHz. Determine the effect of the RC filter on this signal.

**8.42** A microwave radio channel has a frequency response

$$C(f) = 1 + 0.3 \cos 2\pi f T$$

Determine the frequency-response characteristic for the optimum transmitting and receiving filters that yield zero ISI at a rate of  $1/T$  symbols/sec and have a 50%-excess bandwidth. Assume that the additive noise spectrum is flat.

**8.43**  $M = 4$  PAM modulation is used for transmitting at a bit rate of 9600 bits/sec on a channel having a frequency response

$$C(f) = \frac{1}{1 + j \frac{f}{2400}}$$

$|f| \leq 2400$ , and  $C(f) = 0$ , otherwise. The additive noise is zero-mean, white Gaussian with power-spectral density  $\frac{N_0}{2}$  W/Hz. Determine the (magnitude) frequency response characteristic of the optimum transmitting and receiving filters.

**8.44** Binary PAM is used to transmit information over an unequalized linear filter channel. When  $a = 1$  is transmitted the noise-free output of the demodulator is

$$x_m = \begin{cases} 0.3, & m = 1 \\ 0.9, & m = 0 \\ 0.3, & m = -1 \\ 0, & \text{otherwise} \end{cases}$$

1. Design a three-tap zero-forcing linear equalizer so that the output is

$$q_m = \begin{cases} 1, & m = 0 \\ 0, & m = \pm 1 \end{cases}$$

2. Determine  $q_m$  for  $m = \pm 2, \pm 3$ , by convolving the impulse response of the equalizer with the channel response.

**8.45** The transmission of a signal pulse with a raised cosine spectrum through a channel results in the following (noise-free) sampled output from the demodulator:

$$x_k = \begin{cases} -0.5, & k = -2 \\ 0.1, & k = -1 \\ 1, & k = 0 \\ -0.2, & k = 1 \\ 0.05, & k = 2 \\ 0, & \text{otherwise} \end{cases}$$

1. Determine the tap coefficients of a three-tap linear equalizer based on the zero-forcing criterion.

2. For the coefficients determined in part 1, determine the output of the equalizer for the case of the isolated pulse. Thus, determine the residual ISI and its span in time.

**8.46** Show that the gradient vector in the minimization of the MSE may be expressed as

$$\mathbf{g}_k = -E[e_k \mathbf{y}_k]$$

where the error  $e_k = a_k - z_k$ , and the estimate of  $\mathbf{g}_k$ ; i.e.,

$$\hat{\mathbf{g}}_k = -e_k \mathbf{y}_k$$

satisfies the condition that  $E[\hat{\mathbf{g}}_k] = \mathbf{g}_k$ .

**8.47** A nonideal bandlimited channel introduces ISI over three successive symbols. The (noise-free) response of the matched filter demodulator sampled at the sampling time  $t = kT$  is

$$\int_{-\infty}^{\infty} s(t)s(t - kT) dt = \begin{cases} \mathcal{E}_b, & k = 0 \\ 0.9\mathcal{E}_b, & k = \pm 1 \\ 0.1\mathcal{E}_b, & k = \pm 2 \\ 0, & \text{otherwise} \end{cases}$$

1. Determine the tap coefficients of a three-tap linear equalizer that equalizes the channel (received signal) response to an equivalent partial response (duobinary) signal

$$y_k = \begin{cases} \mathcal{E}_b, & k = 0, 1 \\ 0, & \text{otherwise} \end{cases}$$

2. Suppose that the linear equalizer in part 1 is followed by a Viterbi sequence detector for the partial response signal. Give an estimate of the error probability if the additive noise is white and Gaussian, with power-spectral density  $N_0/2$  W/Hz.
- 8.48** Determine the tap weight coefficients of a three-tap zero-forcing equalizer if the ISI spans three symbols and is characterized by the values  $x(0) = 1$ ,  $x(-1) = 0.3$ ,  $x(1) = 0.2$ . Also determine the residual ISI at the output of the equalizer for the optimum tap coefficients.
- 8.49** In LOS microwave radio transmission, the signal arrives at the receiver via two propagation paths, the direct path and a delayed path that occurs due to signal reflection from surrounding terrain. Suppose that the received signal has the form

$$r(t) = s(t) + \alpha s(t - T) + n(t)$$

where  $s(t)$  is the transmitted signal,  $\alpha$  is the attenuation ( $\alpha < 1$ ) of the secondary path and  $n(t)$  is AWGN.

1. Determine the output of the demodulator at  $t = T$  and  $t = 2T$  that employs a filter matched to  $s(t)$ .
  2. Determine the probability of error for a symbol-by-symbol detector if the transmitted signal is binary antipodal and the detector ignores the ISI.
  3. What is the error-rate performance of a simple (one-tap) (DFE) that estimates  $\alpha$  and removes the ISI? Sketch the detector structure that employs a DFE.
- 8.50** Repeat Problem 8.48 using the MMSE as the criterion for optimizing the tap coefficients. Assume that the noise power spectrum is 0.1 W/Hz.
- 8.51** In a magnetic recording channel, where the readback pulse resulting from a positive transition in the write current has the form (see Figure 8.17).

$$p(t) = \frac{1}{1 + \left(\frac{2t}{T_{50}}\right)^2}$$

a linear equalizer is used to equalize the pulse to a partial response. The parameter  $T_{50}$  is defined as the width of the pulse at the 50%-amplitude level. The bit rate

is  $1/T_b$  and the ratio of  $T_{50}/T_b = \Delta$  is the normalized density of the recording. Suppose the pulse is equalized to the partial-response values

$$x(nT) = \begin{cases} 1, & n = -1, 1 \\ 2, & n = 0 \\ 0, & \text{otherwise} \end{cases}$$

where  $x(t)$  represents the equalized pulse shape.

1. Determine the spectrum  $X(f)$  of the bandlimited equalized pulse.
  2. Determine the possible output levels at the detector, assuming that successive transitions can occur at the rate  $1/T_b$ .
  3. Determine the error-rate performance of the symbol-by-symbol detector for this signal assuming that the additive noise is zero-mean Gaussian with variance  $\sigma^2$ .
- 8.52** Sketch the trellis for the Viterbi detector of the equalized signal in Problem 8.51 and label all the states. Also, determine the minimum Euclidean distance between merging paths.
- 8.53** (Carrierless QAM or PSK Modem) Consider the transmission of a QAM or  $M$ -ary PSK ( $M \geq 4$ ) signal at a carrier frequency  $f_c$ , where the carrier is comparable to the bandwidth of the baseband signal. The bandpass signal may be represented as

$$s(t) = \text{Re} \left[ \sum_n a_n g(t - nT) e^{j2\pi f_c t} \right]$$

1. Show that  $s(t)$  can be expressed as

$$s(t) = \text{Re} \left[ \sum_n a'_n Q(t - nT) \right]$$

where  $Q(t)$  is defined as

$$Q(t) = q(t) + j\hat{q}(t)$$

$$q(t) = g(t) \cos 2\pi f_c t$$

$$\hat{q}(t) = g(t) \sin 2\pi f_c t$$

and  $a'_n$  is a phase rotated symbol; i.e.,  $a'_n = a_n e^{j2\pi f_c nT}$ .

2. Using filters with responses  $q(t)$  and  $\hat{q}(t)$ , sketch the block diagram of the modulator and demodulator implementation that does not require the mixer to translate the signal to bandpass at the modulator and to baseband at the demodulator.

**8.54** (Carrierless amplitude or phase (CAP) modulation) In some practical applications in wireline data transmission, the bandwidth of the signal to be transmitted is comparable to the carrier frequency. In such systems, it is possible to eliminate the step of mixing the baseband signal with the carrier component. Instead, the bandpass signal can be synthesized directly, by embedding the carrier component in the realization of the shaping filter. Thus, the modem is realized as shown in the block diagram in Figure P-8.54, where the shaping filters have the impulse responses

$$q(t) = g(t) \cos 2\pi f_c t$$

$$\hat{q}(t) = g(t) \sin 2\pi f_c t$$

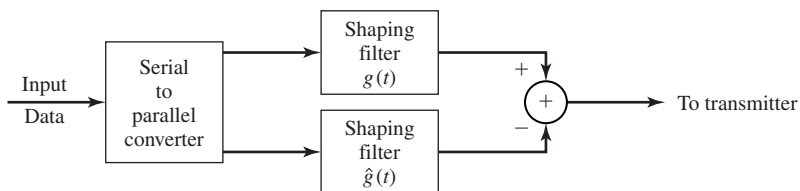
and  $g(t)$  is a pulse that has a square-root raised cosine spectral characteristic.

1. Show that

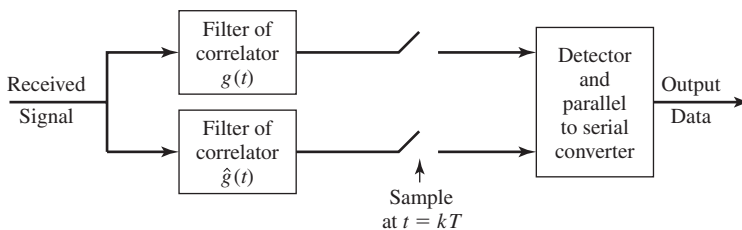
$$\int_{-\infty}^{\infty} q(t)\hat{q}(t) dt = 0$$

and that the system can be used to transmit two dimensional signals, e.g., PSK and QAM.

2. Under what conditions is this CAP modem identical to the carrierless QAM/PSK modem treated in Problem 8-53?



(a) Modulator



(b) Demodulator

Figure P-8.54 CAP modem.

- 8.55** Show that the sequence  $\{x_n, 0 \leq n \leq N - 1\}$  given by Equation (8.7.7) corresponds to the samples of  $x(t)$  given by Equation (8.7.8). Also, prove that  $x(t)$  given by Equation (8.7.6) is a real-valued signal.
- 8.56** Show that the IDFT of a sequence  $\{X_k, 0 \leq k \leq N - 1\}$ , can be computed by passing the sequence  $\{X_k\}$  through a parallel bank of  $N$  linear discrete-time filters with system functions

$$H_n(z) = \frac{1}{1 - e^{j2\pi n/N} z^{-1}}, \quad n = 0, 1, \dots, N - 1$$

and sampling the filter outputs at  $n = N$ .